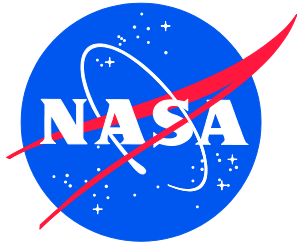# A Comprehensive Analysis of the X-15 Flight 3-65 Accident

Cornelius J. Dennehy/NESC
Langley Research Center, Hampton, Virginia

Jeb S. Orr
Draper Laboratory, Huntsville, Alabama

Immanuel Barshi, and Irving C. Statler
Ames Research Center, Moffet Field, California

NASA STI Program . . . in Profile

Since its founding, NASA has been dedicated to the advancement of aeronautics and space science. The NASA scientific and technical information (STI) program plays a key part in helping NASA maintain this important role.

The NASA STI program operates under the auspices of the Agency Chief Information Officer. It collects, organizes, provides for archiving, and disseminates NASA's STI. The NASA STI program provides access to the NASA Aeronautics and Space Database and its public interface, the NASA Technical Report Server, thus providing one of the largest collections of aeronautical and space science STI in the world. Results are published in both non-NASA channels and by NASA in the NASA STI Report Series, which includes the following report types:

- TECHNICAL PUBLICATION. Reports of completed research or a major significant phase of research that present the results of NASA Programs and include extensive data or theoretical analysis. Includes compilations of significant scientific and technical data and information deemed to be of continuing reference value. NASA counterpart of peer-reviewed formal professional papers, but having less stringent limitations on manuscript length and extent of graphic presentations.

- TECHNICAL MEMORANDUM. Scientific and technical findings that are preliminary or of specialized interest, e.g., quick release reports, working papers, and bibliographies that contain minimal annotation. Does not contain extensive analysis.

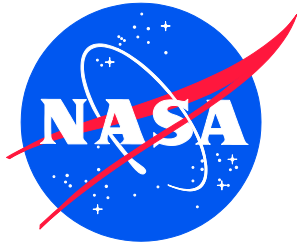- CONTRACTOR REPORT. Scientific and technical findings by NASA-sponsored contractors and grantees.

- CONFERENCE PUBLICATION. Collected papers from scientific and technical conferences, symposia, seminars, or other meetings sponsored or co-sponsored by NASA.

- SPECIAL PUBLICATION. Scientific, technical, or historical information from NASA programs, projects, and missions, often concerned with subjects having substantial public interest.

- TECHNICAL TRANSLATION. English-language translations of foreign scientific and technical material pertinent to NASA's mission.

Specialized services also include organizing and publishing research results, distributing specialized research announcements and feeds, providing information desk and personal search support, and enabling data exchange services.

For more information about the NASA STI program, see the following:

- Access the NASA STI program home page at http://www.sti.nasa.gov

- E-mail your question to help@sti.nasa.gov

- Fax your question to the NASA STI Information Desk at 443-757-5803

- Phone the NASA STI Information Desk at 443-757-5802

- Write to:
  STI Information Desk
  NASA Center for AeroSpace Information
  7115 Standard Drive
  Hanover, MD 21076-1320

NASA/TM–2014-218538
NESC-RP-14-00957

A Comprehensive Analysis of the X-15 Flight 3-65 Accident

Cornelius J. Dennehy/NESC
Langley Research Center, Hampton, Virginia

Jeb S. Orr
Draper Laboratory, Huntsville, Alabama

Immanuel Barshi, and Irving C. Statler
Ames Research Center, Moffet Field, California

Acknowledgments

Available from:

NASA Center for AeroSpace Information
7115 Standard Drive
Hanover, MD 21076-1320
443-757-5802

**A Comprehensive Analysis of the X-15
Flight 3-65 Accident**

September 4, 2014

Report Approval and Revision History

NOTE: This document was approved at the September 4, 2014, NRB. This document was submitted to the NESC Director on September 26, 2014, for configuration control.

Approved:	*Original Signature on File*	9/29/14
	NESC Director	Date

Version	Description of Revision	Office of Primary Responsibility	Effective Date
1.0	Initial Release	Cornelius J. Dennehy, NASA Technical Fellow for Guidance, Navigation, and Control (GN&C), GSFC	9/4/14

Table of Contents

Technical Assessment Report

List of Figures

List of Tables

Technical Assessment Report

1.0   Notification and Authorization

The November 15, 1967, loss of X-15 Flight 3-65-97 (hereafter referred to as Flight 3-65) was a unique incident in that it was the first and only aerospace flight accident involving loss of crew on a vehicle with an adaptive flight control system (AFCS). In addition, Flight 3-65 remains the only incidence of a single-pilot departure from controlled flight of a manned entry vehicle in a hypersonic flight regime. Both the advent of small, commercially developed entry vehicles and a renewed interest in the use of adaptive control to improve performance and flight safety have necessitated a thorough analysis of the causal and contributing factors in this accident.

To mitigate risk to emerging aerospace systems, the NASA Engineering and Safety Center (NESC) proposed a comprehensive review of this accident. The goal of the assessment was to resolve lingering questions regarding the failure modes of the aircraft systems (including the AFCS) and thoroughly analyze the interactions among the human agents and autonomous systems that contributed to the loss of the pilot and aircraft.

Mr. Cornelius J. Dennehy, NASA Technical Fellow for Guidance, Navigation, and Control (GN&C) was selected as the NESC lead, with Dr. Jeb S. Orr assigned as the technical lead. The key stakeholders for this assessment were Mr. Garry Lyles, Space Launch System (SLS) Program Chief Engineer; Mr. Kurt Jackson, SLS Program Integrated Avionics and Software Discipline Lead Engineer; Mr. Mark West, SLS Vehicle Management Discipline Lead Engineer; the Human Exploration and Operations Mission Directorate; and the Commercial Crew Program.

2.0   Signature Page

Submitted by:

Team Signature Page on File – 10/07/14

_____
Mr. Cornelius J. Dennehy   Date

Significant Contributors:

_____   _____
Dr. Jeb S. Orr   Date   Dr. Immanuel Barshi   Date

_____
Dr. Irving C. Statler   Date

Signatories declare the findings, observations, and NESC recommendations compiled in the report are factually based from data extracted from program/project documents, contractor reports, and open literature, and/or generated from independently conducted tests, analyses, and inspections.

3.0   Team List

Name	Discipline	Organization
Core Team		
Neil Dennehy	NESC Lead	GSFC
Jeb Orr	NESC Deputy Lead	MSFC/Draper Laboratory
Immanuel Barshi	Research Psychologist	ARC
Irving Statler	Ames Associate (Retired)	ARC
Patricia Pahlavani	MTSO Program Analyst	LaRC
Administrative Support		
Jonay Campbell	Technical Writer	LaRC/NG

3.1   Acknowledgements

4.0   Executive Summary

The X-15 program operated three hypersonic, high-altitude rocket-propelled single-pilot aircraft from 1959 until 1968. The third aircraft, X-15-3, was involved in a fatal accident on November 15, 1967. X-15-3 was the most advanced aircraft flown during the program and carried a variety of sophisticated instrumentation and electronics, including the MH-96 adaptive flight control system (AFCS).

The X-15-3 aircraft was destroyed during atmospheric entry after entering uncontrolled flight at an altitude of 230,000 feet and a velocity near Mach 5. The pilot, United States Air Force (USAF) Major Michael J. Adams, was incapacitated by the aircraft accelerations and was killed either during the ensuing breakup or upon ground impact.

To better understand the risks to emerging aerospace systems incorporating advanced technologies such as adaptive flight control, the NASA Engineering and Safety Center (NESC) organized a comprehensive assessment of this fatal accident in light of almost 50 years of accumulated experience in flight operations, human factors, and flight control. The report of the 1968 NASA/United States Air Force Accident Investigation Board (AIB) was used as a point of departure for the present assessment. The goal of the study was to characterize the causes of the loss of life, as well as to determine, at a level of detail not addressed in the original report, the exact role of the MH-96 AFCS in the accident.

The NESC assessment confirmed that the root cause of the accident was an electrical disturbance originating from an experiment package using a commercial-off-the-shelf (COTS) component that had not been properly qualified for the X-15 flight environment. Notably, the risks of accelerated and/or limited flight qualification of COTS components have been highlighted in other recent assessments by the NESC. These assessments are referenced in the final report.

The performance of the pilot was found to be commensurate with his experience and qualifications. As noted by the 1968 AIB, spatial disorientation (SD) may have contributed to pilot workload. However, the NESC assessment found no conclusive evidence to support the hypothesis that SD was a causal factor. On the contrary, the evidence suggests that poor design of the pilot-aircraft interface and ineffective operational procedures prevented the pilot and ground control from recognizing and isolating the numerous failures before the aircraft's departure from controlled flight was inevitable.

The MH-96 AFCS limit cycle oscillation (LCO) that contributed to the breakup of the aircraft was analyzed in detail by the NESC team. Using nonlinear simulation and frequency-domain analytical methods, the NESC analysis determined that the LCO was caused by a design oversight in a control system notch filter that was installed only on the X-15-3 aircraft. This notch filter was used to stabilize an unstable structural resonance but introduced a latent failure mode that only appeared in severe off-nominal conditions. The notch filter design issue was not identified in the 1968 AIB report. The MH-96 failure mode was shown to be independent of the adaptive control law. This key NESC finding highlights the fact that the implementation of the

adaptive control hardware, not the underlying theory of adaptive flight control, was the contributing factor in the loss of X-15-3.

Finally, the NESC assessment highlighted several programmatic and cultural themes contributing to the accident, including continued flight operations in the presence of multiple unexplained anomalies and an insufficient focus on the risks of subsystem-level interactions.

This NESC final report documents a total of 10 findings and 18 recommendations, which are directed to the key stakeholders for this assessment.

5.0   Introduction

The X-15 research aircraft (Figure 5.0-1) is widely regarded as one of the most successful high-performance flight research platforms ever developed. Although it encountered numerous technical and programmatic challenges over the course of its development, the X-15 eventually became a test bed for validating numerous concepts that were fundamental enabling technologies for other programs, including the Apollo program and the Space Transportation System. During the X-15's operational lifetime, the breaking of new records of speed and altitude for manned flight became almost routine, and the program continued successfully in spite of several severe, nonfatal accidents. Many advances in the modern understanding of hypersonic flight mechanics, including thermal protection, structural design, shock-impingement heating, air-data sensing, and hypersonic propulsion can be directly attributed to research performed using the X-15 platform. Many research pilots and astronauts contributed substantially to the success of the program during its 199 flights and nearly 10-year operational history [ref. 4].

Figure 5.0-1. X-15 56-6672 in Flight (USAF photo)

Owing to its diverse mission capabilities and the relative immaturity of autonomy in aerospace engineering at the time, the X-15 from its inception was designed to be a piloted aircraft. Only later in the design process did nontraditional approaches to guidance, navigation, and control (GN&C) begin to enter the design space. These approaches were, in all respects, conservative and motivated primarily by functionality and engineering practicality. These included, most notably, an AFCS that eased pilot workload by automatically adjusting the gains of the aircraft's aerodynamic control surfaces in response to changing flight conditions. This experimental flight

control system, designated the MH-96 AFCS, experienced a relatively successful deployment on X-15-3 (serial number 56-6672) [refs. 5 and 6].

In addition, the X-15-3 was considered a test bed for development of advanced GN&C technologies, and along with the advanced flight control system, included an advanced inertial system, a boost guidance and energy management computer, and advanced pilot displays. The other two aircraft (X-15-1 and X-15-2) used a conventional, pilot-selectable fixed-gain stability augmentation system (SAS) and conventional instruments. Erratic behavior of the AFCS during Flight 3-65 was a key factor in the subject accident and will be discussed in detail in the coming sections.

In the course of its operation at the NASA Flight Research Center[1] (FRC), all three X-15 aircraft underwent numerous field modifications, upgrades, and equipment retrofits. This practice of adapting the aircraft capabilities to meet mission needs was a key enabler in the X-15's agility as a science platform. However, this placed a substantial demand on the pilot-engineers that managed the X-15 during its highly dynamic missions.

5.1   Accident Summary

On November 15, 1967, X-15-3 was destroyed in flight due to a structural load exceedance precipitated by a loss of control [ref. 3]. The research pilot, USAF Major Michael J. Adams, did not survive the event. The flight (denoted 3-65-97) was the 65th flight of X-15-3 and the 191st flight of the X-15 program.

The causes of the accident are complex, beginning with an electrical anomaly associated with an experiment motor that had not been properly qualified for the space environment. This electrical anomaly led to a series of electrical and instrumentation failures that required continuous attention from the pilot to diagnose and troubleshoot. Ground controllers, lacking adequate aircraft information displays and believing the pilot would effectively manage the emergency, did not inform the pilot of the multiple subsystem anomalies or recommend that the mission be discontinued.

In the already high-demand environment of the ballistic hypersonic flight regime, the excessive workload contributed to the pilot's apparent loss of spatial and instrument mode awareness. The pilot, apparently mostly unaware of the condition of the aircraft systems, provided control inputs that allowed the aircraft to enter a hypersonic spin that evolved into an inverted dive. The dive may have been recoverable, but a persistent high-amplitude flight control system LCO originating in the MH-96 AFCS prevented the pilot from regaining control of the aircraft. The LCO also contributed to the airframe load exceedances that eventually caused the aircraft to break up at approximately 60,000 feet.

---

[1] Later Dryden Flight Research Center (DFRC), and now Armstrong Flight Research Center (AFRC).

5.2   Motivation

A concern has recently arisen within the aerospace community as to the implications of the X-15-3 accident for the design of emerging manned hypersonic vehicles, launch vehicles, and spacecraft. For example, the renewed interest in boost-glide concepts for transportation and suborbital space tourism necessitates the use of ballistic trajectories that are not unlike those experienced by the X-15 [ref. 5]. In addition, orbital space planes whose nominal entry trajectories differ substantially from the X-15's often encounter conditions similar to an X-15 entry in the event of a powered abort. While avionics, sensing, and autonomy technologies have advanced by orders of magnitude in the last 50 years, the fundamental challenges associated with hypersonic ballistic flight remain largely unchanged. Insofar as it relates to the ability of a flight crew to successfully manage a space plane through the highly dynamic phases of boost, suborbital coast, entry, and glide, the lessons learned from the X-15-3 accident lend insight as to potential requirements for flight control design, vehicle instrumentation, crew spatial/situational awareness, and abort modes. These lessons are relevant and applicable even if vehicle manual or semi-manual control is implemented only as a backup to a fully automatic guidance and control system.

In addition, in recent years some aspects of the anomalies experienced on Flight 3-65 have been incorrectly reported in the literature, probably owing to the limited availability of the flight test data and failure report outside the NASA community [refs. 7 and 8]. No comprehensive account of the accident exists in the open literature that treats the issue at a system level and discusses the human factors, flight controls, and other subsystem anomalies simultaneously. The present report attempts to bridge the gap in the accident understanding by examining in detail the relevant systems (i.e., instrumentation and flight control) and the programmatic and cultural factors that led to this fatal accident.

5.3   Sources

Several excellent references exist regarding X-15 program history, design, engineering, operation, and subsystems. Many of the technical data are in original program documents and technical reports with several available in the open literature; these are referenced where appropriate. The most complete historical accounts are those of Jenkins [refs. 4 and 9]. These works provide a comprehensive look at the evolution of the program and the aircraft, with many first-hand accounts by participants in the X-15's design and operation.

The January 1968 report of the joint NASA/USAF Accident Investigation Board (AIB) [ref. 3] that reviewed the causes of the destruction of the X-15-3 is a primary source for the present discussion. This report is extensive, and while it contains technical data in the attached appendices, some of the references therein are unfortunately lost. For various reasons, reference 3 is not available outside the NASA community as of the time of this writing. While the NASA/USAF AIB report contains the most comprehensive assessment of the accident available, it is limited in depth and self-contradictory in some respects. Importantly, the report

lacks detail, especially with respect to the AFCS function. After an extensive search, many important references were identified that provide additional insight into the operation of various aircraft subsystems.

Much of the critical design data on the X-15 has been lost. This issue is complicated by the fact that much of the design and engineering work was performed across disparate organizations. While the X-15 program as a whole was effective at documenting research results [ref. 10], design data were rarely consolidated and maintained for future use. In the event design data were consolidated, their self-consistency is often questionable since the vehicle configurations varied widely over the program's 10-year lifespan [ref. 4]. Various surviving documents related to the flight control system are dispersed among NASA, the Department of Defense (the USAF and the United States Navy (USN)), and contractor archive libraries, owing to the diverse heritage of the AFCS as an incrementally developed technology with its origins in the USAF research organizations.

A careful and concerted effort has been undertaken to assemble a picture of the aircraft and systems configuration at the time of the accident. Given the substantial changes in the vehicle design that occurred during its development and operation, as well as the lack of a single source that details its final configuration, it is surprisingly easy to draw erroneous conclusions about the operational vehicle's characteristics from the data available in the open literature. The authors have attempted to construct a cohesive and self-consistent description of the X-15-3 aircraft as flown in November 1967 through careful checking and cross-referencing of numerous reports and technical data.

It is important to note that the formal assessment of the appropriateness or correctness of the original AIB recommendations is not within the scope of the present study. While some findings and recommendations of this study both supplement and extend, and in some cases, contradict, the findings of the AIB report, the present study was conducted considering all of the available objective evidence, with more than 45 years of human factors, flight control, and flight test operations experience accumulated since the end of the X-15 program.

Finally, it is with full cognizance that the present report appears at a time when residual "tribal knowledge" associated with the X-15 program is sparse. The number of living persons having direct engineering development and test experience with the X-15 program is likely less than a few dozen. This is a solemn reminder that current and future aerospace vehicle development programs must include a strong emphasis on retaining a documentation tree focused on requirements and specifications, and on the corresponding design motivation, underlying reasoning, and innovations.

5.4   Report Structure

The structure of this report is as follows. In Section 6, a systems-level overview of the X-15 aircraft and its mission profile is provided. Various aspects of the pilot instrumentation and flight control system are discussed to aid in understanding the phenomena that were present at

the time of the accident. In Section 7, a timeline of Flight 3-65 is provided with detailed information as to the aircraft state throughout the trajectory based on an analysis of the available flight data.

Section 8 provides a detailed look at the fundamental subsystem failure modes that contributed to the accident. In Section 9, the human factors, programmatic, and engineering culture aspects of the accident are discussed. Summary conclusions and the NASA Engineering and Safety Center (NESC) recommendations are presented in Section 10. Finally, a comprehensive simulation analysis was conducted in an effort to better characterize and understand the conditions under which the MH-96 AFCS could exhibit behavior commensurate with that which contributed to the accident. While the results are summarized in Section 8, a detailed description of the modeling methodology appears in Appendix A. Supplementary information, including detailed plots of reconstructed flight data, appears in Appendix B.

6.0   The X-15 Research Aircraft

The X-15 was a piloted, single-seat rocket-propelled hypersonic research aircraft developed under cooperative funding and program management from the USAF, the USN, and NASA. Initial design concept engineering was completed in the early 1950s, and a prime contract for three aircraft was awarded to North American Aviation in September 1955. The first of three airframes was completed in October of 1958. The charter of the X-15 program was primarily to provide a platform for high-speed aerothermodynamic and high-altitude aeromedical research, and the design approach followed a capability-driven model anchored to specific performance targets expressed in terms of speed, altitude, and flight duration. Military interest in the X-15 development by the USAF and the USN stemmed from the applications of manned hypersonic systems for reconnaissance and strategic weapon delivery. The ill-fated X-20 Dyna-Soar skip-entry bomber program, being developed in parallel to the X-15, was to have adopted numerous technologies from the X-15 had it not been cancelled in late 1963. In fact, several mature technologies from the canceled X-20 (e.g., a version of the inertial navigation system) were used on the X-15 [ref. 11].

6.1   Design Overview

The X-15 aircraft was a reusable winged space plane with a launch mass of about 33,000 lbm, depending on the particular airframe and equipment loadout [ref. 4]. By 1967, all X-15s were powered by a single, regeneratively cooled YLR99-RM-1 throttleable rocket engine providing a thrust at altitude of 57,000 lbf with a specific impulse of 265 seconds and a total burn time capability of 180 seconds [ref. 12]. The X-15 structure was comprised primarily of Inconel® X, a high-strength nickel-steel alloy that was capable of withstanding the high aerothermal loading and peak temperatures of approximately 1,300 degrees Fahrenheit in the stagnation regions [ref. 10]. The airframe volume was occupied by integral pressure-stabilized propellant and oxidizer tanks containing anhydrous ammonia and liquid oxygen, with ullage and purge pressures maintained via an integral helium supply. Liquid nitrogen was stored for cooling and

cabin pressurization, and a hydrogen peroxide supply provided propellant for the two auxiliary power units (APUs) used to supply electrical power and run the hydraulic systems. A separate hydrogen peroxide supply was used for the ballistic control system (BCS) monopropellant thrusters in the nose, now commonly referred to as a reaction control system (RCS). A third hydrogen peroxide supply in the aft compartment, cross-strapped to the RCS and APU tanks, was used to provide power to the YLR-99 turbopumps that supplied propellants to the main propulsion system [ref. 13].

An internal layout drawing of the X-15 is shown in Figure 6.1-1. The X-15 cockpit consisted of a single seat aft of the RCS compartment and forward of the equipment bay. The cockpit used a canopy having two planar windows, and pilots reported that despite the small windscreen the outside view during approach and landing was acceptable [ref. 14].
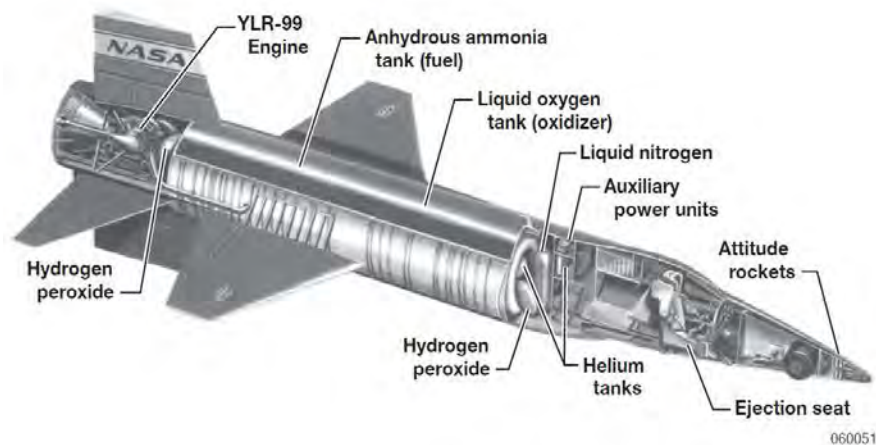
Figure 6.1-1. X-15 Research Aircraft Internal Layout (NASA)

Aft of the pilot station was an equipment bay containing most of the research instrumentation. Each X-15 airframe was extensively instrumented, and a large portion of the research and flight instrumentation data (about 90 distinct measurements) was telemetered to the ground. The remainder was recorded onboard using a combination of film oscillographs and tape recorders. Each aircraft was instrumented with approximately 1,000 aerodynamic and aerothermal transducers, thermocouples, and pressure taps [ref. 15].

6.2   Trajectory

The X-15 was carried to a launch altitude of 45,000 feet by a NASA NB-52 carrier aircraft on a launch pylon below the starboard wing, and nominally flew a ballistic or depressed high-altitude trajectory with a launch point 200 to 300 nautical miles uprange of the landing site. Trajectories were generally flown along an azimuth southwest from the launch point along a fixed magnetic heading toward the landing site. Most X-15 flights lasted about 10 minutes from carrier aircraft launch to touchdown [ref. 4].

The X-15 mission profiles and target flight conditions varied substantially based on specific research objectives but were generally classified into the two major categories of altitude and speed profiles. Altitude profiles, such as the design reference mission shown in Figure 6.2-1, consisted of a ballistic atmospheric exit to an altitude exceeding 200,000 feet after experiencing an engine burn of 80–100 seconds and a peak axial acceleration nearing 4 g.

The X-15 altitude trajectory consisted of an immediate engine ignition and throttle up after separation from the NB-52 carrier aircraft, followed by a 2- to 2.5-g pull-up to maintain a prescribed angle of attack (α) or pitch attitude, typically around 12 or 32 degrees, respectively. The aircraft velocity during the propulsive phase increased from Mach 0.7 at launch to approximately Mach 5. The aircraft was stabilized after atmospheric exit using the RCS system throughout the trajectory, with the aircraft experiencing about two minutes of 0-g before a rapid onset of dynamic pressure associated with atmospheric reentry. The aircraft was stabilized at a predetermined entry α and decelerated at a nominal normal load of 5 g before being recovered into an equilibrium glide at a high supersonic Mach number. Energy management procedures were then executed to null entry dispersions and preparation for a landing on Rogers Dry Lake, California [ref. 10].
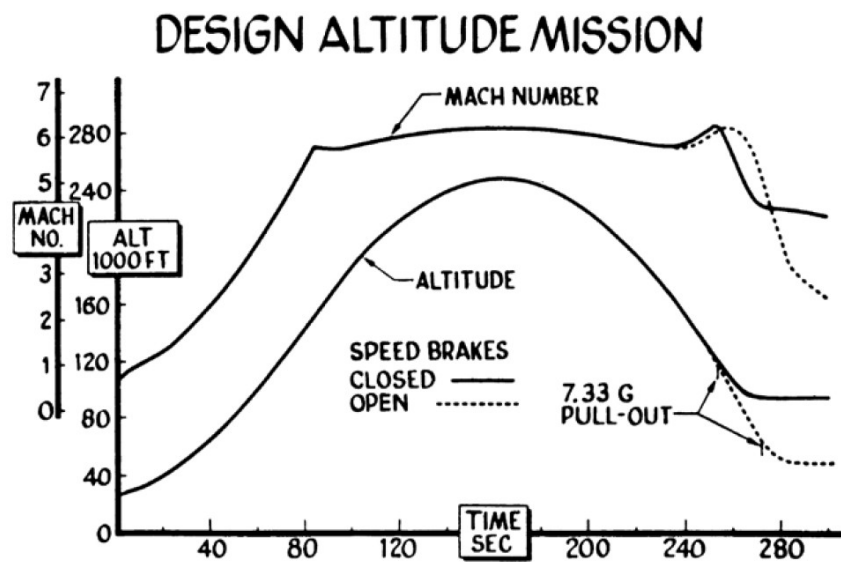
Figure 6.2-1. X-15 Altitude Design Reference Mission (NASA)

6.3 Flight History

The X-15 program conducted 199 research flights over a period of nearly 10 years. The first unpowered drop test was conducted on June 8, 1959, and the final powered flight was completed October 24, 1968. During this period, the program routinely set altitude and speed records for a piloted aerospace plane and ultimately held the record for the highest altitude (354,200 feet;

August 22, 1963) and highest Mach number (Mach 6.7; October 3, 1967). These official records persisted until the orbital reentry of Space Shuttle STS-1 in April 1981.

The X-15 program was not without frequent anomalies and several serious accidents. This era of flight research was characterized by a fast pace of system and mission development, quick advancement of envelope expansion, and relatively poor hardware reliability compared with currently acceptable standards for safety-critical components. Aborts due to subsystem malfunctions were commonplace, but safety precautions were a regular facet of mission planning (e.g., trajectories were designed such that abort-to-landing capability was available with sufficient energy at all points in the mission profile). While the acceptance of risk during flight test operations was a common feature of the X-15 program, numerous test and checkout procedures were employed prior to flight, and go/no-go criteria were established for critical subsystems. However, owing to the short flight duration, the generally poor radio communications between the flight controllers and the X-15 pilots, and a high reliance on the research pilot to troubleshoot subsystem issues, the pilot's role in mitigating the effects of component failures was paramount. In nearly all cases where major subsystem anomalies threatened the safety of flight, direct action by the pilot successfully prevented a catastrophic accident [ref. 4].

The X-15 program suffered four major accidents, three of which were in-flight with only one occurring at a high altitude and Mach number. In the only major ground accident, a propulsion system malfunction caused an explosion in the X-15-3 airframe during ground operations in June 1960 but caused no major injuries.

In November of 1959, the first serious landing accident resulted in a structural failure on X-15-2 when it landed heavy after an abort. The pilot sustained no major injuries. In the second nonfatal flight incident in November of 1962, the pilot made an emergency landing in the same airframe. The aircraft again landed heavy and the wing flaps failed to deploy, causing a collapse of the left main landing skid upon touchdown. The vehicle tumbled, and the pilot was seriously injured, but recovered after several weeks [ref. 10]. The only fatal accident of the program, the subject of the present report, occurred in November 1967.

6.4 Instrumentation

Instrumentation aboard the aircraft, excluding supplemental research instrumentation, was used to measure the aircraft dynamic states for the purposes of flight control and pilot display. All three X-15 aircraft were similar in terms of instrumentation subsystems. Flight instrumentation onboard the X-15-3 aircraft available to the AFCS and the pilot included an inertial measurement unit (IMU), a dual-redundant rate gyro package, an aerodynamic flow direction sensor, and flight control accelerometers.

6.4.1 Stable Platform and Inertial Flight Data System (IFDS)

The stable platform was a three-axis IMU contained in the forward equipment bay. In the initial design, the stable platform was a Sperry FRC-66 3-axis IMU coupled to an analog navigation computer. Together, the sensor package and its navigation hardware were referred to as the IFDS (inertial flight data system). In 1964-65, the FRC-66 package on X-15-1 and X-15-3 was replaced with the digital X-20 IFDS, which provided better computational accuracy at the expense of degraded gyro drift and higher mass [ref. 11].

As a gimbaled platform, the attitude solution was available directly from the IMU gimbal resolvers. The attitude director indicator (ADI) "ball," the pilot's primary attitude instrument, was slaved directly to the IMU output [ref .11]. The ADI could be operated in a gross attitude mode or one of two selectable precision indicator modes. One of the precision modes, called precision attitude indicator (PAI), used horizontal and vertical needles on the display to indicate fine pitch and roll error in place of the usual α and sideslip (β) error.

The stable platform was a four-gimbal system designed to avoid attitude singularities ("gimbal lock"). IMU data were available for use in attitude (roll, pitch, and heading) hold modes, which were provided by the MH-96 AFCS [ref. 16]. At low dynamic pressure of less than 50 psf, the IFDS could provide α based on velocity and attitude for use in the MH-96 α hold mode in place of the measured α from the flow direction sensor [ref. 2].

The IFDS was used to derive inertial estimates of altitude, altitude rate, and velocity magnitude. Experience showed that the inertial estimates of the velocity and altitude were acceptably accurate for about 300 seconds of flight [ref. 17] but were expected to drift following entry and thus were seldom relied upon for ranging decisions [refs. 11, 18, and 19].[2] While the IFDS was the primary source of pilot information during the boost trajectory phase, it was not considered mission critical for two reasons. First, flight planning relied on reaching a particular burnout velocity, and with engine performance relatively well characterized, pilots flew to a specified burn time (or burned all propellant available) rather than attempting to meet a velocity constraint [ref. 18]. Secondly, the availability of more accurate radar velocity data communicated from ground control supplanted the use of inertially derived measurements.

In progress at the time of the Flight 3-65 incident was the development of a boost and entry guidance capability by Ames Research Center, related to work that had been performed in support of the canceled X-20 program [refs. 20 and 21]. This supplemental guidance computer (AN/AYK-5), referred to as ALERT, was installed on X-15-3 with an advanced instrument panel having vertical tape displays versus the conventional instruments [ref. 4]. The ALERT system was installed on X-15-3 at the time of the accident, and its boost-guidance mode was used for pitch steering cues during the power-on phase [ref. 3].

---

[2] Based on flight data, the digital IFDS exhibited a 1-σ altitude error of approximately 5,000 feet at 500 seconds [ref. 11].

6.4.2 Rate Gyros

While the stable platform contained a triad of rate gyros used in maintaining the platform orientation, a separate set of body-fixed ("strapdown") gyros were used for flight control rate damping [ref. 16]. The flight control rate gyros were located in the aft equipment bay, and were packaged into two identical three-axis assemblies to support the MH-96 AFCS's dual-channel redundant configuration. The other X-15 airframes had only one gyro package. One notable feature of the flight control rate gyro was its failure monitor circuit, which was intended to mitigate failure effects that could be manifested as a full-scale output. In the event that the gyro output rate exceeded 22.5 degrees/second, the failure monitor was tripped and the input from the gyro to the flight control system was zeroed. Reset was automatic upon reduction of rate below the critical threshold. No indication of this behavior was provided to the pilot [ref. 3].

6.4.3 Flow Direction Sensor

The innovative X-15 "ball nose" air data system, or Q-ball, was a hypersonic flow direction sensor mounted in the aircraft nose [ref. 22]. Using a servo feedback loop on an articulated spherical differential pressure sensor, accurate estimates of α and β at high Mach number could be provided to the pilot to a dynamic pressure of approximately 50 psf. Below 50 psf, estimates of α and β were generally accurate except during RCS pulses from the nose jets [ref. 23]. Usable measurements were available to a dynamic pressure as low as 3.5 psf.[3] The flow-field interaction near the nose corrupted the measurements, but the effect was transient and pilots were aware of the phenomenon (Figure 6.4-1). However, the transient behavior precluded the use of measured data for α-hold at low dynamic pressure. A calibrated measurement of dynamic pressure was provided by the ball nose and was considered accurate within 2 percent above Mach 2.5 [ref. 17].

---

[3] The 3-65 flight plan called for the pilot to establish and hold α at 7 psf.
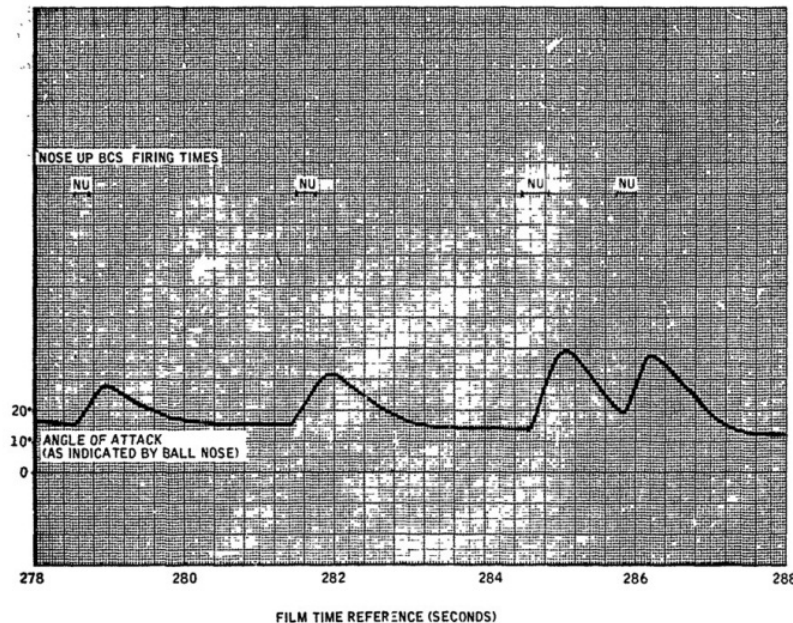
***Figure 6.4-1. RCS Jet Flow-field Interaction with Flow Direction Sensor at 3 psf,
240,000 feet, Mach = 4.4 [ref. 1]***

6.4.4   Accelerometers

Separate from the IFDS IMU was an accelerometer package collocated with the AFCS hardware
in the forward equipment bay. While lateral acceleration feedback was used to augment
directional stability in the early design, it was removed with yaw rate to roll feedback by late
1963 to be consistent with the deletion of the ventral fin [ref. 19]. Normal acceleration
measurements were used primarily in the pitch control loop and to provide a normal load
limiting function in the MH-96. This limiting function provided nose-down feedback as the
normal acceleration approached 5.5 g [refs. 1 and 2]. The pilot's display of normal acceleration
was provided by a separate, self-contained accelerometer mounted in the instrument panel
[ref. 17].

6.5   Flight Control System

The X-15 flight control system configuration differed based upon the airframe. On all three
vehicles, aerodynamic control surfaces consisted of a vertical stabilizer with an all-moving
rudder surface and an all-moving horizontal tail with differential actuation for roll control
[ref. 24]. Three-axis attitude control during exoatmospheric flight was provided by dual string of
RCS monopropellant peroxide jets in the nose and wingtips [ref. 25]. Wing trailing surfaces
included landing flaps that were deployed on final approach but were unused during powered,
ballistic, or entry flight. Aft speed brakes were available for energy management after engine
shutdown. The jettisonable lower ventral fin was used to increase lateral-directional stability

above Mach 6, but after determining that aircraft stability characteristics were improved during high-altitude reentries without the fin, it was removed from the X-15-3 after 1963 [ref. 26].

Aerosurface motion control (Figure 6.5-1) was provided by a set of power-boost hydraulic actuators supplied by a dual-redundant hydraulic system. The interface to the hydraulic servocylinders was mechanical and was interlinked to the pilot inceptors via a set of pushrods and cables with spring bungees and nonlinear gearing for artificial feel [ref. 24].
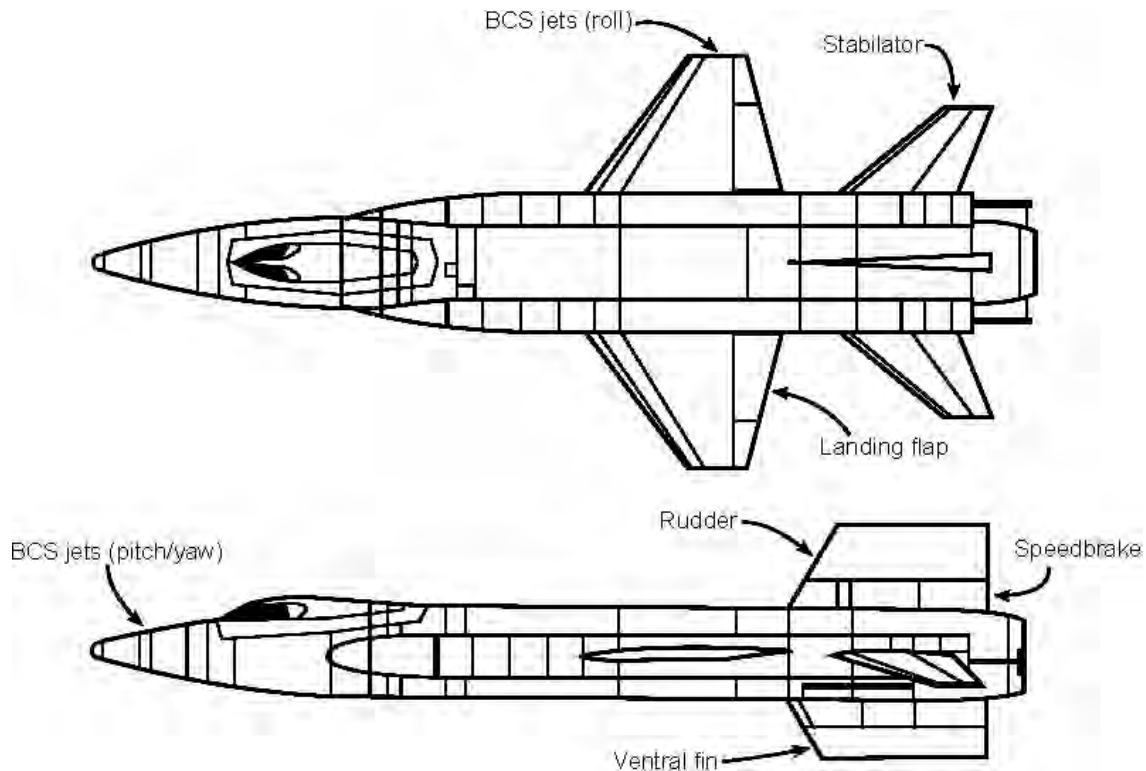
Figure 6.5-1. X-15 Flight Control Effectors

X-15-1 and X-15-2 (serial numbers 56-6670 and 56-6671) used a pilot-selectable "fixed-gain" three-axis SAS with rate gyro feedback having a range of ten preset gains in each axis available for pilot selection during flight [ref. 24]. The fixed-gain system design was consistent with systems conventionally deployed on research aircraft at the time, and as such, pilots were familiar with the process of adjusting SAS gains during flight to maintain acceptable handling qualities. Until the ventral fin removal in 1963, the SAS was required for entry from most flight conditions due to an unstable lateral-directional ("dutch roll") mode exhibited by the X-15 at high Mach numbers and moderate α [ref. 26]. The SAS stabilized the unstable airframe in this flight regime to allow the pilot to safely complete the entry. Exoatmospheric stabilization was provided by manual inputs on the left-hand controller, or a rate-damping reaction augmentation system (RAS). The RAS used one-half (one string) of the reaction control authority in each axis [ref. 27] to damp body rates during the ballistic coast.

X-15-3 used a substantially more advanced experimental flight control system, the MH-96 [ref. 28]. The MH-96 was referred to as a "self-adaptive" flight control system. The MH-96 AFCS provided better reliability and fail-safety than the basic SAS through the use of a dual-redundant architecture with extensive internal failure monitoring. A principal function of the MH-96 was to enable automatic blending of the reaction controls and aerosurfaces during the atmospheric exit and entry transition phases. For this reason, X-15-3 was preferred for extended high-altitude trajectories due to the improvement in controllability, decreased pilot workload, and reduced RCS propellant expenditures [ref. 5].

The MH-96 aerodynamic control function was based upon a sophisticated adaptive approach that maintained a small-amplitude limit cycle in the aerodynamic control surface servoactuators via the modulation of the forward gain in the inner loop (Figure 6.5-2). In essence, the system was designed to bring the gain of the aerodynamic control to its maximum permissible value at all times, thus operating the system at its upper stability limit. Since the servoactuator limit cycle frequency was approximately invariant with respect to flight condition, the MH-96 gain changer electronics were able to maintain a nearly constant aircraft dynamic response over the entire flight envelope as the dynamic pressure and control surface effectiveness changed. Since these parameters were highly uncertain and not believed to be reliably measurable with the air data system, the adaptive approach provided an effective method of decreasing sensitivities to the time-varying aircraft parameter variations (Figure 6.5-3).
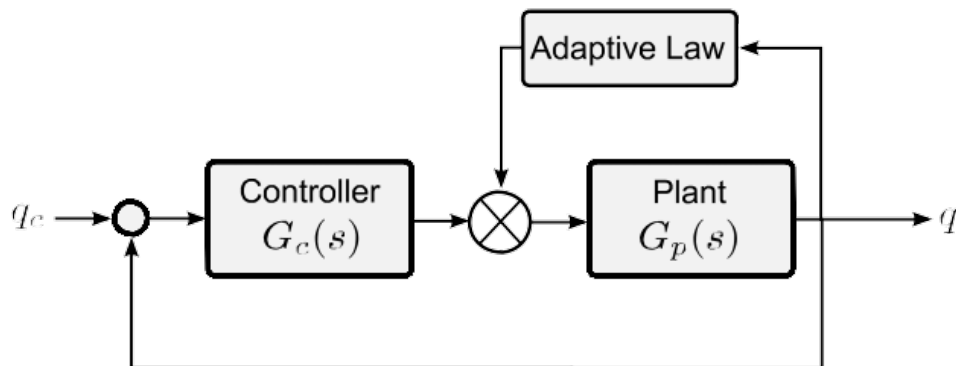
Figure 6.5-2. MH-96 Adaptive Concept
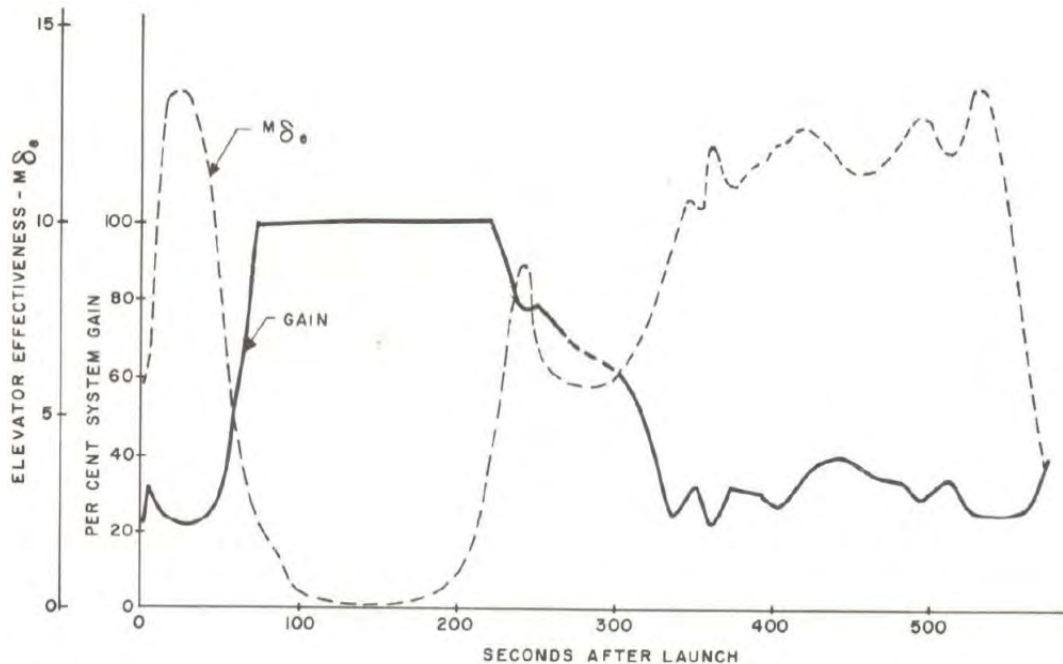
Figure 6.5-3. MH-96 Typical Gain Variation [ref. 2]

The MH-96 designers recognized that since the adaptive gain was inversely proportional to the control surface effectiveness, the adaptive gain could be used to determine the necessity of supplemental reaction control. To that effect, the MH-96 incorporated an attitude-rate RCS phase plane controller[4] with an "R/C AUTO" mode that automatically engaged and disengaged the RCS based upon the value of the sum of the adaptive gains in all three axes. RCS was enabled when the adaptive gains reached 90 percent of their maximum sum, and RCS was disengaged at 75 percent of the maximum sum[5] [ref. 29]. RCS control with the MH-96 was provided through the right-hand control inceptor used for aerodynamic surfaces, such that the pilot was not required to transition to the left stick during atmospheric exit. Manual RCS engage/disengage for the MH-96 and the left-hand inceptor was provided in addition to the "R/C AUTO" mode, but manual control was seldom needed during high-altitude flights with the MH-96.

---

[4] The MH-96 RCS actuators were solenoid valves, providing on-off control authority in contrast to the proportional control authority available on the left hand manual controller. The designers of the left-hand controller implemented proportional control when exoatmospheric piloting technique was in its infancy, and it was later recognized that pilots exclusively used the left-hand control in an on-off pulsed mode.

[5] The reported values vary. These are taken from the contractor final report in the post acceptance-test configuration [ref. 29].

Detection of the desired limit cycle to adjust the gain relied upon a filtering operation, or frequency-domain discrimination (the MH-96 gain modulation element was configured to respond to changes only in a narrow portion of the frequency spectrum of the sensed control signal, which was taken at the output of the servocylinder). The assumption was that only the limit cycle activity would be present in this narrow frequency range and, thus, would be isolated from other signals below (i.e., rigid-body control motions) or above (i.e., structural flexibility) this band. A more extensive discussion of the MH-96 AFCS design and operation appears in Appendix A.

6.6   Emergency Egress System

Cockpit egress was enabled by a rocket-propelled ejection seat that was developed specifically in support of the X-15 aircraft. The seat was a necessarily complicated, but functional design that included a deployable stabilization system to ensure the seat would not tumble after separation from the aircraft. The canopy was jettisoned during the ejection sequence using a separate pyrotechnic system, or it could be actuated manually.

The ejection seat was certified for operation to approximately Mach 4 and 120,000 feet altitude. While it was qualified to a limited extent using rocket sled tests, it was never demonstrated in conditions of high Mach number or high dynamic pressure. In the event of a high-altitude or high-Mach malfunction, pilots planned to stay with the aircraft as long as possible or until flight conditions allowed ejection [ref. 4]. The ejection system was never used during the X-15 program, although the canopy jettison mechanism was actuated by the pilot during the November 1962 landing accident.

6.7   Pilot Interface

The X-15 cockpit layout was relatively conventional for aircraft of the era, with the exception of having three control inceptors and vertical-tape displays for several instruments. Panel changes were frequent throughout the program. Panel modifications were incorporated, to some extent, into the simulator using interchangeable modules such that simulated missions could be flown using a panel similar to that in the aircraft [ref. 4]. While the X-15-3 originally had a cockpit layout nearly identical to the other two aircraft, an updated panel was installed in the fall of 1965, primarily to include instrumentation for the experimental boost and entry guidance systems (see Figures 6.7-1 and 6.7-2) [ref. 4].

Figure 6.7-1. X-15-3 Original Panel (1960–1965)
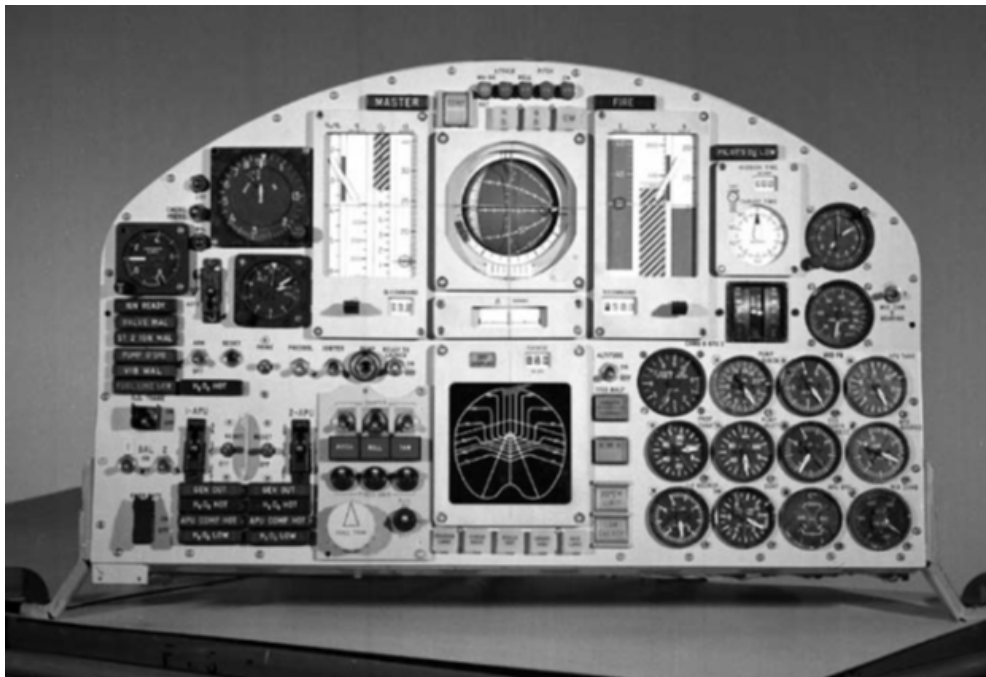
Figure 6.7-2. X-15-3 Vertical Tape Panel (1965+)

6.7.1   Control Inceptors

A conventional center stick directly actuated the control surface servocylinders and was mechanically connected to a right-hand side stick controller. The right-hand controller provided hydraulically boosted inputs to the center stick, such that the center stick tracked the side stick and vice-versa. The side stick was intended for high-G operation. In addition, the RCS manual control inceptor was positioned on the pilot's left side. This mechanical stick was directly connected to metering valves that drove the RCS jets.

In normal operation with the MH-96, the right-hand stick was used to provide rate commands to the autopilot. The left-hand stick, as a mechanical override, was not used without first disabling the automatic system [ref. 2]. The autopilot was responsible for responding to the rate commands using an automatically blended combination of the aerosurfaces and the RCS jets.

The left-hand manual controller drove both RCS jet strings in parallel, while the automatic system commanded only a single string. In this arrangement, the pilot had double the control authority of the automatic system, such that commands issued by the automatic system could be force-overridden by the pilot. This was not without consequence, in that opposing a rate damping command from the automatic system would expend three times the RCS propellant per unit time while the automatic and manual jets fired simultaneously.

6.7.2   Flight Instruments

The primary instruments available to the pilot for deducing the aircraft state included the ADI "ball," a set of attitude deviation needles with selectable reference, a β indicator, a selectable heading/roll rate indicator, and a set of navigated state outputs (e.g., altitude, altitude rate, and velocity). Dynamic pressure and normal acceleration were displayed primarily for use during the entry and pullout maneuver.

The instrument configuration and operation and the pilot interface was primarily driven by engineering need and functionality, and lacked a formal approach to human-machine integration. This is evidenced by the exceptionally complicated procedures associated with subsystem status, enable, disable, and reset functionality. Several instruments had multiple modes, one of which was of critical importance during the accident.

A summary of the instrumentation that was intended to be functional and presented to the pilot on Flight 3-65 is summarized in Table 6.7-1. An attempt has been made to detail each instrument's functional status during Flight 3-65.

***Table 6.7-1. Sources of Aircraft Dynamic State Information Available to Pilot,
Flight 3-65 Configuration***

Display	Data	Source	Limitations	Malfunctioned?
ADI	Aircraft inertial roll, pitch, and heading (ϕ, θ, ψ)	IFDS IMU	None applicable	No
Attitude indicator deviation needle (vertical)	β or roll error (ϕ_e), depending on PAI mode	Ball nose flow direction sensor or IFDS computer (depending on computed α/β mode); IFDS IMU (in PAI mode)	α/β from ball nose inaccurate due to RCS jet interaction below 50 psf	Yes
Attitude indicator deviation needle (horizontal)	α or pitch error (θ_e), depending on PAI mode	Same as above	Same as above	Yes
Sideslip indicator	β	Ball nose flow direction sensor or IFDS computer (depending on computed α/β mode)	Same as above	Yes
Precision heading indicator	Heading error (ψ_e), roll rate ($\dot{\phi}$) depending on roll rate mode	IFDS IMU	None applicable	No
Dynamic pressure vertical tape	Dynamic pressure ($\bar{q}$)	Ball nose	Accuracy degraded below Mach 2.5	No
Velocity vertical tape	Earth-relative velocity magnitude (V)	IFDS computer	Accuracy degraded after ~300 sec due to navigation error	Yes
Altitude vertical tape	Inertial altitude with respect to reference (h)	IFDS computer	Same as above	Yes
Altitude rate vertical tape	Inertial altitude rate ($\dot{h}$)	IFDS computer	Same as above	Yes
Normal acceleration vertical tape	Normal acceleration N_z (g)	Self-contained	None applicable	No

In normal operation, the X-15 pilot's ADI in the center of the control panel (Figure 6.7-3) was a standard freely rotating sphere called the "8-ball." The sphere was bisected into white and black areas representing sky and earth, respectively. The ADI was a critical instrument because the

typical X-15 ballistic flight profile prevented pilots from seeing Earth's horizon until reentry and the degree of precision flying required by the mission demanded constant reference to flight instruments until landing. Moreover, the pilot was dependent on the ADI to perform the experimental maneuvers with the required precision. Normally, the needles labeled "8a" and "8b" in Figure 6.7-3 indicated α error from preset and β error from zero, respectively. Needle "8c" displayed error from a ground preset of the pitch attitude desired during climb. Needle "8d" indicated error from a ground preset heading.
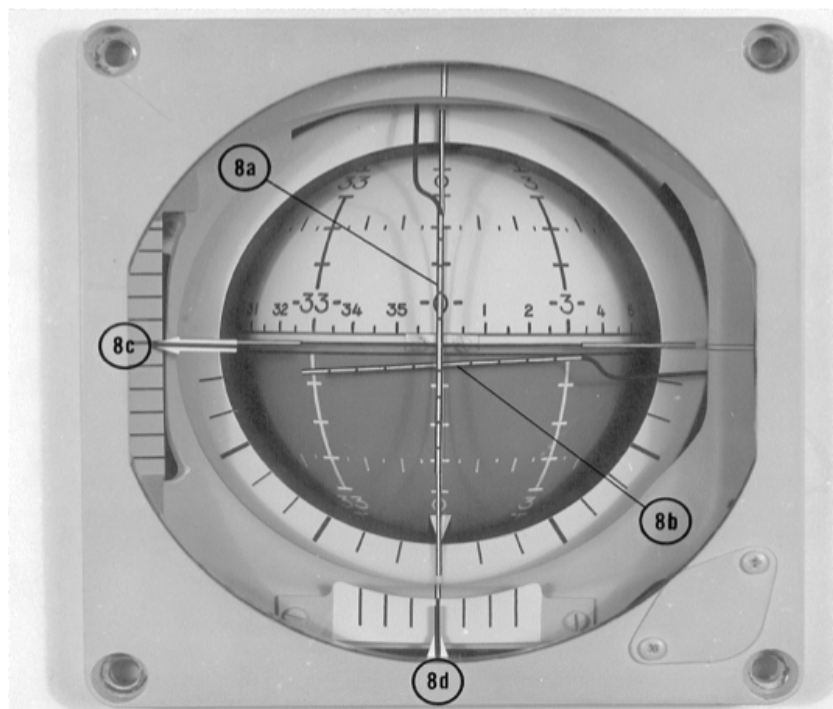
Figure 6.7-3. X-15-3 Attitude Director Indicator

However, the ADI in the X-15-3 aircraft was modified to an alternate display configuration, called the PAI, which was needed to perform scheduled experiments with the desired precision. Switches on the display panel upper right section controlled the functions of the horizontal and vertical needles independently (in the PAI mode, they indicated pitch- and roll-attitude errors, respectively, rather than pitch and yaw). This was a major design departure for a performance instrument considered critical to maintaining controlled flight. This design was incorporated because the X-15 instrument panel had limited area available.

An additional complexity of the ADI in either of its modes was that the standard ball nose air data system, which provided a measurement of α and β, was not reliable at dynamic pressures less than about 50 psf. When the pilot received the displayed information that the dynamic pressure was less than 50 psf, he was expected to use a switch to change the source of α and β data for the ADI displays from the ball nose to an inertially computed source.

7.0   Accident Detail

Flight 3-65 on November 15, 1967, was planned as an altitude flight. The pilot was conducting his seventh X-15 flight and his third flight in X-15-3. The flight was attempted 2 weeks earlier on October 31, 1967, but was aborted prior to launch due to a propulsion system issue.

The two flights immediately preceding Flight 3-65 were high-altitude flights and were made with the aircraft in nearly the same configuration. The only configuration exceptions were that, for purposes of performing additional aerothermal and aerodynamic experiments on Flight 3-65, a panel of ablative material was added to the left-hand upper speed brake to test the adhesive and insulating properties of a material proposed for use on the Saturn launch vehicle, and a traversing probe experiment was added to the starboard wing pod.[6]

7.1   Flight Plan

The flight plan for this altitude flight was similar to prior altitude flights. X-15-3 was to launch from Delamar Dry Lake, Nevada, at an altitude of 45,000 feet and depart southwest toward NASA FRC on a heading of 216 degrees magnetic (232 degrees true). There were eight primary science objectives, including boost guidance evaluation, solar spectrum and plume measurement experiments, the traversing probe experiment, micrometeorite collection, ablative materials testing, and several instrumentation tests. Orienting the aircraft during the ballistic coast involved use of a PAI mode of the ADI display to perform a tracking task at or near peak altitude such that the solar spectrum experiment located in the aft experiment compartment could be oriented toward the sun. The flight plan called for a maximum velocity of 5,100 fps, a maximum altitude of 250,000 feet, and a maximum entry dynamic pressure of approximately 820 psf. Emergency procedures and landing sites were established for major subsystem failures, including premature engine shutdown.

7.2   Timeline

The pilot entered the cockpit at approximately 08:15 Pacific Standard Time (PST), and the NB-52 carrier aircraft departed Edwards Air Force Base for the launch lake at 09:12 PST. The carrier aircraft was enroute approximately 1 hour and 15 minutes before making the final turn to align with the launch azimuth. All captive-carry systems checkout procedures were normal, except for a peroxide leak from a yaw RCS jet, which was determined to be of no consequence prior to launch. Most X-15 instrumentation and systems, including the traverse probe experiment, were activated prior to launch. The traverse probe experiment was powered on at 10:27:20 PST with the flight data recorders.

---

[6] Wing pods were not part of the original X-15 design, but had been aerodynamically qualified for use and were safely demonstrated on several flights prior to Flight 3-65 and on the X-15-1 and X-15-3 airframes.

Launch from the NB-52 took place at 10:30:07 PST with all systems operating normally. Ignition occurred at 10:30:08 PST (mission elapsed time (MET) +0 seconds)[7]. During the final 40 seconds of the power-on phase, a gradual β to about 5 degrees nose left was noticed by ground control. This deviation was considered normal and was attributed to engine misalignment.[8]

Radio communications throughout the flight were reported to be poor, but this was not considered unusual during high-altitude missions [ref. 3]. However, in this case communications with the pilot were intermittent throughout the entirety of the powered flight phase and did not become intelligible until after the end of the powered flight phase.

At 10:31:28 PST (MET + 80 seconds) just prior to engine shutdown, which occurred at 10:31:30 PST (MET + 82 seconds) and at about 140,000 feet altitude, the IFDS computer and instrument malfunction lights illuminated, indicating an IFDS malfunction. Eight seconds later, the pilot attempted to reset the system, but malfunction light stayed on. The IFDS continued to malfunction, and the warning light could not be reset.

At 10:31:34 PST (MET +86 seconds) and about 154,000 feet altitude, the pilot received ground control instruction to switch the ADI to the PAI mode. Due to poor radio communication conditions, this message was relayed via the NB-52 crew. The pilot had switched the ADI into PAI mode at 10:31:33 PST (MET + 85 seconds) in accordance with the flight plan, even though that mode was not required until the precision attitude-tracking task later in the flight.

At 10:31:42 PST (MET + 94 seconds) ground control called for the wing-rock maneuver, which the pilot had initiated at 10:31:37 PST (MET +89 seconds). At 10:31:58 PST (MET + 110 seconds), the pilot reported the computer and instrument malfunction lights were on. Ground control acknowledged the pilot's report.

The wing-rock maneuver was completed at 10:32:20 PST (MET + 132 seconds), at which time the aircraft had started a slow yaw drift to the right.

Although ground control had acknowledged that the IFDS computer was malfunctioning, at 10:32:09 PST (MET + 121 seconds) and about 220,000 feet altitude, the pilot was instructed to perform the computed α/β-check maneuver using the display of IFDS computed α and β when the altitude reached 230,000 feet. The pilot performed this maneuver immediately following completion of the wing-rock maneuver at 10:32:20 PST (MET + 132 seconds). During the maneuver, the RCS did not respond normally to pilot inputs. The pilot delayed depressing the computed α/β switch for several seconds, possibly due to his attention to the control malfunction. The pilot selected IFDS α/β at 10:32:23 PST (MET + 135 seconds). At this time, the aircraft was

---

[7] For clarity, the present report adopts the convention that MET + 0 seconds coincides with ignition. The AIB report uses range clock time only.

[8] The ventral fin had been designed in part to reduce β due to thrust misalignment, but the program elected to fly high-altitude flights without the ventral fin after fall of 1962, which probably increased the "expected" power-on β.

sideslipping approximately 6 to 8 degrees nose right, as displayed by the precision heading and β indicators. The aircraft roll attitude was nearly wings level and the ADI vertical wand displaying roll in PAI mode did not indicate any significant error.

By 10:32:25 PST (MET + 137 seconds), the negative side β slip deviation had increased to off-scale nose right as displayed by the cockpit precision heading and β indicators. At this time, lacking a control room indication of heading information, ground controllers were not aware of the heading error.

Immediately after selecting IFDS α/β, the MH-96 AFCS disengaged automatically at 10:32:26 PST (MET + 138 seconds), illuminating a caution light. The pilot recognized that the light was on and immediately reset the MH-96 while concurrently reporting to ground control that the pitch and roll stability augmentation channels had disconnected. The MH-96 was re-engaged by the pilot at 10:32:31 PST (MET + 143 seconds).

At approximately 10:32:50 PST (MET + 162 seconds), the pilot initiated the Precision Attitude Tracking Task in accordance with instructions from ground control. At this time, the β angle had increased to 20 degrees. The RCS momentarily resumed normal operation, arresting the positive yaw rate. However, due to a lack of normal response from the AFCS right-hand reaction control inceptor, at 10:33:05 PST (MET + 177 seconds) the pilot elected to use the left-hand manual control inceptor. The pilot did not disable the AFCS, although normal procedures for transition to manual control would have required this action. By the time the pilot began to use the manual control inceptor, the aircraft had rolled left through zero bank angle and the precision roll indicator needle called for the aircraft to be rolled to the right. However, the pilot applied manual right-yaw reaction control, further increasing the deviation from the planned heading.

At 10:33:14 PST (MET + 186 seconds) and about 258,000 feet altitude, ground control instructed the pilot to check the status of the pitch and roll dampers. The pilot reset them manually at 10:33:21 PST (MET + 193 seconds).

The aircraft entered a spin at approximately 10:33:30 PST (MET + 202 seconds) at an altitude of 250,000 feet and a velocity of 5,000 fps. At 10:33:39 PST (MET + 211 seconds) and about 240,000 feet altitude, the pilot reported that the aircraft control seemed "squirrelly." At 10:34:01 PST (MET + 233 seconds), the pilot transmitted, "I'm in a spin." At that time, the aircraft had reached peak altitude and was in a descent through 210,000 feet. The aircraft attitude was approximately 40 degrees above the horizon and was approximately 90 degrees right of the planned heading with a roll rate of 20 degrees per second. The aircraft had completed one yaw revolution. The dynamic pressure in this flight condition was increasing through approximately 1.5 psf. At this time, reaction controls were still required. The pilot reported the spin a second time at 10:34:16 PST (MET + 248 seconds).

The aircraft continued uncontrolled motion until about 10:34:34 PST (MET + 266 seconds), where at an altitude of approximately 130,000 feet, the spin was arrested by a combination of automatic and manual reaction controls, aerodynamic controls, and inherent aerodynamic

stability. At this point, the aircraft had a velocity of about 4,700 fps and was subject to a dynamic pressure of about 200 psf.

At about 10:34:37 PST (MET + 269 seconds), within seconds after the aircraft came out of the spin and went into an inverted dive, the MH-96 AFCS entered into a divergent limit-cycle oscillation in the pitch axis with the stabilators moving at their maximum rate of about 26 degrees per second. As dynamic pressure increased during rapid descent, the horizontal stabilizer motions produced rapidly increasing accelerations that exceeded structural limits. By-products of the MH-96 AFCS limit-cycle instability in pitch were rolling and yawing oscillations that produced excessive structural loads.

At 10:34:54 PST (MET + 286 seconds) at an altitude of 62,000 feet and a dynamic pressure exceeding 1,300 psf, a catastrophic buckling of the fuselage occurred and the aircraft disintegrated into several large fragments. The pilot did not successfully eject and was killed during the breakup or upon ground impact.

7.3   Data Reconstruction

Reconstructed flight data depicting key events with respect to the aircraft attitude angles are shown in Figure 7.3.1. These data were derived from filtered measurements of the IMU resolver angles recovered from the original stripchart recordings. The correctness of the IMU angle data was verified by the post-accident investigation team via correlation of the estimated attitude with a known solar angle in recovered film footage from onboard cameras [ref. 3]. The remaining trajectory data appear in Appendix B.

In Figure 7.3-1, MET is referenced to ignition, which occurred at 10:30:08 PST. The onset of spin entry at approximately 10:33:30 PST (MET + 202 seconds) was based on the rapid increase in yaw rate and the observation of the first traversal of the sun across the instrument panel as seen from the cockpit camera. Note that the aircraft was tumbling after approximately MET + 215 seconds, and the attitude resolver angles wrap through 360 degrees, but are masked by noise filtering.

Based on the assumption the pilot recognized the spin entry about 31 seconds prior to reporting it (when the sun traversed the instrument panel), just over 1 minute elapsed during the pilot's attempts to regain control until the aircraft was destroyed.
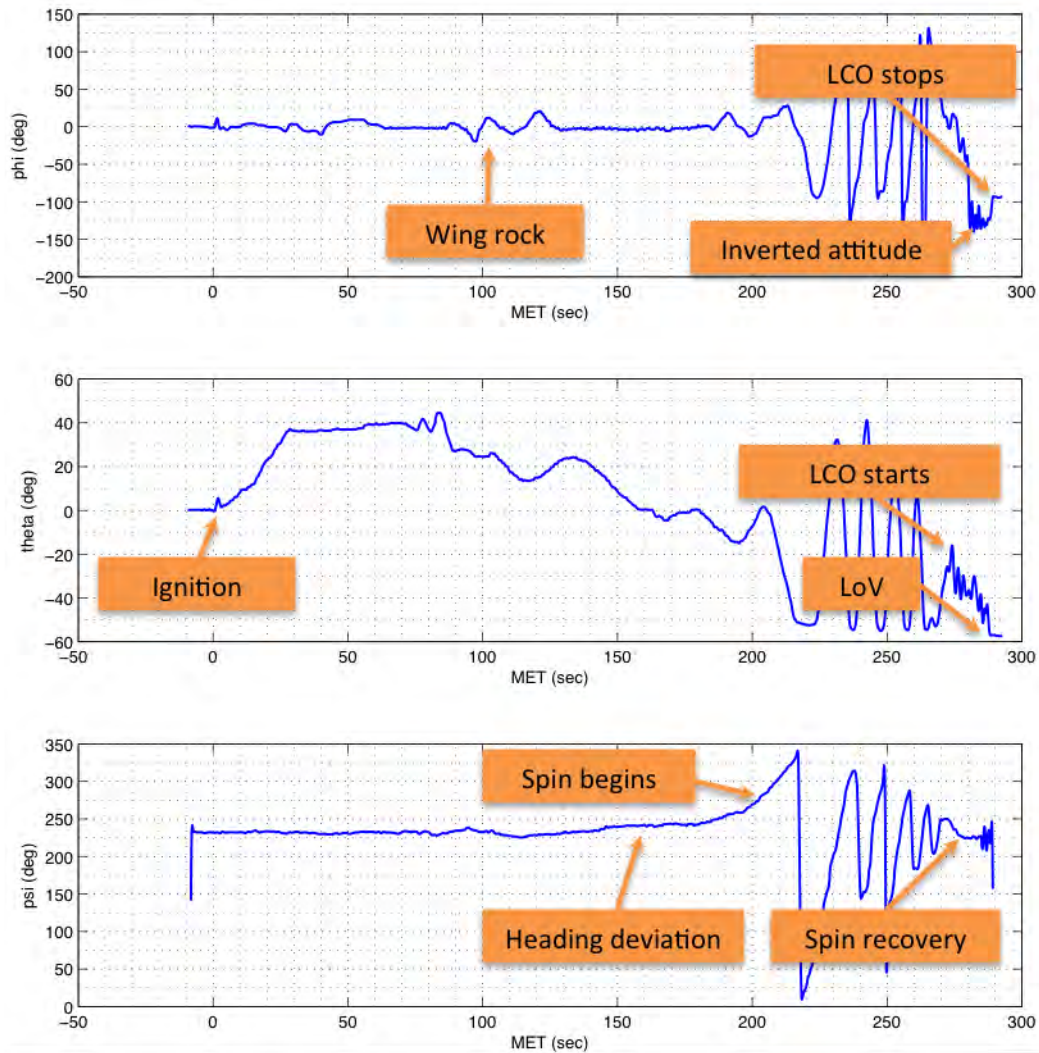
Figure 7.3-1. X-15 3-65 Reconstructed Flight Data (attitude angles[9])

8.0 Failure Analysis

In the following subsections, analyses of individual subsystem failures and their effects will be detailed. These include the failure of the traverse probe experiment; the subsequent instrumentation, RCS control, and display anomalies; and the development of the MH-96 large-amplitude limit cycle. In Section 9.0, an analysis of the human factors related to the accident

---

[9] Although not indicated in the original flight data, based on [ref. 11] it is assumed the Euler angles are referenced to a geodetic north, east, down (NED) frame centered at the landing site. The Euler sequence is unknown, but was probably 3-2-1.

will be detailed, with a focus on piloting performance and the role of ground control in the incident.

8.1   Traverse Probe Experiment Failure

The traverse probe contained in the starboard wing pod consisted of a servo-controlled pressure boom whose design was such that it would oscillate across the bow shock boundary, providing a measurement of the shock location. The traverse probe relied on power from the aircraft and was interfaced to the primary 115V (volt) 400-Hz (Hertz) alternating current (AC) power bus supplied from the aircraft APU generators. The traverse probe experiment had been flown on two prior missions in 1963, although neither achieved an exceptionally high altitude [ref. 4]. Flights 1-35-56 and 1-36-57 on the X-15-1 airframe reached maximum altitudes of 124,200 and 111,800 feet, respectively. No anomalies related to the traversing probe were noted on these flights.

Post-flight tests of the reconstructed traversing probe hardware concluded that below pressures corresponding to approximately 90,000 feet pressure altitude, a starting capacitor associated with the traverse probe drive motor would first develop a corona discharge and then exhibit arcing to ground across an approximately 0.25-inch gap between the capacitor terminal and the experiment chassis. Continued testing revealed this behavior would persist until power supply line fuses, rated at 2 amps, interrupted the power to the traverse probe motor. This interruption is consistent with the cessation of the electrical disturbance prior to the pilot and aircraft loss during Flight 3-65, and it was verified the flight fuses recovered from the wreckage exhibited characteristics consistent with the fuse burn-through reproduced on the ground [ref. 3].

Dielectric breakdown in low-pressure gases is a known phenomenon in high-voltage systems [refs. 30–32]. Dielectric breakdown phenomena obey the semi-empirical Paschen's Law, which describes the minimum breakdown potential (in V) associated with a parallel plate electrode configuration as a function of the product of pressure and gap distance (*pd*). The breakdown voltage approaches a minimum at a specific value of the pressure-gap product and increases elsewhere (see Figure 8.1-1, reproduced from data appearing in reference 32).

Paschen's Law implies, for a fixed gap distance and potential, the likelihood of breakdown increases until reaching a maximum at a specific absolute dielectric pressure and then decreases as the dielectric pressure approaches zero. The result is counterintuitive, but is driven by the physics of the underlying electron transport phenomena and ionization processes. The shape of the Paschen curve for a given dielectric depends on the gas composition and its temperature. Breakdown may be influenced by electrode composition and contaminants, and particularly in space environments, by electrons liberated by incident radiation.
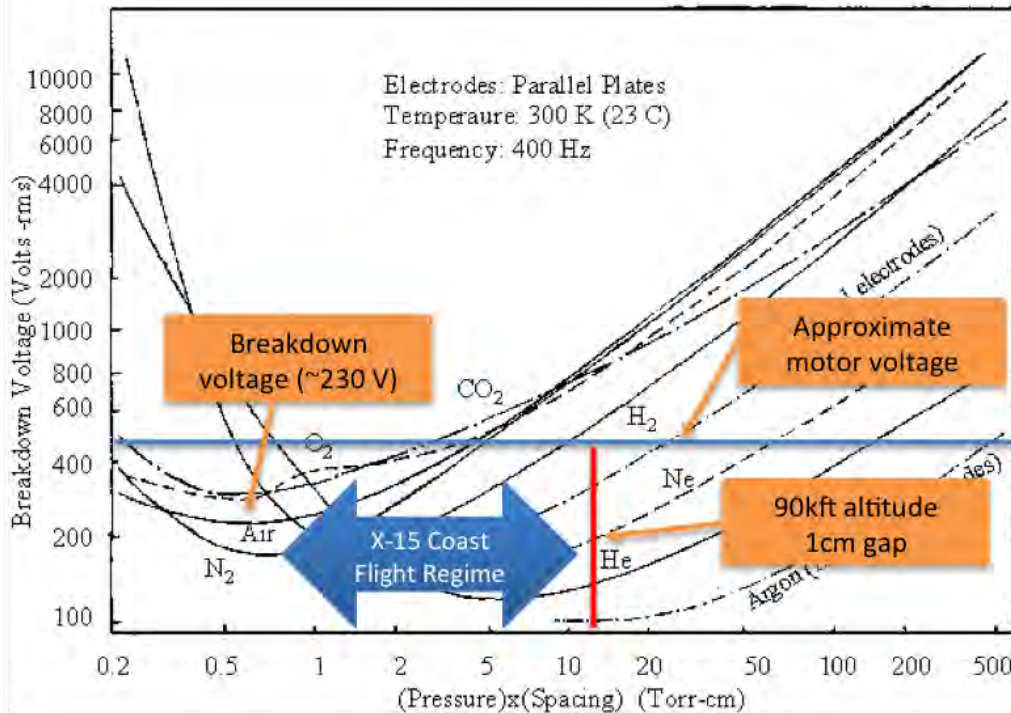
Figure 8.1-1. Paschen Curve for 400 Hz Potential at 300 degrees Kelvin [ref. 32]

Even at the critical *pd* value, quiescent breakdown in air generally will not occur below 300V. However, deviations from the basic Paschen law result from various factors, including the presence of nonuniform or oscillating electric fields (e.g., conductors with sharp radii and AC potentials, respectively). In the latter case, 400 Hz AC potentials as were used in the X-15 AC power bus reduce the threshold to about 230V. Unknown to the traverse probe experiment developers, the commercial-off-the-shelf (COTS) AC motor selected from existing inventory contained a transformer circuit that multiplied the 115V input by a factor of about 4, yielding a peak potential in the experiment exceeding 630V. Under reduced-pressure conditions, arcing was practically guaranteed across uninsulated gaps of modest spacing. As the design was not thoroughly reviewed for environmental compatibility or tested in simulated altitude conditions prior to installation on the aircraft, the breakdown phenomena was first seen in flight. The investigating board theorized that during the relatively short exposure to the high-altitude environment on the previous two flights, arcing may have occurred, but could have gone undetected as no particularly sensitive electronics were installed on the other X-15 aircraft [ref. 3].

The effects of the traverse probe electrical disturbance during the accident flight were severe. Post-accident laboratory testing indicated that 30 μs transient spikes of at least 300V would appear on the aircraft power bus and would be transmitted to all common-ground electrical components. Systems that operated on 28V direct current (DC) power and/or had robust power

supply electronics (e.g., the IFDS IMU) were not substantially impacted. However, the majority of the electronic and electromechanical systems, including the servoactuators, MH-96 AFCS gain changer electronics, IFDS computer, and telemetry and voice transceivers, were affected.

8.2 IFDS Computer Failure

The IFDS installed on the X-15-1 and X-15-3 airframes consisted of a digital inertial computer and an analog stable platform (IMU) that was originally designed and environmentally qualified for the X-20 program. The digital component of the IFDS contained the mechanization of the navigation equations and was used to accumulate (integrate) velocity data from the stable platform and transform this information into a coordinate frame suitable for use by the pilot and the boost guidance algorithm. The principal IFDS outputs were the altitude, altitude rate, and Earth-relative velocity magnitude. In addition, body-relative velocity vectors were used to establish estimates of α and β.

By 1960s-era accuracy standards, the IFDS IMU was a coarse aviation-grade instrument with a gyro bias in the range of 3.0 deg/hr, and an acceleration sensitivity of approximately 10 μG. As such, it was shown to be useful only during the boost and ballistic phases of flight, after which accumulated errors tended to yield estimates of aircraft state too inaccurate for use in safety-critical ranging decisions. However, while range radar was relied upon for determining energy during and after entry, the use of IFDS for pilot situational awareness was common. During Flight 3-65, the accuracies of the computed α and β were being experimentally evaluated. Nevertheless, flight planning called for the IFDS to replace the air-data derived indications of these quantities on the pilot display panel at dynamic pressures below 50 psf.

At the onset of the Flight 3-65 electrical disturbance, the IFDS began a series of resets. In each case, transient upsets to the power supply induced as a result of the traverse probe breakdown phenomena caused the IFDS to temporarily halt integration of the navigation equations and resume shortly thereafter. This event occurred at least 61 times [ref. 3] during the less than 3 minutes of electrical disturbance. Due to the loss of integrated velocity during the halt period, a substantial error, on the order of 100,000 feet and 1,000 fps, accumulated in the IFDS estimates of the altitude and velocity. Importantly, the failure in the IFDS did not affect the ADI ball. Therefore, the pilot's indications of gross and fine (PAI) attitude were correct throughout the flight. The same telemetered indications of the aircraft attitude, derived from the IMU resolver angles, were independently used to drive the ADI ball servos [ref. 11] and were unaffected by the IFDS dropouts. This conclusion can be verified by comparing the sun and shadow angles in the cockpit with the position of the ADI ball, and by noting that the IFDS GROSS failure indicator was not illuminated in the cockpit film [ref. 3].

The principal effects of the IFDS failure were erroneous indications of altitude, altitude rate, total velocity, α, and β on the pilot displays. While the aircraft control was lost in part due to an unrecognized β deviation at a point in time that the IFDS was selected as a source of β information, and while the timeline reveals that the data was likely in error, the IFDS output was

off-scale and with the correct sign at the time the pilot selected it. Thus, the erroneous data from the IFDS do not appear to be a direct contributor to the vehicle loss of control. However, the deteriorating state of the IFDS displays, especially in that the altitude and velocity tapes were substantially different from the expected values, combined with repeated warnings from the IFDS error annunciator suggests that the pilot was suspect of any data originating from the IFDS. This may have contributed to a loss of spatial orientation, which is discussed in further detail in Section 9.0.

The susceptibility of the digital IFDS computer to power supply transients was a known problem, but regrettably, it had been considered benign and/or unlikely since it had apparently only occurred on X-15-1 and was suspected to have been due to a particularly high electrical load. As of July 1968, the problem on X-15-1 was still unresolved, but under investigation [ref. 11].

8.3   Servo Transient Anomaly

An anomaly highlighted in the 1968 NASA/Air Force AIB report was the presence of servo transients whose behavior could not be reconciled with any known cause [ref. 3]. Servo transients were considered a benign behavior, but due to the nature of the MH-96 AFCS, any uncommanded, rapid servo motion could be interpreted as an excessively high servo limit cycle, thus triggering a momentary drop in gain. The AIB reported the X-15 had operated for some time with the servo transient issue and the momentary gain reduction (on the order of 5 to 10 seconds) was often unnoticed by the pilot.

The X-15 servoactuator assembly was a two-stage hydraulic power-boosted design operated in series with direct pilot mechanical inputs to the aerodynamic surface power actuators [ref. 24]. The servocylinder torque motor and servocylinder feedback electronics had a relatively high electrical sensitivity to current transients [ref. 29]. Given the extent of the electrical anomaly caused by the traverse probe failure, the most plausible explanation for the excessive servo motion is that a known and poorly characterized sensitivity to electrical interference in the servo was exacerbated by the severe electrical noise.

Servo transients during Flight 3-65 had two distinct and equally problematic effects. First, the aforementioned coupling with the gain changer electronics caused the MH-96 to interpret the occasional servo motions as excessive servo limit cycles, and the MH-96 correctly responded by rapidly decreasing the gain to recover stability. In doing so, the hysteresis logic associated with the automatic RCS blending was activated, and the RCS was disengaged. The pilot was not notified of the disengagement.

Second, the MH-96, similar to the other X-15 SAS designs, included a failure monitor circuit on each servocylinder to protect for hardover failures. Hardover failures were considered credible anomalies and were protected for, when detected, by a complete disengage of the associated roll, pitch, or yaw axis [ref. 24]. Both systems used a simulated servocylinder model implemented using analog electronics. In the baseline SAS, the hardover detection circuit consisted of an

absolute travel error monitor that was triggered when the expected value of the servo position exceeded the measured value by more than 10 percent. In the MH-96, detection was triggered when the rate of the servo travel differed in sign from the expected rate. In the event of a "damper reset," two lights were illuminated on the panel to notify the pilot, and pilot action was required to re-engage the failed channels by returning the damper select switches to the "up" position.

To reduce the potential for supercritical operation in the event that the MH-96 was disengaged at a low dynamic pressure condition and re-engaged at a high dynamic pressure condition, the gain changer electronics were configured to reset the gain to minimum following any reset. Under normal conditions in exoatmospheric flight, the adaptive gain would return to maximum in 10 to 20 seconds. A reset would interrupt access to the RCS during that time.

During Flight 3-65, a servo monitor disengage, precipitated by a large servo transient, occurred simultaneously in the pitch and roll channels at 10:32:26 PST (MET + 138 seconds). This condition was immediately recognized and reset by the pilot in about 4 seconds. However, since the yaw channel was severely affected by the traverse probe electrical noise, the sum of adaptive gains did not return to a value sufficient to reactivate the RCS for nearly 20 seconds after the channels were reset [ref. 3]. A similar disengage manually triggered by the pilot occurred about 1 minute later when the pilot was asked by ground control to "check [his] dampers." This manual action interrupted access to the RCS.

8.4   Yaw Rate Gyro Channel Disconnect

In addition to the hardover monitor responsible for the pitch and roll axis disengage, each of two redundant channels of each axis in the MH-96 architecture included a rate hardover monitor on the flight control rate gyro. An ability to recover from a flight control rate gyro fault was a requirement of the MH-96 design, but a simultaneous failure of both gyros in a single axis was not considered credible. Thus, the architecture was designed so a single failure could be accommodated by disconnecting the failed gyro, in which case the total adaptive gain (i.e., the sum of both channels) would automatically increase to return the total system gain to a normal range [ref. 29]. Unlike the case of a servo failure detection, the adaptive channels were not disengaged.

The flight envelope provided to the MH-96 designers specified the range of angular rates in each axis would not exceed 20 degrees per second, and the gyro output amplifiers were designed to saturate at 30 degrees per second. As such, the hardover monitor threshold in pitch and yaw was empirically set to a value of approximately 22.5 degrees per second.[10] The roll channel used a differential trigger, but essentially operated the same way.

---

[10] The exact value of the threshold differs. This value is taken from the MH-96 engineering documentation, WADD-TR-60-651 Part VII, whereas the AIB report specifies 30 degrees per second, which was probably confused with the gyro saturation limit.

During Flight 3-65, the onset of a spin brought the true body yaw rate above the hardover-failure disconnect threshold simultaneously in both yaw channels, which were operating normally. As designed, both channels simultaneously disconnected, essentially opening the yaw damper loop and providing no yaw rate feedback from approximately 10 seconds after spin entry until 10:34:29 PST (MET + 261 seconds) when the disconnect circuits reset and re-enabled both channels. No indication of the open condition in the loop was provided to the pilot. Lacking any closed-loop feedback, the MH-96 total gain in yaw increased to maximum and remained there so that RCS control was available to the pilot so long as the pitch and yaw gains were near maximum. However, regardless of the RCS state, the pilot had transitioned to the left-hand stick and RCS yaw rate damping was unavailable due to the lack of rate gyro inputs. The primary effect of this failure was to exacerbate spin development with no rate damping augmentation.

8.5 MH-96 Large-Amplitude Limit Cycle

The AIB report provides little detail regarding the MH-96 LCO that contributed to the aircraft breakup. To isolate the most probable cause of the MH-96 instability, an extensive analysis was undertaken to gain insight into the exact mode(s) of failure (see Appendix A). The AIB report indicated the rate-limited power actuator was a contributor, and it appeared the large-amplitude LCO could be sustained in the event of rapidly increasing dynamic pressure, as was seen during the entry of Flight 3-65. However, a review of the trajectory data revealed the maximum dynamic pressure rate of change was less than seen on previous flights, and the MH-96 adaptive gain law provided sufficient response to maintain gains below supercritical operation in these conditions. Furthermore, it appears the presence of supercritical gains in the MH-96 would seldom lead to a loss of rigid-body stability, but rather to an excitation of the servo-limit cycle mode to a higher, but nondestructive amplitude.

The present analysis revealed the AFCS, coupled to the X-15-3 airframe at a fixed flight condition above approximately Mach 3.0, could exhibit two distinct oscillation modes. The first was dominated by the desired limit cycle associated with small-amplitude surface motion at the critical forward gain with no rigid body motion. The second was a divergent large-amplitude LCO[11] involving the rigid body, but not directly involving the adaptation dynamics. The presence of the divergent LCO appears to have been the result of a latent design oversight in a structural notch filter installed on the MH-96 configuration.

8.5.1 History

In May 1960, a severe high-frequency LCO in the baseline (fixed-gain) stability augmentation system was discovered during a X-15-2 flight, which involved a 12- to 13-Hz oscillation in a stabilator resonant mode at certain flight conditions [refs. 1, 6, 24, and 33].

---

[11] "Divergent" LCOs are oscillations that grow to sufficient amplitude to cause divergent (destructive) aircraft dynamics before reaching their theoretically limiting behavior.

	NASA Engineering and Safety Center Technical Assessment Report	Document #: NESC-RP-14-00957	Version: 1.0
	A Comprehensive Analysis of the X-15 Flight 3-65 Accident		Page #: 41 of 107

Title:

The NASA FRC maintained the fixed-gain SAS for X-15-1 and X-15-2, and underwent a redesign of the fixed-gain SAS filters to mitigate the high-frequency LCO. The FRC engineering personnel were aware of the nonlinear saturation and rate limiting characteristics of the power actuators, and incorporated these features in their design model when developing the filter modifications [ref. 34]. The modified filter was verified through hardware-in-the-loop simulation and installed on both fixed-gain SAS airframes, where flight tests confirmed the elimination of the high-frequency LCO. No further issues were seen on the fixed-gain system.

In late 1960, a basic model of the problematic structural mode was sent to the MH-96 contractor for evaluation. At the time, the contractor was in the late stages of preparing the MH-96 for flight qualification tests, which were scheduled to begin in the fall of 1961. The contractor reviewed the structural model and concluded that a notch filter would be needed in the rate damping loop to mitigate the issue. An appropriate filter was designed, fabricated, and incorporated into the MH-96 design [ref. 35].

The redesigned MH-96 was installed and tested at FRC in the Hardware in the Loop (HWIL) facility and in September 1961 was installed on the aircraft for ground testing.[12] During ground aircraft testing, an additional unstable inertial-servoelastic coupling effect appeared in the closed-loop dynamics. The designers were challenged by the appearance of an additional adverse structural-mode limit cycle caused by the notch filter due to the additional lag at higher frequency. Additional filter modifications were made, with a reduction in authority of the adaptive gains and the installation of a deadband, to ensure that the small-amplitude oscillation would not appear in flight [ref. 35].

Due to facilities problems and other practical limitations, the HWIL and ground testing was not extensive, and the modified MH-96 was moved forward to begin preparation for initial flight tests in only a few months. The first flight test was conducted on December 20, 1961. Notwithstanding a yaw channel oscillation at approximately 12 Hz caused by excessive gain in the lateral acceleration loop, the filter modifications proved successful in mitigating the risk of a high-frequency limit cycle caused by the stabilator dynamics.

However, while NASA FRC had used a nonlinear model of the servo and power actuator with more extensive HWIL simulation to verify the filter design, the contractor apparently did not have access to the same type of model data and used a simple first-order lag model with hysteresis only (Figure 8.5-1). As such, a latent design sensitivity was introduced into the inner loop of the MH-96 SAS that would allow the SAS rate loop to become unstable in the presence of actuator rate saturation.

---

[12] X-15-3 had been rebuilt following the catastrophic propulsion test failure.

Figure 8.5-1. Surface Actuator Models Used in Design [refs. 34 and 35]

8.5.2   Mode of Failure

The transition from the desirable small-amplitude LCO to the large-amplitude destructive LCO was an artifact of the rate-limited power actuator with its semi-integrating servo loop. A known effect of power actuator rate limits is the introduction of an amplitude-dependent equivalent phase lag in the inner loop, which plays an important role in the sensitivity to pilot-induced oscillations (PIO). As can be seen in Figure 8.5-2, the presence of rate limits severely degrades the equivalent nonlinear frequency response of the X-15 actuator. The severe landing PIO encountered on X-15 Flight 1-1-5 was an effect of the same rate-limited actuators, albeit in a different failure mode [ref. 36].

The adverse high-amplitude limit cycle behavior was not directly related to the AFCS adaptation dynamics, but to the SAS loop linear filter design, which differed from the linear filters used in the fixed-gain SAS on the other X-15 aircraft. Since the MH-96 required special loop shaping to attain the desired LCO conditions, the AFCS's high-order notch filter induced substantially more phase lag near the rigid body short period frequencies. The mechanism by which a destructive limit cycle could be introduced involved an abrupt maneuver at relatively high forward gain, where the power actuator would reach rate saturation while inducing large angular acceleration on the rigid body. If this event occurred at a flight condition where the rigid-body short period

damping was particularly low, as it did during Flight 3-65, then the rigid-body oscillation was divergent, even with fixed adaptive gains.
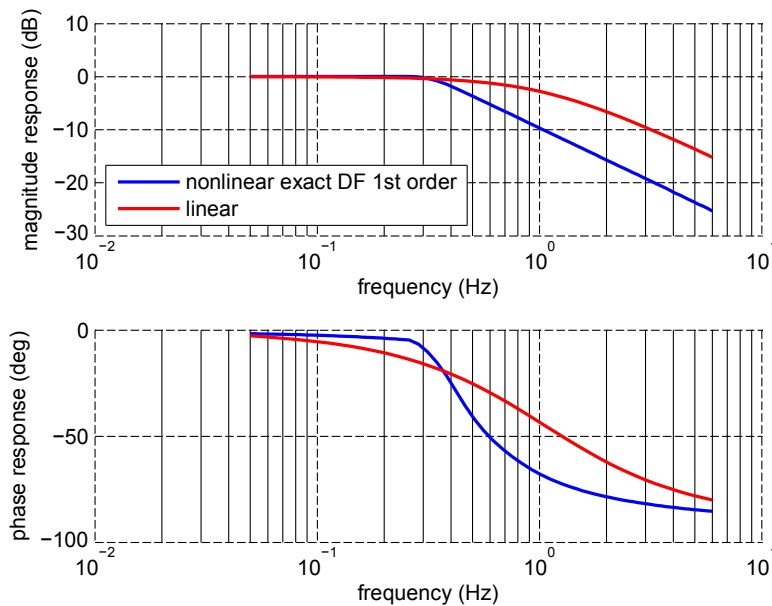
Figure 8.5-2. X-15 Power Actuator under Rate Saturation, 15-degree Amplitude

During entry, the X-15 bare airframe exhibited a short-period pitch mode of approximately 0.5 Hz with a damping ratio of less than 10 percent while at a flight condition between Mach 4.5 and 5.0 [ref. 37]. In an environment of increasing dynamic pressure, especially rapid entries, the system gains were often supercritical for a few seconds until the desired limit cycle was established and the MH-96 gain changer reduced the gain. This unfortunately meant that rapid inputs at these flight conditions were accompanied by large servo commands that could saturate the power actuators. This was especially true for combined pitch-roll maneuvers due to the shared stabilator authority. While the adaptation dynamics were not directly involved in the LCO phenomenon, the limiting circuitry associated with the MH-96 adaptive loop could be saturated by large DC signals [ref. 33]. If this occurred, then the gains would ramp to maximum in an effort to reestablish the desired high-frequency limit cycle. This behavior further amplified the large-amplitude limit cycle, leading to a loss of rigid-body control.

A comparison of the reconstructed rigid body limit cycle appears in Figure 8.5-3. Using fixed aerodynamic parameters consistent with the onset of the LCO at $M = 4.7$ and the entry dynamic pressure profile from reconstructed flight data, the LCO can be triggered by a large or abrupt control surface motion. This occurs during normal adaptation behavior that otherwise does not lead to adverse oscillations. The resultant motion is divergent and couples with the rigid body at a frequency of about 0.5 Hz.
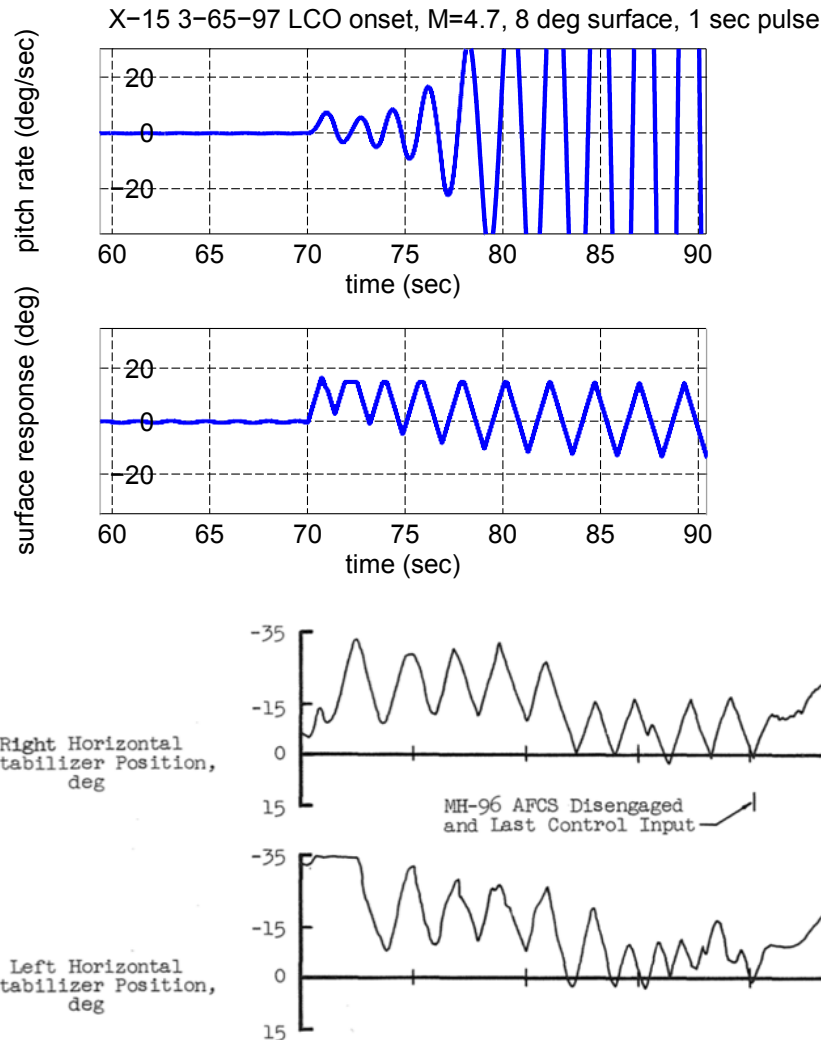
Figure 8.5-3. X-15 3-65 MH-96 Servo Actuator LCO (simulated) versus Flight Data

The presence of this adverse operation mode apparently went unnoticed until Flight 3-39 on January 13, 1965, when the LCO appeared during the flight boost phase [ref. 3]. It quickly attenuated due to decreasing dynamic pressure, which decoupled the rigid body from the loop. The MH-96 contractor conducted a study, which concluded that the adverse LCO could be avoided if such abrupt inputs in the pitch axis were avoided while dynamic pressure was rapidly increasing. This recommendation is consistent with the failure mode identified through the present analysis. Pilots and engineering staff were briefed of the possibility of such adverse behavior and cautioned regarding its effects [ref. 3]. The contractor report stated:

> *The MH-96 adaptive system can continue flying without modification if the following precautions are observed: avoid planning flights where large, rapid angle-of-attack changes might be encountered while simultaneously rolling the vehicle when at Mach numbers greater than 3.0; brief pilots on the potential consequences of abrupt control motions, especially when in the flight conditions described above. If the above precautions are considered too restrictive, the nonlinear stability (pitch limit cycle) of the MH-96 pitch axis can be improved through modification.*

Replication of this behavior in simulation is non-trivial, as it requires a high-fidelity model of the power actuator, servocylinder, servo feedback, valve dynamics, and associated nonlinearities. The semi-analytical methods used in Appendix A to predict the instability were known in the 1960s, but could not be exercised at the level of detail now available using rapid numerical simulations. However, there is some evidence suggesting this behavior had been encountered in HWIL simulation before it appeared in flight, as a brief report [ref. 38] contains plots of a large-amplitude roll oscillation that reappear in the 1971 report [ref. 33] commissioned by the AIB. Therein, an X-15 controls engineer remarks:

> *When a large...command is made, rate limiting occurs and causes [a] greatly deteriorated response...nonlinearities in system components cannot be ignored in high-gain control systems.*

It is reasonable to expect the X-15 flight control team, having had recent experience with a rate-limited PIO during the first piloted flight, could postulate the existence of a rate-limited large-amplitude LCO in the pitch axis. However, it seems this knowledge was not communicated to the program, or it was thought not to be a credible failure in flight, since according to the AIB it came as enough of a surprise in 1965 that a contract was issued to study its implications [ref. 3]. However, by the time of the accident, this behavior seems to have been known. A control room MH-96 monitor engineer remarks in a witness statement [ref. 3]:

> *...the limit cycle operation which occurred...is a rarely seen characteristic of this system which is undesirable and did prevent the pilot from having full...control capability.*

8.5.3   The Role of Adaptive Control

The investigation following the 3-65 accident concluded from simulation studies that the adverse LCO could have been avoided had the pilot disabled the MH-96 and reverted to fixed-gain operation prior to entry. However, the AIB noted the pilot would have been unfamiliar with the LCO since he had not experienced it in the simulator [ref. 3]. Although the existence of this failure mode was known, it may have been difficult to reproduce on the ground since the HWIL simulation facility was seldom operated at full flight hydraulic pressures [ref. 5].

It is unlikely that disabling the adaptive mechanism *per se* successfully recovered stability, but rather that the fixed-gain mode in X-15-3 reverted to the lowest acceptable gain, which was

below the threshold that would sustain rate limiting. While the adaptive mechanism exacerbated the problem by increasing the system sensitivity to large or spurious inputs, it is likely that an alternate filter design would not have been susceptible to this phenomenon. Pilots executing high-altitude reentries using the fixed-gain SAS typically did so with a pitch gain preset at 40 to 60 percent of the maximum gain in that axis [ref. 19]. Had the same structural filter been installed on the X-15 aircraft with the fixed-gain SAS, whose inner loop was functionally identical to the adaptive inner loop, the fixed gain controller may have exhibited the same unstable behavior at a higher dynamic pressure.

Following the accident, the AIB concluded that a detailed failure mode analysis was unnecessary, since the only example of the MH-96 system in a flight configuration had been destroyed [ref. 3]:

> *The destruction of the only X-15 airplane equipped with an adaptive control system makes detailed recommendations in this area unnecessary.*

The AIB recommended that a report be released summarizing the general experience with adaptive flight control technology within 90 days [ref. 3]. However, the report was released more than 3 years later in March 1971 [ref. 33]. While this brief summary mentioned the severity of the pitch-and-roll axis limit cycle instability and its relationship to the actuator rate limits, it did not adequately discuss the contributions of the AFCS to the Flight 3-65 accident:

> *An example of gain reduction caused by electrical noise is shown...in this particular instance, the performance of the AFCS became so poor that the pilot resorted to the use of the manual reaction control system, rather than continue to use the poorly performing AFCS blended reaction controls...*

> *...when these [pilot] commands were large or rapid, the effect on the gain changer was serious. In each flight incident, the gain changer was misled by the direct-current or low-frequency signals which were large enough to saturate the electrical limits, thus masking signals within the bandpass frequency range. The gain increased to values exceeding the critical gain, and the servoactuator loop became unstable...*

> *...saturation in one axis resulted in complete loss of control in the other axis. This problem occurred immediately following recovery from a high-altitude spin in the last flight of the X-15 airplane with the AFCS.*

The report refers the reader to an earlier document [ref. 6], which does not appear to have received widespread dissemination. The present authors conjecture that this critical lack of detail may have led to the commonly held misconceptions about the root causes of the Flight 3-65 failure.

It is regrettable that the role of the adaptation law in the development of the adverse limit cycle behavior has been largely misunderstood in the modern flight controls community and has been

incorrectly reported in the literature [refs. 7, 8, and 39]. In the cited examples, the X-15 airframe and controller models were used to simulate a loss of control, but excepting magnitude saturation, the nonlinear actuator was not modeled, and the destructive limit cycle oscillation shown did not involve rate limiting. In these models, the failure was induced by simulating an 80-percent asymmetry in stabilator control surface effectiveness (control surface damage), an event that is completely unrelated to the Flight 3-65 accident.

9.0   Human Factors

From a human factors perspective, for Flight 3-65 the design of the pilot interface, the interaction of the pilot with the aircraft and with ground control, and the conduct of the program at the time of the accident were important aspects of the event and are addressed in detail in this section.

9.1   Critical Events

Figure 9.1-1 illustrates the timeline of the major events leading to the loss of the pilot and the aircraft, and diagrams the sequence of key events during the 3 minutes following the initial traverse probe electrical disturbance. Note that the timeline in Figure 9.1-1 ends at about 10:34:17 PST (MET + 249 seconds), or about 37 seconds before breakup. The time history of the MH-96 AFCS gains is shown in Figure 9.1-2.

Beginning at 10:31:07 PST (MET + 59 seconds), the electrical disturbance caused erratic fluctuations in the automated gain control from maximum to minimum as seen in Figure 9.1-2, which caused the pilot's access to the RCS through the right side stick to be intermittent throughout the 2-minute, 46-second duration of the electrical disturbance.

At 10:31:00 PST (MET + 52 seconds), all three input gains to the aerodynamic controls were at their maximums so that the MH-96 had automatically enabled RCS inputs and the pilot's right side stick was operational at that point. Seven seconds later, the total gain of the three aerodynamic controls had decreased below 75 percent of its maximum, so access to the RCS was closed by the MH-96. From then on, the pilot's right side stick RCS control was intermittent because of the erratic fluctuations in the automated gain controls due to the continuing electrical disturbance. The pilot was unable to detect the intermittent RCS control for nearly 3 minutes. Cockpit indicators showed that the engagement of the pitch and roll dampers was also intermittent during the electrical disturbance.

At 10:31:58 PST (MET + 110 seconds), the pilot reported the IFDS computer- and the instrument-malfunction lights had come on and could not be reset. Ground control acknowledged the pilot's report.

At 10:32:09 PST (MET + 121 seconds), ground control instructed the pilot to perform the scheduled experiment of the computed α/β-check maneuver, which required the use of the display of IFDS computed α and β, even though the flight controller had acknowledged the pilot's prior reports that the IFDS computer was malfunctioning.

Figure 9.1-1. 3-65 Event Timeline

At 10:32:27 PST (MET + 138 seconds), the pilot reported that the pitch and roll dampers had tripped out.

Despite the indications of aircraft system malfunctions, ground control seemed unaware of the pilot's severe situation. At 10:33:01 PST (MET + 173 seconds), the flight controller told the pilot that he was looking "real good."

However, at 10:33:05 PST (MET + 177 seconds), the pilot apparently noticed for the first time the aircraft's lack of responsiveness due to the intermittent, and ultimately the deactivation of, access to the RCS through the right side stick and switched to direct control bypassing the AFCS using the left side stick. Normally, the procedure for switching to direct manual control would have involved deactivating the RCS "auto" mode or disabling the MH-96, but the pilot did not execute this step and continued to try to perform the precision attitude-tracking task.

At 10:33:25 PST (MET + 197 seconds), the flight controller again assured the pilot that he was "a little bit high," but "in real good shape."

However, 14 seconds later, at 10:33:39 PST (MET + 211 seconds) and about 240,000 feet, the pilot reported that the aircraft control seemed "squirrelly." Twenty-two seconds later at 10:34:01 PST (MET + 233 seconds), the pilot said, "I'm in a spin." Ground control did not acknowledge either of these transmissions. The pilot repeated, "I'm in a spin," at 10:34:16 PST (MET + 248 seconds). At 10:34:17 PST (MET + 249 seconds), the flight controller said, "Say again." At 10:34:17 PST (MET + 249 seconds), the aircraft was in descent at 184,000 feet with a velocity of 5,100 fps. The aircraft would begin to break apart 37 seconds later.

Figure 9.1-2. AFCS Gain Variation during Flight 3-65

9.2 Causal and Contributing Factors

As in most accidents, the destruction of the X-15-3 during Flight 3-65 was due to a confluence of latent and proximate factors. This review of the events from the human factors perspective identified latent, proximate causal, and contributing factors. The contributing factors were those that exacerbated the causal factors. Although unlikely, it is conceivable that if certain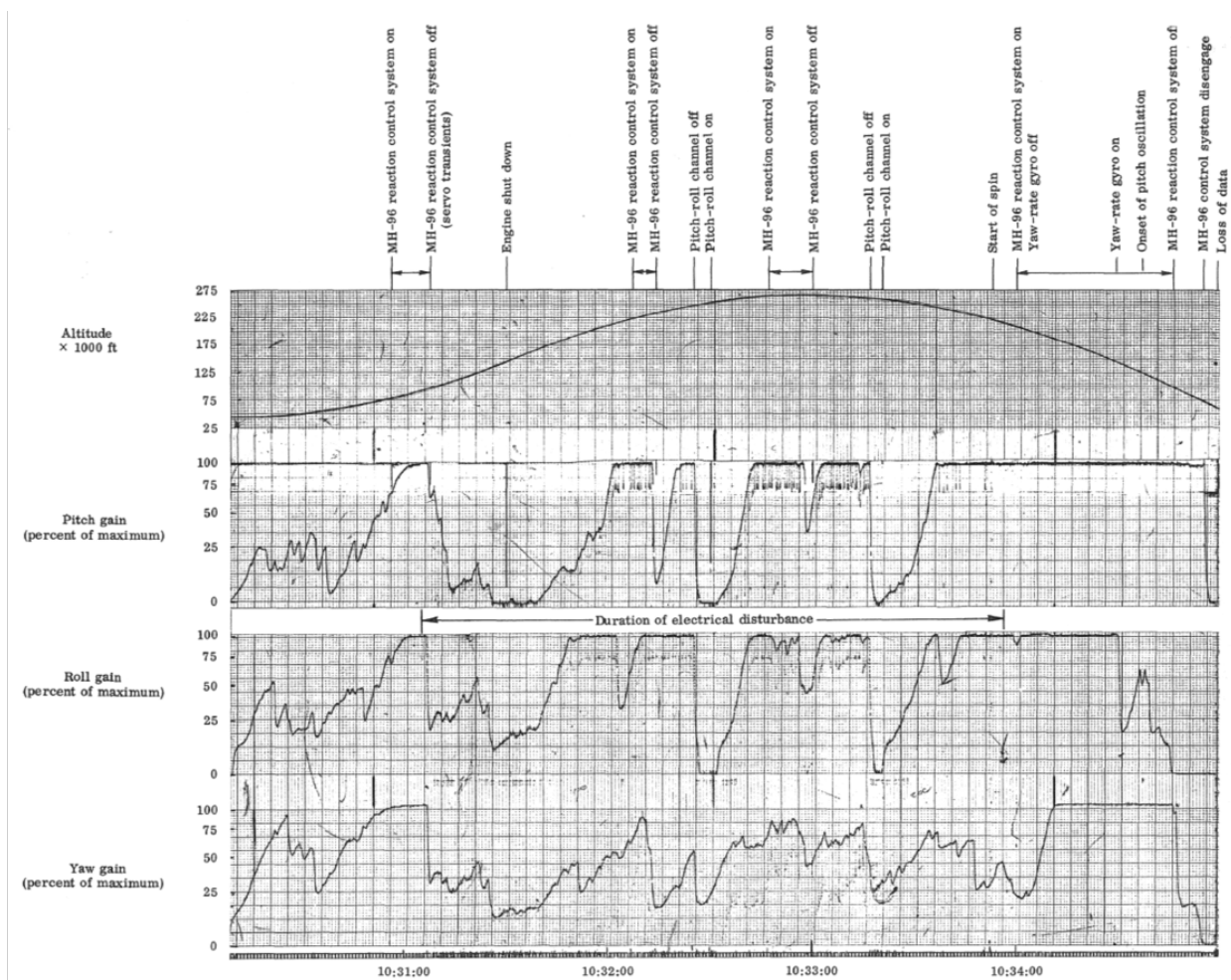 contributing factors had not been present, then the pilot might have been able to recover control of the aircraft and effect a safe landing.

9.2.1 Causal Factors

A latent causal factor in the Flight 3-65 accident was the installation of experimental equipment (i.e., the apparatus for the traversing-probe experiment) without adequate certification. The consequences of the traversing-probe motor arcing on Flight 3-65 show that the procedures for designing and testing X-15 experimental flight equipment were incomplete.

A proximate causal factor was the confluence of aircraft subsystem failures and of ground control to alert the pilot to the possibility of control problems and of erroneous data as soon as indications of malfunctions were observed. The AFCS design, the pilot's interface, and the ground control procedures contributed to the pilot's illusion that his aircraft was operating properly during almost 3 minutes when the electrical systems were malfunctioning. The pilot and ground control should have recognized that the inability to reset the IFDS computer and instrument malfunction lights was an indication of a major subsystem failure, but it seems the system (including the pilot and ground control) tended not to consider the IFDS to be critical. While there was an indicator of the failure of the IFDS computer on the pilot's display and while the MH-96 could detect and alert the pilot to numerous types of major component failures, there was no display to indicate that the MH-96 gain control was erratic. If the pilot had been alerted so that he could have changed to direct manual control and reverted to the fixed-gain mode of the MH-96 in a timely manner (e.g., when ground control observed indications of control problems during the wing-rock maneuver), then he may have been able to recover control. Therefore, the failure of the system to alert the pilot to the problem in the aircraft's control and displays was a causal factor in the accident.

The failure in the system design was that there were no provisions for alerting the pilot to the erratic behavior of the automated flight control system, or to the erroneous information on aircraft α, β, altitude, and altitude rate generated by the malfunctioning IFDS computer. Also, the intermittent aspect of the access through the AFCS to the RCS, which is an inherently on/off system, caused the pilot to assume that the system was operating properly for several minutes. As the AIB report [ref. 3] states, access to the automated RCS was "propitiously" operating during the few brief instants when the pilot moved the right side stick control as he performed the first two tasks (i.e., the wing-rock maneuver and the computed α/β-check maneuver) and as he initiated the precision attitude tracking task. The report states:

> *Since the MH-96 provides no visual indication to the pilot of reaction control system status, i.e., whether or not the system has been automatically selected, the pilot must rely on being able to detect rocket operation by sound, visual exhaust observation, or control response to determine if the reaction controls have been properly selected. Since no attitude-rocket firing occurred during the initial 11-second engage time of the MH-96 reaction controls on Flight 3-65, it would have been virtually impossible for the pilot to detect that the system had automatically engaged and then disengaged 11 seconds later.*

Consequently, with no visual display of the failure, there was little possibility the pilot would have recognized the intermittency of his control based solely on aircraft response.

Ground control was a contributor to this proximate causal factor because its primary principle was not followed. The AIB report states:

> *The philosophy associated with X-15 research flights is to discontinue the research objectives when aircraft malfunctions impair safe recovery of the aircraft or when the pilot has become so overloaded with aircraft malfunctions and/or experiment tasks that he is unable to do either.*

This is the proper philosophy for flight-testing, but did not appear to have been effectively implemented during Flight 3-65.

The AIB report states that ground control did not have access to all the information needed for effective and timely problem detection. If this was the case, then ground control was unable to perform its primary function of protecting pilot and aircraft safety in accordance with the philosophy the AIB had noted. It is hard to understand why the status of the critical automated RCS was not being monitored on the ground, whereas the aerodynamic control system servomotors were being monitored. The MH-96 AFCS should have been viewed as experimental equipment. In its key role as safety backup to the pilot in such an experimental flight, all critical flight information should be available to ground control regardless of whether or not it is available to the pilot.

However, regardless of the lack of certain key information, ground control had substantial evidence of Flight 3-65 problems. The continuing fluctuations in the telemetered data with the indications of the IFDS malfunction should have been sufficient evidence of problems to status the pilot and potentially abort the mission. Within 80 seconds after the start of the electrical disturbance, ground control had several indicators of serious aircraft problems. These include:

- At 10:31:07 PST (MET + 59 seconds), the telemetered data became and remained erratic for several minutes. For example, ground control was aware of continuing anomalous servo transients from these telemetered data. The AIB report states:

  The transient motion of the three servos was not due to pilot inputs or aircraft motion, but was apparently electrical and was of sufficient frequency content and

amplitude to drive all three control gains well below their normal values for the particular flight conditions at which it occurred. The gain reduction in all three channels was great enough to cause the primary reaction controls to automatically disengage.

- Starting at 10:31:07 (MET + 59 seconds), the telemetered data on altitude and velocity differed from the radar data and was noted by ground control personnel.

- At 10:31:58 (MET + 110 seconds), the pilot reported the IFDS computer and instrument malfunction lights were on. The flight controller acknowledged the pilot's report.

- About 20 seconds later, during the wing-rock maneuver, a member of the ground control team reported to the flight controller that the pilot was having a control problem based on his observations of larger than normal pitch-roll servo excursions.

- Simultaneously, the telemetered indication of β data, which was monitored by the flight controller, was observed to deviate to off-scale nose right indicating the aircraft had undergone a large heading deviation.

- At 10:32:26 (MET + 138 seconds), disengagement of the pitch and roll dampers was reported by the pilot and acknowledged by the flight controller.

The proactive approach to safety is to advise the pilot of a problem as soon as there is any indication of that possibility. Such a warning is mandatory even if it may be redundant. The failure of ground control to notify the pilot of a possible control problem as soon as they had a suspicion of a problem was a causal factor in the loss of Flight 3-65.

Moreover, throughout the flight, ground control continuously assured the pilot that he was on the planned flight profile and instructed him to proceed with planned experiments despite the evidence of problems. Not only did ground control potentially delay the pilot's recognition of the problem and cause him to discount the computer and instrument malfunction lights and the disengagement of the pitch and yaw dampers, but they also added to the pilot's workload by instructing him to execute the experiments rather than focus on the problem. For example:

- During the wing-rock maneuver, it became apparent to ground personnel monitoring the telemetry records that something was amiss with the aircraft control. Nevertheless, the flight controller instructed the pilot to continue with the computed α/β-check maneuver. This experiment was a part of a continuing study to determine the highest altitude at which the ball-nose display could be considered reliable by comparing its indications of α and β with the values calculated by the IFDS computer. Ground control knew the IFDS computer was malfunctioning and there was a control problem, yet the pilot was instructed to proceed with this experiment that relied on the IFDS computed α and β.

After 190 successful flights, the ground control personnel for Flight 3-65 may have become complacent and may have chosen to ignore the reported evidence of a problem onboard the

aircraft. The flight controller appears to have been unable to recognize the integrated significance of the several indications of problems that were reported by the pilot and ground-control personnel. Evidence of this failure is in the following testimony reported by the AIB [ref. 3]. A member of ground control during Flight 3-65 testified:

> "The first problem indication was the computer malfunction light call from the pilot. I did not hear him call reset. The next thing was pitch-roll damper dropout, and reset. ... With the apparent A/C problems I asked the controller to have the experiments closed." The flight controller did not request that the science objectives be terminated until at least 2 minutes later, after the pilot had reported the development of a spin.

Another ground control member testified:

> "Upon initiation of the planned roll maneuvers, the pilot appeared to have a roll control problem as evidenced by larger than normal pitch-roll servo excursions. .... stop to stop excursions continued on the pitch-roll servo traces. In addition, the ball nose β indication moved off scale, showing the aircraft nose right. Ball nose α and β are not used for flight guidance during the ballistic portion of altitude flights."

The flight controller did not consider this evidence of continuing control problems.

In addition, the flight controller continually assured the pilot that he was "on track" and "on heading." The pilot and flight controller were aware that heading information could not be determined from radar track data. No display of heading information (e.g., telemetered IMU yaw data) was available in the control room. Although the ball nose data correctly indicated a large β angle, it was discounted by the flight controller due to his past experience with unreliable ball-nose indications at low dynamic pressure [ref. 3].

For more than 2 minutes, until the pilot recognized that he had problems, ground control encouraged the pilot to operate the aircraft even though it was known that the control system was malfunctioning and that much of the displayed information on aircraft states was probably erroneous. These actions on the part of the flight controller and the ground control team were a causal factor in the accident.

9.2.2 Contributing Factors

During the nearly 3 minutes after the electrical arcing from the traversing probe that precipitated the events leading to the destruction of the X-15-3, there were several factors that exacerbated the causal factors. It is conceivable the pilot might have regained control of the aircraft and effected a safe landing had certain of these factors not prevailed at the time.

One contributing factor was the design that allowed a failure in the AFCS to interfere with the pilot's ability to control the aircraft without any indication to the pilot of the failure other than a reliance on the pilot noticing a lack of response to his control inputs. In addition, each time the MH-96 adaptive gains were reset to minimums, either via external inputs or as a result of pilot

action, there was a delay of several seconds before RCS could be reengaged so as to prevent startup transients if the adaptive channels were reset. While this aspect of the MH-96 design had merit for protection of the aerodynamic controls, the designers apparently failed to consider the negative impact of the delayed reengagement on controllability when the only control useful to the pilot was the RCS. The intermittency of this ineffectiveness was particularly insidious because, with no other signal of malfunction and the inherently on-off nature of RCS, the pilot's recognition of the failure was obfuscated.

A second contributing factor was the complexity of the pilot's interface to the MH-96. The problem of understanding the functioning of the AFCS is exemplified by the following instructions in the pilot's manual:

> *If the damper switches are down and the lights are out, power for the system is off. If the damper switches are down and the lights are on, the system is disengaged but in a state of readiness to be engaged. If the damper switches are up (DAMPER position) and the lights are out, the dampers are engaged. If the damper switches are up and the lights are on, only the fixed-gain portion of the dampers are engaged.*

This type of design is conducive to human error. The procedure to switch from RCS control through the MH-96 to direct manual control was similarly complex. The pilot's manual states that before the pilot switches to the left side stick for direct access to the RCS he must first turn off the MH-96 AFCS. Otherwise, the automated system would oppose the pilot's commands. The pilot would be expected to take this action when he recognized that the AFCS has failed. When the MH-96 failed on Flight 3-65, the pilot would have had to rely on the aircraft response to recognize that the RCS was not being activated by his right side stick inputs. However, as was indicated and noted in the AIB report, the small control inputs required for the experiments and the intermittent effectiveness of control made it virtually impossible for the pilot to detect the failure. Further, had the pilot recognized that the AFCS was not functioning properly, it is questionable whether he could have identified and taken the necessary steps to disengage it under the stressful conditions and the aircraft motions that existed at the time he entered into the spin. The procedure design did not take into account the operational context under which the procedure would be used.

A third contributing factor was the known tendency of the stability augmentation system to undergo large-amplitude limit cycle oscillation under some flight conditions. The possibility of this failure mode (having experienced it on a prior flight) should have resulted in a suspension of flight operations using the MH-96 until the design issue was resolved. While the previous failure incidence was of concern but caused no damage, in this case it destroyed the aircraft, leading to the loss of the pilot. Although this pitch control system instability resulted in the destruction of the X-15-3, it is considered a contributing factor because the instability would have been avoided if the pilot had disengaged the AFCS when he switched to direct manual control just prior to the spin.

	NASA Engineering and Safety Center	Document #:	Version:
	Technical Assessment Report	NESC-RP-14-00957	1.0

Title: A Comprehensive Analysis of the X-15 Flight 3-65 Accident	Page #: 55 of 107

A fourth contributing factor was in the design of the pilot's display that used the ADI in two different modes (i.e., normal mode and the PAI). Even though this instrument was flown successfully on previous X-15-3 flights, it was a fundamentally poor design from a human factors perspective. In its normal configuration, the horizontal and vertical needles of the ADI indicated α and β, respectively. When the ADI was switched to the PAI mode, the horizontal needle indicated the pitch angle, and the vertical needle indicated the roll angle. Using such a critical display in two different configurations without a clear and salient mode indication is conducive to mode confusion, especially when the pilot is under stress and high workload. The switch position was the only indication of the PAI mode.

A fifth contributing factor was that, during the time period and the altitudes at which most of the critical events occurred, information displayed came from the IFDS computer. The only other source, the ball nose, was known to be unreliable at these flight conditions. There was no provision for backup source of reliable information for the pilot at high altitude in case of failure of the IFDS computer.

When the dynamic pressure became less than about 50 psf, the normal procedure for the pilot was to push a switch on the display panel that changed the source of data for the α and β from the aerodynamic source of the ball nose to the IFDS computer. During Flight 3-65, the dynamic pressure fell below 50 psf at about 155,000 feet altitude at 10:31:35 PST (MET + 87 seconds), by which time the IFDS computer had failed and the computer and instrument malfunction light had illuminated. Although the pilot did not make a verbal report, the post-accident examination of the cockpit film shows that after hesitating at the switch for several seconds he pushed the data-source switch as planned, despite the IFDS computer malfunction light. After switching the source, the β indication was correctly indicating off-scale nose-right, but the α information was erroneous. During Flight 3-65, the dynamic pressure did not increase above 50 psf until after the pilot reported he was in a spin. The cockpit film indicates that he never switched back to the aerodynamically driven source of aircraft data and may not have been able to switch once the aircraft entered into a spin.

Finally, the evidence in the AIB report was reviewed to ascertain what actions taken or not taken by the pilot during the critical 3 minutes may have been contributing factors in the X-15-3 accident.

It was not until 2 minutes after the access to the RCS through the right side stick had become intermittent that the pilot realized the aircraft was not responding to his inputs and switched to the left side stick control. Coincidentally, the controls worked when called upon during the wing-rock and the computed α/β-check maneuvers. This coincident response contributed to the deception that the controls were operating normally. It was not until the pilot was trying to maintain control for the precision attitude-tracking task that access to the RCS through the AFCS from his right side stick was determined to not be working. The delay in the pilot's ability to recognize the failure contributed to the accident.

The pilot failed to correct the error in yaw when he switched to direct RCS control through the left side stick. The AIB report attributes this failure to the pilot's misinterpretation of the PAI after he earlier selected that mode for the ADI. However, the AIB report states:

> *Since it did not require excessive control inputs to keep the needle close to center, the pilot may not have realized his error until it was too late or he may never have realized his error, in that he could not or did not recognize any problem with his attitude control.*

It is important the AIB recognized the pilot might not have been able to discern the aircraft had reached a large yaw error until he discovered that he had no control. The pilot's failure to correct the yaw error, or his inability to detect it, contributed to the accident.

The evidence suggests the pilot forgot he was in the PAI mode when he switched to the left-hand stick RCS control. However, at the moment he switched control, he was performing the precision attitude-tracking task (Figure 9.2-1) and he continued to try to complete that task after he switched hands. It is difficult to believe that the pilot would have forgotten that he was in the PAI mode while he was in the process of performing the very maneuver for which the PAI mode was specifically designed.

The evidence indicates that the pilot did not disengage the MH-96 AFCS when he switched to the left side stick control. This was an important failure because the subsequent instability could have been avoided had the pilot had remembered to disengage the AFCS when he switched to direct manual control, and recovery from the dive might have been possible. While this action was practiced as part of the captive carry AFCS equipment checkout procedure, it does not appear on the Flight 3-65 radio transcript and may have been skipped to save time [ref. 3].

The pilot's apparently impaired performance might be explained by the high stress and workload at the moment that he switched controls. By the time the pilot realized he had no control using the right side stick and changed to direct manual RCS control through the left side stick, he must have recognized that the aircraft had attained large attitude angles and angular velocities, the computer and instrument malfunction lights were on, and the displayed information was suspect. The pilot may have found himself trying to cope with an uncontrollable aircraft and questionable information just as he was starting into the critical descent phase. The aircraft was at an altitude at which the aerodynamic controls were ineffective and the AFCS was behaving erratically. Coping with these multiple problems could have demanded all of the pilot's attention, possibly causing him to forget actions he had taken (e.g., switching the ADI mode to PAI) or should have taken (e.g., disengaging the AFCS).
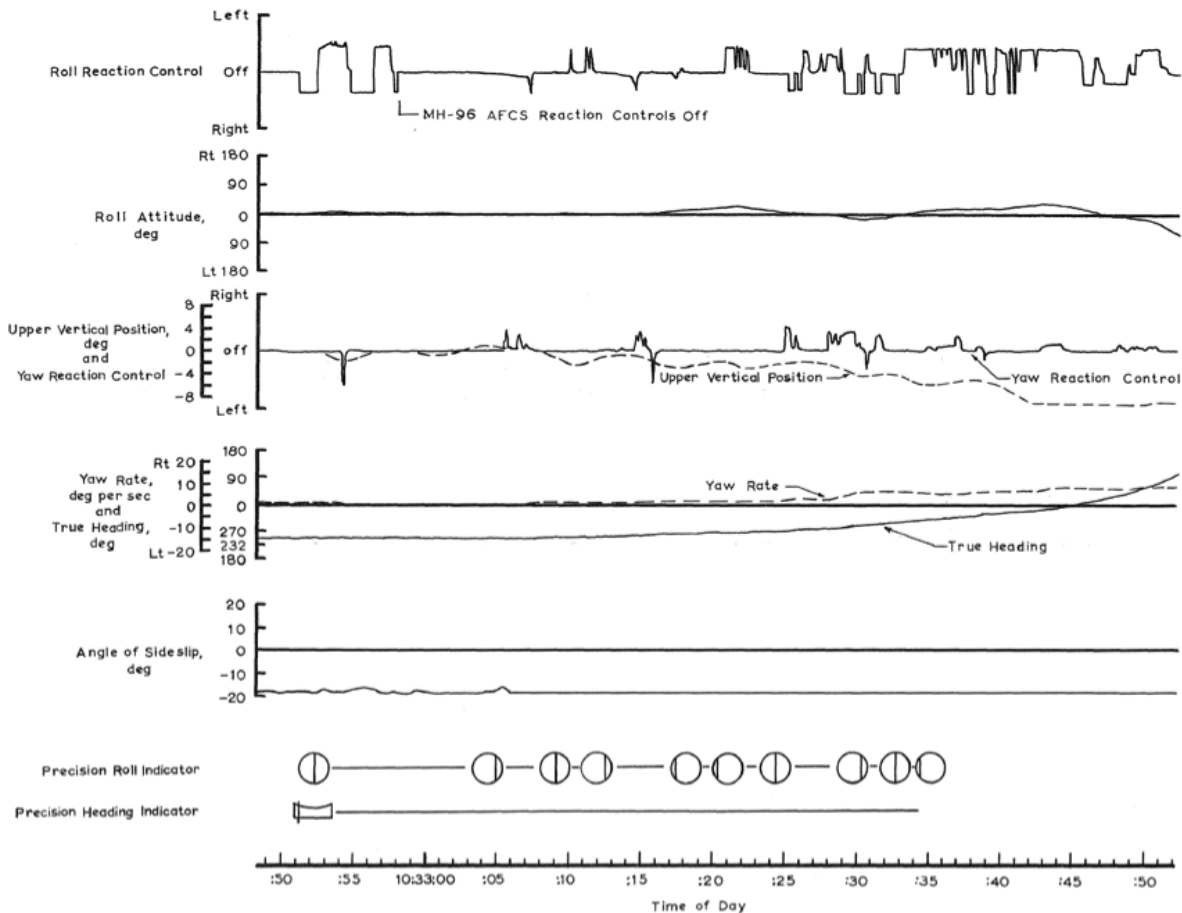
Figure 9.2-1. Time History of Precision Attitude Tracking Task at Peak Altitude [ref. 3]

9.2.3 Alternative Hypotheses

The hypotheses appearing in this section are recognized as speculative and lack conclusive evidence but are provided since they cannot be discounted as possible contributing factors in the Flight 3-65 accident.

9.2.3.1 Hypoxia

A hypothesis considered by the AIB was that the pilot was hypoxic due to an unknown equipment malfunction [ref. 3]. The X-15 cabin was sealed, pressurized, and thermally regulated using gaseous nitrogen derived from the aircraft's liquid nitrogen supply. The cabin temperature was maintained at a maximum of approximately 80 degrees Fahrenheit, and the cockpit and instrumentation bays were insulated to minimize heat transfer into the cockpit during high aerothermal loading conditions. A cabin pressure differential of 3.5 psi with respect to ambient pressure was maintained by the cabin pressure regulator.

By 1967, X-15 pilots wore a custom-fitted A/P22S-2 pressure suit containing anti-g bladders. The suit pressure and cockpit pressure were equalized, and breathing oxygen was supplied only to the face area by partitioning the helmet with a face seal. This design was primarily to mitigate the risk of fire associated with an oxygen-based cockpit pressurization system. Oxygen was supplied by self-contained seat-mounted bottles with a regulator that forced oxygen into the helmet at a differential pressure higher than the suit pressure, ensuring that normal breathing would not allow the pilot to inhale pressurization nitrogen. It was known that rapid deep inhalations could exceed the differential pressure maintained by the oxygen regulator and result in transient inhalation of nitrogen, and that pilots' respiration rates increased precipitously during the boost phase [refs. 4 and 40].

It is possible that the pilot may have been experiencing hypoxia due to some equipment malfunction (e.g., a failure leading to low differential pressure) and that the situation may have been exacerbated during the boost phase as a result of rapid or deep breathing and increased stress. Limited testing was performed on the oxygen system components that survived the impact, and while the AIB concluded that those components had no direct evidence of failure, the pilot's lactate levels were 10 percent higher than the threshold considered indicative of hypoxia at that time. However, results were inconclusive since several hours had elapsed before the laboratory analysis could be conducted [ref. 3].

9.2.3.2 Spatial Disorientation

A speculation of the AIB was the pilot's susceptibility to Type-II spatial disorientation (SD), which the AIB report refers to as "vertigo," was a contributing factor in this accident. Despite the pilot's and other X-15 pilots' self-reported sensitivity to the somatogravic illusion during the boost phase, there is no direct evidence that the pilot's performance was affected by SD during the boost phase and performance of the maneuvers, nor was there evidence that he was misinterpreting the PAI during these two experiments.

However, at the moment the pilot switched to direct manual control, he had just come "over the top" at about 266,000 feet and had been in a 0-g condition since the end of the engine burn. Under these circumstances, the pilot's susceptibility to SD may have contributed to his forgetting to switch off the AFCS, especially as it seems he was still focused on completing the precision attitude-tracking task. As the AIB report states, "Vertigo [SD] could have coupled with the added workload of sorting the various malfunctions," and perhaps caused his lack of recognition of the yaw attitude if he did in fact misinterpret the ADI in its PAI mode during his subsequent actions. Most of the pilot's experience in the X-15 aircraft was with a normal ADI (i.e., with the vertical needle indicating yaw) when he used the left side stick for the RCS. When he switched to manual control, he was under stress and high workload, and it is a common human tendency under such conditions to revert to the basics in which one is most highly trained. Thus, the pilot may have mentally reverted to the normal ADI mode when he switched to manual control.

It is also possible the pilot was confused as to what to believe in the displays. Pilots are trained that the only way to overcome SD is to fly basic instruments and disregard the attitudes

suspected by their physical senses. The pilot had been taught that the ball nose did not provide reliable information at dynamic pressures less than about 50 psf. He knew he had switched to the IFDS computer as the source of data to his displays when the panel display light indicated that he should do so, and he knew that the IFDS computer and instrument malfunction lights were on. However, the assurances from ground control and the instructions to perform experiments that relied on the IFDS computed data may have contributed to the confusion. The AIB report states:

> *The pilot seemed unaware of a gross heading deviation in spite of three separate correctly reading instruments...He apparently was concentrating on a single instrument, the vertical needle of the ADI, as a pilot might do if he were trying to overcome vertigo [SD].*

When some instruments are displaying erroneous information, it is difficult to determine which instruments are correct and which are not. When the pilot is focused on a specific instrument for the sake of the particular maneuver to be performed, other instruments receive lower priority. With the added effect of the flight controller's assurance the aircraft was "on heading," the heading deviation may have gone unnoticed. Furthermore, tunneled attention and disregard for other displays, including audible alarms, are known tendencies of humans under high stress and workload, regardless of SD.

9.2.3.3 Egress System

Post-flight analysis of the aircraft emergency egress (ejection) system revealed the canopy jettison mechanism had been actuated at an altitude in excess of 60,000 feet and had operated abnormally. A detailed description of the anomalous canopy jettison activation appears in reference 3. The AIB noted that while it was contrary to the flight surgeon's opinion, the physical evidence suggested that the pilot may have attempted to activate the ejection system and was unable to do so. A contributing factor may have been the pilot's physical compatibility with the seat design:

> *One possibility would be that the pilot could have raised the ejection handles far enough to fire the M-3 initiator [canopy jettison] but not far enough to fire the M-32 initiator [seat]… If the canopy jettison were the result of pilot action, which is contrary to medical opinion, the possibility that Major Adams was unable to complete the movement of the ejection handles to the locked position must be considered. It was known that Major Adams was large for the seat, and although he had successfully passed the egress training, he had some difficulty in moving the handles far enough to reach the locked position that must be attained for ejection to take place.*

The noted difficulty in actuating the ejection mechanism [ref. 3] may have been amplified in a high-stress, time-critical situation.

9.2.3.4 Pilot Training and Past Performance

The pilot was known to be an exceptionally proficient research pilot and had demonstrated his performance on a prior flight when a failed propulsion system mandated an emergency landing [ref. 4]. However, while the pilot was adequately qualified for the operation of the X-15-3, it is undoubtable that the additional complexity of the human-machine interface in the X-15-3 versus the other two aircraft contributed to the pilot's apparent negative transfer that he exhibited under a high-workload and high-stress situation. Furthermore, the pilot had not, unlike more experienced pilots, been directly involved in the development and test of the experimental flight control system. Finally, the majority of the pilot's flight and training experience was in the X-15-1 aircraft with conventional controls and instrumentation panel. Only 20 percent of his logged simulator time was flown in the X-15-3 configuration (Table 9.2-1).

Table 9.2-1. Pilot Flight and Simulator Experience

Flight Experience				Simulator Experience		
Flight	*Flight No.*	*Airframe*	*Date*	*Airframe*	*Logged Hours*	*Fraction (percent)*
173	1-69-116	56-6670 (#1)	October 6, 1966	56-6670 (#1)	165.2	~69
176	3-57-86	56-6672 (#3)	November 29, 1966	56-6671 (#2)	25.5	~11
177	1-70-119	56-6670 (#1)	March 22, 1967	56-6672 (#3)	47.5	~20
179	1-71-121	56-6670 (#1)	April 28, 1967			
182	1-72-125	56-6670 (#1)	June 15, 1967			
187	3-62-92	56-6672 (#3)	August 25, 1967			
191	3-65-97	56-6672 (#3)	November 15, 1967			

10.0 Findings, Observations, and NESC Recommendations

The analysis of the fatal accident of X-15-3 Flight 3-65 has highlighted several recurring themes in the complex scenario leading to and during the flight that resulted in the loss of life. As is often the case in aerospace vehicle accidents, a confluence of latent failure modes and sensitivities was compounded by the unique flight circumstances. It is plausible that had one or more of these factors been mitigated prior to the flight, the accident would not have occurred or would have resulted in a serious but nonfatal mishap. The major themes contributing to the accident were:

1. Insufficient focus on characterizing risks associated with subsystem-level interactions.

2. Continued flight operations in the face of multiple unexplained system anomalies.

3. Inadequate documentation, communication, and analysis of failure effects.

4. Ineffective design for human-machine integration.

5. Development of a complacent culture surrounding experimental systems and flight test operations.

Specific findings, observations, and NESC recommendations are detailed in the following subsections.

10.1 Findings

The following findings were identified:

F-1. The X-15 3-65 accident was precipitated by an electrical failure in an experiment package using COTS components that had not been properly qualified for the X-15 flight environment.

- The electrical isolation mechanism for the experiment package (line fuses) did not adequately protect the aircraft main power bus. The ensuing electromagnetic interference effects caused numerous subsystem failures, interrupted pilot access to the RCS, and led to an eventual loss of control.

F-2. The pilot's inability to recognize and isolate the subsystem failures and safely regain control of the aircraft was largely caused by the lack of adequate display of safety-critical information to the pilot and to ground control, lack of communication of the status of the aircraft to the pilot, excessive reliance on the autonomy of the pilot, lack of redundant pilot information displays, and the flight controller's decision to continue with the mission despite multiple indications that the safety of flight was compromised.

F-3. A principal cause of the aircraft destruction was a large-amplitude divergent limit cycle oscillation in the MH-96 AFCS caused by a latent design error in the structural notch filter that did not account for the nonlinear behavior of the X-15 servoactuator under rate saturation when coupled with the lightly damped aircraft longitudinal mode at high Mach numbers.

F-4. The high-gain nature of the MH-96 AFCS, in which it would operate at or near the critical stability limit, decreased robustness to unmodeled nonlinearities and parametric uncertainty and accelerated the onset of the divergent limit cycle oscillation.

F-5. By the time of its deployment, the MH-96 had undergone multiple modifications to compensate for operational factors not accounted for in its initial concept designs that reduced its overall performance and robustness below that of its theoretically ideal operating characteristics.

- These factors included the pilot interface, hysteresis effects, structural flexibility, and servoelasticity. There is no evidence to suggest that the effects of these modifications were verified analytically against the original design models or that design models were updated to reflect observed flight behavior.

F-6. Loss of control was compounded by pilot actions resulting from some combination of mode confusion, attentional tunneling, negative transfer, and possibly hypoxia and SD.

F-7. A major contributor to the loss of control was a poor human interface design of the X-15-3 aircraft, consisting of (1) lack of clear and salient mode indication on flight-critical instruments, (2) a complex and counterintuitive interface, and (3) design such that the automated flight control system could interrupt access to the pilot's only control effector without notifying the pilot.

F-8. The successful deployment of an experimental AFCS in an operational mission mode led to a dilution of the perceived risks associated with its use and prevented the pilot and ground controllers from recognizing and isolating its failure before the destruction of the aircraft was inevitable.

F-9. Failure detection features of the MH-96 AFCS that were designed to improve reliability, when exercised outside their intended design envelope, malfunctioned and caused degraded performance, which contributed to the loss of control.

F-10. Of the five major subsystem failures contributing to the accident, three (i.e., the IFDS computer failure, the servo transient anomaly, and the MH-96 limit cycle) had shown some evidence of failure on previous flights.

- The program's decision to continue flight operations without assessing risk and identifying the root cause(s) of these anomalies was a causal factor in the 3-65 accident.

10.2 Observations

O-1. The effectiveness and availability of ground control to assist flight crews in diagnosing and troubleshooting subsystem anomalies can be compromised due to operational aspects of the flight profile.

- For example, known flight regimes with poor radio communication can limit ground control situational awareness; critical maneuvers and dynamic events that occur on short timescales (e.g., ballistic atmospheric reentry) lend insufficient time for action.

O-2. Complete or near-complete reliance on a flight crew to troubleshoot and resolve subsystem anomalies in a complex experimental system carries excessive risk.

- This is especially true in single-pilot operation and even more so in flight regimes that have extremely demanding, time-critical piloting tasks.

O-3. Ballistic space planes are more susceptible to electrical arcing in high-voltage components than aircraft, launch vehicles, or spacecraft due to the extended time spent in the critical *pd* region.

O-4. The use of COTS components and subsystems in aerospace vehicle designs is accompanied by the risk that an unknown design element of the component or subsystem may interact negatively with other subsystems.

O-5. Actuator nonlinearity, especially rate limiting, continues to play a role in the introduction of latent instabilities in flight control systems that become apparent in high-gain modes of operation and with large commands.

- Such high-gain modes may arise due to high pilot gain (e.g., PIO) or high control system gain. Such conditions are generally associated with off-nominal scenarios involving large or abrupt maneuvers and may not have been fully exercised in simulations.

10.3 NESC Recommendations

The following NESC recommendations are directed to the Human Exploration and Operations Mission Directorate:

R-1. Minimize the use of high-voltage electronics, and especially AC potentials, to the greatest extent possible. *(F-1)*

- In particular, systems with peak potentials exceeding 100V should be scrutinized to ensure that the design is not at risk of corona discharge or breakdown. Environmental qualification of high-voltage components for the target environment is mandatory and should include testing at simulated flight conditions when practicable. Departures from the assumptions of the ideal breakdown theory and the implications of violating these assumptions should be rigorously assessed. These include, but are not limited to, frequency, wave shape, gas composition and temperature, external radiation, contamination, and electrode composition. Assessed risk should be used to inform the scope of detailed analysis, simulation, and test activities.

R-2. Qualify all experimental equipment for the target environment, even if it is electrically and mechanically isolated from safety-critical systems. *(F-1)*

R-3. Rigorously analyze the reliability and efficacy of electrical isolation and grounding schemes to ensure malfunctioning equipment cannot cause cascaded electrical failures. *(F-1)*

R-4. Thoroughly understand the implications of using COTS components in a system. *(F-1)*

- System integrators should assess COTS designs in detail and structure vendor requirements such that potentially safety-critical design information is not withheld.

- The risks of accelerated and/or limited flight qualification of COTS components have been highlighted in other recent assessments by the NESC [refs. 41–44].

R-5. Explicitly account for saturation and rate limiting behavior to the greatest extent possible in flight control system analysis and design. *(F-3, F-5)*

- Simulations and, when practical, incremental flight testing must exercise regions outside the expected flight envelope, to include specific cases that induce nonlinear behavior.

- The value of nonlinear simulations can be greatly enhanced by companion approximation methods for assessing linear and nonlinear system stability, for example, describing function analysis.

R-6. Carefully weigh the benefits and risks of advanced flight control with the cost and schedule impacts required to decrease uncertainty in the design models through high-fidelity modeling, element testing, or incremental flight testing and post-flight validation. *(F-3, F-4, F-5, F-8)*

- Adaptive control is most applicable when system dynamics change in a rapid and uncertain way and the environment is potentially uncertain and/or unpredictable. Adaptive control should be employed when relevant and warranted by fundamental limitations in the predictability or measurability of the system to be controlled.

- In some cases, the use of a conventional flight control algorithm with improved design models and/or high-reliability flight instrumentation (e.g., air data systems) may provide equivalent performance to an adaptive system and may have behavior that is more easily predictable and analytically tractable.

R-7. Conduct training of research pilots for experimental systems using piloted simulations, especially with respect to off-nominal scenarios and emergency situations, in a simulated cockpit environment that is functionally identical to that of the flight vehicle so as to minimize the likelihood of negative transfer. *(F-6)*

R-8. Ensure priority of pilot and ground control in the event of an anomaly be placed on restoring the aircraft to a safe state, which may require the immediate cessation of science objectives. *(F-2, F-6, F-7)*

R-9. Identify possible subsystem malfunctions prior to flight and categorically assign mission rules based upon their relative severity to assist controllers and flight crews in recognizing and diagnosing failures. *(F-2, F-8, F-9, F-10)*

R-10. Maintain, to the greatest extent possible, adequate telemetry coverage and voice communication with the flight crew. *(F-2, F-6)*

- Risk assessments should dictate requirements for mission planning that minimize the duration of exposure to flight regimes in which access to ground assistance is impeded.

R-11. Enable ground controllers access to all information on the aircraft systems status needed to perform their primary responsibility of maintaining safety of operation. *(F-2, F-6, F-7)*

R-12. Ensure that ground controllers inform flight crews on the state of the aircraft and its subsystems. *(F-2, F-6, F-7, F-8)*

- Anomalies that may have any significance to the safe operation of the aircraft should be immediately reported to the flight crew.

R-13. Preclude an automated system, the failure of which would compromise the safety and/or the operability of the aircraft, from relying on a single source of aircraft or environmental data for computation of its automated actions. *(F-2, F-9)*

R-14. Immediately notify the pilot of a flight control system failure. *(F-2, F-6, F-7, F-9)*

- If manual control is possible, then any failure must not interfere with the pilot's manual and direct aircraft control.

R-15. Reconcile modifications with the baseline design methodology if the control system is altered to improve the behavior of a fielded design. *(F-3, F-5, F-8)*

- If the design process is found to be deficient or poorly correlated with flight, then these deficiencies should be resolved and properly documented.

R-16. Design automation to provide for effective dynamic cooperation between the human and the nonhuman agents responsible for operating any complex system. *(F-2, F-6, F-7, F-8, F-9)*

R-17. Ensure the active mode is clearly and saliently indicated, preferably on the relevant display itself, to minimize mode confusion if a critical display is used in two different configurations. *(F-6, F-7)*

R-18. Suspend flight operations to assess risk in the event that unexplained anomalies or uncharacterized failure modes occur during flight-testing of safety-critical systems. *(F-10)*

11.0   Alternate Viewpoint

There were no alternate viewpoints identified during the course of this assessment by the NESC team or the NRB quorum.

12.0   Other Deliverables

No unique hardware, software, or data packages, outside those contained in this report, were disseminated to other parties outside this assessment.

13.0   Lessons Learned

No applicable lessons learned were identified for entry into the NASA Lessons Learned Information System (LLIS) as a result of this assessment.

14.0   Recommendations for NASA Standards and Specifications

No recommendations for NASA standards and specifications were identified as a result of this assessment.

15.0   Definition of Terms

Corrective Actions	Changes to design processes, work instructions, workmanship practices, training, inspections, tests, procedures, specifications, drawings, tools, equipment, facilities, resources, or material that result in preventing, minimizing, or limiting the potential for recurrence of a problem.
Finding	A relevant factual conclusion and/or issue that is within the assessment scope and that the team has rigorously based on data from their independent analyses, tests, inspections, and/or reviews of technical documentation.
Lessons Learned	Knowledge, understanding, or conclusive insight gained by experience that may benefit other current or future NASA programs and projects. The experience may be positive, as in a successful test or mission, or negative, as in a mishap or failure.
Observation	A noteworthy fact, issue, and/or risk, which may not be directly within the assessment scope, but could generate a separate issue or concern if not addressed. Alternatively, an observation can be a positive acknowledgement of a Center/Program/Project/Organization's operational structure, tools, and/or support provided.
Problem	The subject of the independent technical assessment.

Proximate Cause	The event(s) that occurred, including any condition(s) that existed immediately before the undesired outcome, directly resulted in its occurrence and, if eliminated or modified, would have prevented the undesired outcome.
Recommendation	A proposed measurable stakeholder action directly supported by specific Finding(s) and/or Observation(s) that will correct or mitigate an identified issue or risk.
Root Cause	One of multiple factors (events, conditions, or organizational factors) that contributed to or created the proximate cause and subsequent undesired outcome and, if eliminated or modified, would have prevented the undesired outcome. Typically, multiple root causes contribute to an undesired outcome.
Supporting Narrative	A paragraph, or section, in an NESC final report that provides the detailed explanation of a succinctly worded finding or observation. For example, the logical deduction that led to a finding or observation; descriptions of assumptions, exceptions, clarifications, and boundary conditions. Avoid squeezing all of this information into a finding or observation

16.0   Acronym List

α	Angle of Attack
β	Sideslip Angle
AC	Alternating Current
ADI	Attitude Director Indicator
AFCS	Adaptive Flight Control System
AFRC	Armstrong Flight Research Center
AIB	Accident Investigation Board
APU	Auxiliary Power Unit
BCS	Ballistic Control System
COTS	Commercial off the Shelf
DC	Direct Current
DFRC	Dryden Flight Research Center
FRC	Flight Research Center
GN&C	Guidance, Navigation, and Control
HWIL	Hardware in the Loop
Hz	Hertz
IFDS	Inertial Flight Data System
IMU	Inertial Measurement Unit
LCO	Limit Cycle Oscillation
MET	Mission Elapsed Time

MSFC   Marshall Space Flight Center
NESC   NASA Engineering and Safety Center
PAI   Precision Attitude Indicator
pd   Pressure and Gap Distance
PIO   Pilot-induced Oscillation
PST   Pacific Standard Time
RAS   Reaction Augmentation System
RCS   Reaction Control System
RRA   Range Reference Atmosphere
SAS   Stability Augmentation System
SD   Spatial Disorientation
SLS   Space Launch System
USAF   United States Air Force
USN   United States Navy
TDT   Technical Discipline Team
V   Volts

17.0 References

1. Lindahl, J., McGuire, W., and Reed, M.: "Advanced Flight Vehicle Self-Adaptive Flight Control System, Part V: Acceptance Flight Tests," WADD-TR-60-651, Part V, Flight Control Laboratory, Aeronautical Systems Division, USAF Systems Command, May 1963.

2. Mellen, D.: "The Development and Flight Test of an Adaptive Flight Control System for the X-15 Vehicle," Technical Report, Minneapolis-Honeywell, February 1963.

3. Bellman, D. et al.: "Investigation of the Crash of the X-15-3 Aircraft on November 15, 1967," NASA Flight Research Center, January 1968.

4. Jenkins, D.: "X-15: Extending the Frontiers of Flight," NASA SP-2007-9-001-HQ, 2007.

5. Holleman, E.: "Control Experiences of the X-15 Pertinent to Lifting Entry," NASA TN D-3262, NASA Flight Research Center, February 1966.

6. Thompson, M. and Welsh, J.: "Flight Test Experience with Adaptive Control Systems," *Advanced Control Systems Concepts, AGARD Conference Proceedings*, No. 58, pp. 141-147, January 1970.

7. Dydek, Z.: "Guaranteed Margins and Performance for an Adaptive Flight Control System and Application on the X-15 Research Airplane," Master's Thesis, Massachusetts Institute of Technology, 2007.

8. Dydek, Z., Annaswamy, A., and Lavretsky, E.: "Adaptive Control and the NASA X-15 Program: A Concise History, Lessons Learned, and a Provably Correct Design," in *Proceedings of the American Control Conference*, Seattle, Washington, 2008.

9. Jenkins, D.: "Hypersonics before the Shuttle: A Concise History of the X-15 Research Airplane," NASA SP-2000-4518, 2000.

10. Stillwell, W.: "X-15 Research Results," NASA SP-60, 1965.

11. Burke, M.: "X-15 Analog and Digital Inertial Systems Flight Experience," NASA TN D-4642, July 1968.

12. Maher, J., Ottinger, C., and Capasso, V.: "YLR99-RM-1 Rocket Engine Operating Experience in the X-15 Aircraft," NASA TN D-2391, NASA Flight Research Center, July 1964.

13. Wiswell, R.: "X-15 Propulsion System," in *Proceedings of the 33rd Joint Propulsion Conference and Exhibit*, AIAA, July 1997.

14. *Proceedings of the X-15 First Flight 30th Anniversary Celebration*, NASA CP-3105, 1989.

15. Sanderson, K.: "The X-15 Flight Test Instrumentation," NASA TM X-56000, NASA Flight Research Center, April 1964.

16. Mellen, D., Cole, G., and Lindahl, J.: "Advanced Flight Vehicle Self-Adaptive Flight Control System, Part II: Design of MH-96 System," WADD-TR-60-651, Part II, Flight Control Laboratory, Wright Air Development Division, USAF Air Research and Development Command, February 1961.

17. Fischel, J. and Webb, L.: "Flight-Informational Sensors, Display, and Space Control of the X-15 Airplane for Atmospheric and Near-Space Flight Missions," NASA TN D-2407, NASA Flight Research Center, 1964.

18. Holleman, E.: "Piloting Performance during the Boost of the X-15 Airplane to High Altitude," NASA TN D-2289, NASA Flight Research Center, April 1964.

19. Holleman, E.: "Summary of High-Altitude and Entry Flight Control Experience with the X-15 Airplane," NASA TN D-3386, NASA Flight Research Center, April 1966.

20. Schultz, P., Soufl, C., and Grubin, C.: "A Boost Guidance Scheme for the Dyna-Soar Mission," SSD-TDR-63-336, Systems Research and Planning Division, The Aerospace Corporation, December 1963.

21. Cockayne, W.: "Description of an Energy Management System for the X-15," NASA CR-96006, NASA Flight Research Center, June 1968.

22. Cary, J. and Keener, E.: "Flight Evaluation of the X-15 Ball-Nose Flow-Direction Sensor as an Air-Data System," NASA TN D-2923, NASA Flight Research Center, July 1965.

23. Wolowicz, C. and Gossett, T.: "Operational and Performance Characteristics of the X-15 Spherical, Hypersonic Flow-Direction Sensor," NASA TN D-3070, NASA Flight Research Center, November 1965.

24. Tremant, R.: "Operational Experiences and Characteristics of the X-15 Flight Control System," NASA TN D-1402, December 1962.

25. Jarvis, C. and Adkins, E.: "Operational Experience with X-15 Reaction Controls," NASA TM X-56002, NASA Flight Research Center, April 1964.

26. Day, R.: "Coupling Dynamics in Aircraft: A Historical Perspective," NASA SP-532, NASA Dryden Flight Research Center, 1997.

27. Jarvis, C. and Lock, W.: "Operational Experience with the X-15 Reaction Control and Reaction Augmentation Systems," NASA TN D-2864, NASA Flight Research Center, June 1965.

28. Boskovich, B., Cole, G., and Mellen, D.: "Advanced Flight Vehicle Self-Adaptive Flight Control System, Part I: Study," WADD-TR-60-651, Part I, Flight Control Laboratory, Wright Air Development Division, Air Research and Development Command, USAF, September 1960.

29. Lindahl, J., McGuire, W., and Reed, M.: "Advanced Flight Vehicle Self-Adaptive Flight Control System, Part VII: Final Report on Study, Development, and Test of the MH-96 System for the X-15," WADD-TR-60-651, Part VII, Air Force Flight Dynamics Laboratory, Research and Technology Division, USAF Systems Command, December 1963.

30. Meek, J. and Craggs, J.: *Electrical Breakdown of Gases*, Oxford, 1953.

31. Sutton, J. and Stern, J.: "Spacecraft High-Voltage Power Supply Construction," NASA TN D-7948, NASA Goddard Space Flight Center, April 1975.

32. Dunbar, W. and Seabrook, J.: "High Voltage Design Guide for Airborne Equipment," AFAPL- TR-75-41, Air Force Aero-Propulsion Laboratory, June 1976.

33. "Experience with the X-15 Adaptive Flight Control System," NASA TN D-6208, NASA Flight Research Center, 1971.

34. Taylor, L. and Smith, J.: "An Analysis of the Limit-Cycle and Structural-Resonance Characteristics of the X-15 Stability Augmentation System," NASA TN D-4287, NASA Flight Research Center, December 1967.

35. Reed, M., Wolfe, J., and Mellen, D.: "Advanced Flight Vehicle Self-Adaptive Flight Control System, Part IV: Notch Filter Development," WADD-TR-60-651, Part IV, Flight Control Laboratory, Aeronautical Systems Division, USAF Systems Command, June 1962.

36. Klyde, D. and Mitchell, D.: "Investigating the Role of Rate Limiting in Pilot-Induced Oscillations," *J. Guidance, Control, and Dynamics*, Vol. 27, No. 5, 2004, pp. 804–813.

37. Yancey, R.: "Flight Measurements of Stability and Control Derivatives of The X-15 Research Airplane to a Mach Number of 6.02 and an Angle of Attack of 25 Degrees," NASA TN D-2532, NASA Flight Research Center, November 1964.

38. Taylor, L.: "Recent X-15 Flight Test Experience with the MH-96 Adaptive Control System," in *Intercenter Technical Conference on Control, Guidance, and Navigation Research for Manned Lunar Missions*, NASA TM X-14568, July 1962.

39. Dydek, Z., Annaswamy, A., and Lavretsky, E.: "Adaptive Control and the NASA X-15-3 Flight Revisited," *IEEE Control Syst. Mag.*, Vol. 30, No. 3, June 2010, pp. 32–48.

40. Bratt, H. R.: "Biomedical Aspects of the X-15 Program 1959–1964," Technical Report No. 55-24, Air Force Flight Test Center, Edwards AFB, CA, August 1965.

41. "SpaceX Dragon Power and Avionics Review," NESC Assessment TI-14-00949, final report in progress.

42. "Implementation Case Study of Electronic Components in Safety-critical Avionics Systems," NESC-RP-13-00850, June 26, 2014.

43. "Use of Commercial Electrical, Electronic, and Electromechanical (EEE) Parts in NASA's Commercial Crew Program," NESC-RP-12-00762, March 15, 2012. Also published as NASA/TM-2012-217558, April 2012.

44. "The Use of Commercial-off-the-Shelf (COTS) Electronic Components in Safety-critical Human-rated (Commercial Crew) Space Avionics Systems," NESC-RP-12-00759, February 27, 2014. Also published as NASA/TM-2014-218261, May 2014.

18.0 Appendices

Appendix A.   Analysis of the MH-96 Adaptive Flight Control System

Appendix B.   Reconstructed Flight Data

Appendix A. Analysis of the MH-96 Adaptive Flight Control System

A   Analysis of the MH-96 Adaptive Flight Control System

The MH-96 AFCS was a form of forward gain adaptive control, which is based upon the idea of multiplicative modulation of the error gain in the inner loop (the "forward gain") in order to maximize performance and maintain stable operation [1]. As is well-known in classical control theory, under certain circumstances the maximum performance can be achieved when the forward gain is as high as possible. However, in all real control systems, the maximum forward gain is limited by the dynamics of the actuators, sensors, structural filters, and other parasitic effects such as flexible modes and sloshing propellant. At forward gains exceeding the critical value, the system will either exhibit instability (exponential or periodic divergence) or will enter a limit cycle (due to nonlinear effects). The latter often is manifested in real systems where a physical limitation, such as finite actuator power, ultimately bounds the amount of energy input to the system.
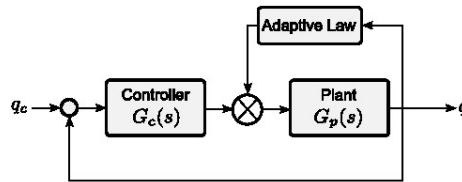
Figure A.1: Forward gain adaptive control (FGAC) concept

In all control systems, the existence of stability bounds on feedback gains limit the achievable performance. For fixed-gain or gain-scheduled control systems, the maximum gain is set as high as practicable while maintaining some *stability margin* to ensure that the system remains stable even when parametric variations and model imperfections present a system that is slightly different than that for which the control system was designed. Ensuring that the system provides acceptable operation under some assumed variation in the actual system provides *robustness* in the control design.

The challenge for all aerospace vehicle flight control systems is that the actual plant dynamics differ from those assumed during the design phase due to limitations in model fidelity or stochastic variations in the environment. Even if models are accurate, the parameters of the system change as a function of flight condition in a way that is difficult to predict accurately. Take, for example, the control of the second-order short period pitch dynamics of an aircraft in a trimmed configuration. The aircraft short-period mode has the response

$$G_p(s) = \frac{M_\delta \left(s + \frac{1}{\tau_a} \right)}{s^2 + 2\zeta_a \omega_a + \omega_a^2} \tag{A.1}$$

where M_δ is the control effectiveness coefficient, τ_a is the short-period zero, and ω_a, ζ_a are the bare airframe natural frequency and damping, respectively [2]. In order to design a fixed-gain or gain-scheduled control system for the short period mode, the control effectiveness coefficient M_δ must be known to a reasonable degree of accuracy; this parameter affects, among other things, the *gain margin* in the control loop. Prudent design practice for fixed-gain or gain-scheduled systems is to maintain at least 6 dB (approximately 2:1) margin in the forward gain, such that the system is robust to about a 2:1 variation in the *actual* parameter M_δ [3].

However, even in the simplest aerodynamics models, the parameter M_δ is a function of the flight condition, including (linearly) the dynamic pressure $\bar{q}$, and (nonlinearly) the Mach number, angles of attack and sideslip, and even the control deflection δ itself:

$$M_\delta = \frac{\bar{q}}{\bar{q}_0} M_\delta(M, \alpha, \beta, \delta, \dots). \tag{A.2}$$

Given a reasonable estimate of M_δ, it is generally straightforward to design a robust control system so long as the linear gain factor (dynamic pressure) is available online for computation. In the case of the X-15, an estimate of dynamic pressure would have to be derived either from inertially navigated velocity or an air data system suitable for hypersonic operation (such as the flow direction sensor). Even with current technology, both are difficult to mechanize accurately and reliably over a wide range of flight conditions. Furthermore, the value of M_δ is challenging to predict in flight regimes that are not well-characterized, notoriously so at hypersonic velocities. In the case of the X-15, the dynamic pressure alone ($\bar{q}$) could vary by a factor of more than 10, and the remaining characteristics were low-confidence estimates due to essential limitations in aerodynamic theory and test capability.

The MH-96 AFCS concept implemented a novel approach for adjusting the gain to provide aircraft response characteristics that were approximately constant at all flight conditions. The AFCS concept was based upon the knowledge that at some critical value of the gain, the system would become marginally stable (in a linear, time-invariant sense) and would develop into a limit cycle oscillation (LCO). The type of limit cycle oscillation depends on the frequency response characteristics of the aircraft, control system, and servomechanisms. The MH-96 designers recognized that if the control loop was designed such that the servo-actuator dynamics were the dominant parasitic mode (the first to become marginally stable), the frequency of the LCO would be almost completely invariant with respect to the control authority parameter M_δ. Once a limit cycle is established in the servo, the limit cycle amplitude is approximately a function only of the forward gain. The gain is a function of the unknown parameter M_δ and the controlled parameter, the feedback gain k_a. Thus, by maintaining a prescribed LCO magnitude, the MH-96 was able to continually maintain the forward gain near the critical value, tracking the changes in M_δ, while requiring no external measurements of dynamic pressure or estimates of the control authority.

The concept of gain modulation in a nonlinear control system was not new at the time of the MH-96 design, but its method of implementation was quite advanced. Similar systems had been designed and successfully tested on other aircraft, including the Lockheed F-94C and the McDonnell F-101. In addition, the F-101 was used as a flight test platform for the MH-96 prior to its first test on the X-15. A system conceptually similar to the MH-96 was used operationally on the General Dynamics F-111 from 1964 until its retirement from foreign military service in 2010 [4].

A.1   MH-96 Architecture

The MH-96 design philosophy was motivated by its intended use for high altitude flights. The first was to provide fail-safety and some amount of redundancy for the flight control system, given that at the time, the baseline SAS had already been shown to be required for stable aircraft control at some flight conditions. Second, the MH-96 was to automate the selection of the forward loop gain based upon the aforementioned limit cycle concept. Finally, the MH-96 was to provide automatic blending of the reaction control system with the aerodynamic surfaces as the dynamic pressure varied during atmospheric exit and entry, and allow the use of hold modes for attitudes and airflow angles based on pilot selections.

The basic inner-loop architecture of the MH-96 is shown below in Figure A.2. The core components consist of the SAS pitch-rate feedback loop, which is functionally the same as that in the fixed-gain SAS. The inner loop gain is adjusted by a variable gain amplifier having a nonlinear gain characteristic with respect to the input of the gain changer integrator. The integrator is driven by the output of a rectifier whose output is compared with a set point. Since the rectifier output is approximately proportional to the signal power of the servo output in a specified band, the LCO amplitude can be controlled directly using this signal as a reference. The system as implemented contained several additional filters that are not depicted in Figure A.2.

The MH-96 was implemented using only analog electronics, and as such the designers were subject to limitations in the range and frequency response of the active and passive electronic components.
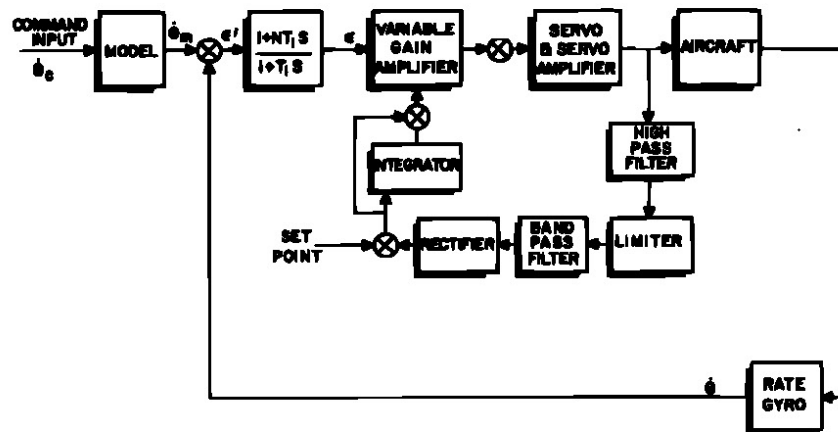
Figure A.2: MH-96 Pitch Axis Architecture

A.1.1 Development History and Design Features

The X-15 MH-96 AFCS began development in June 1959 and concluded in December 1962. The design concept arose as an evolution of adaptive concepts developed in the late 1950's, and relied extensively on development and flight test experience of a similar system for the F-101A aircraft [5].

The MH-96 was designed primarily with high-altitude mission-critical operation in mind, and was engineered with a high level of attention to subsystem reliability and redundancy. The MH-96 system was implemented in two independent strings, each having a dedicated rate gyro package, control electronics, gain changer hardware, and stick force transducers. The gain changers ran in parallel and the total loop gain at the servo input was based upon the sum of both gain changer outputs. Failure monitoring electronics were implemented to disable one channel of the MH-96 in the event of a detected anomaly. In this case, the other channel was able to provide sufficient gain to maintain acceptable handling qualities within a few seconds, since the single channel would increase the gain to compensate for the loss of the other channel [1].

Servo hardover failures were considered a credible failure mode by the design team, and were mitigated via an internal servo monitor associated with each servo. The servo command and response were compared to that of an internal analog model, and if the actual servo output rate differed in sign from the modeled output rate, the servo was disconnected and hydraulically locked [1]. Finally, a mechanical link from the pilot's center stick (and by interlink, the side stick) directly to the power actuator valve was provided in parallel with the servo input. This provided a mechanical override of the servo behavior, and the servo sizing and gearing allowed the pilot to overpower the servo with brute force if it opposed his commands. This feature was called upon during early flight tests of the MH-96; multiple pilots incorrectly engaged hold modes and mechanically overrode the pitch servo commands in order to maintain angle of attack [6].

Failure modes analysis was conducted and redundancy was included, within the limitations of the analog implementation, where it was warranted [7]. As implemented, the system was tolerant to any single-subsystem or component failure excepting the power actuator servo, which was not redundant. Failure modes were evaluated in the X-15 fixed-base simulation using actual flight control hardware where possible [5]. Reliability of the integrated system in the adaptive mode was computed to be greater than

99% during typical X-15 mission scenarios; the reliability of the fixed-gain subcomponent of the MH-96 was computed to exceed 99.4% [1]. Since the decision to remove the ventral fin had not yet been made at the time of the MH-96 development, the reliability guidelines considered the requirement for stability augmentation of the otherwise unstable airframe at certain entry conditions.

The MH-96 system was developed with substantial engineering support from NASA and USAF research pilots, including active X-15 pilots with flying experience on the other two aircraft. During the MH-96 development and beginning in July 1960, flight characterization of prototype flight control hardware in the MH-96 configuration was conducted using an F-101 that had previously used an earlier version of the AFCS, the MH-90 [1].

RCS control in the MH-96 was provided by a conventional linear phase-plane design that provided rate damping or attitude hold based upon the selected mode. The RCS engage thresholds were originally adjusted to provide engage/disengage at relatively high dynamic pressures, but initial flight tests concluded that a substantial savings in propellant could be realized through adjustment of the hysteresis thresholds, which eventually were set at 90% and 75% of the full-scale adaptive gain for engage and disengage, respectively. Extensive assessment of the RCS jet characteristics was conducted in support of the design, including the development of jet models based upon test data [7].

The transparency of the MH-96 reaction control blending, unfortunately, was also its most significant design flaw. Indication of the state of the reaction controls was not provided to the pilot, and proper operation of the RCS could only be deduced from visual observation of the attitude rockets [8]. This behavior would come to play a pivotal role in the 3-65 accident.

Although considered an experimental flight control system up to and including the demise of X-15-3, the MH-96 AFCS was qualified for flight operations in a two-tiered flight campaign consisting of "pre-acceptance" demonstration flights followed by "acceptance" qualification flights in 1961-1962. The first X-15 flight with the MH-96 activated was on December 20th, 1961. The first seven flights (engineering test and evaluation) were conducted by Neil Armstrong (NASA) and Robert White (USAF). The NASA/USAF acceptance flights (flights 8-11) were flown by Joe Walker (NASA) and Robert Rushworth (USAF). All subsequent flights on this airframe (more than 60) were made with the MH-96 engaged [9].

A.1.2 Known Shortcomings

During its greater than 6 years in use, the MH-96 demonstrated reliable operation and came to be accepted as an "operational" rather than "experimental" component of the X-15-3 aircraft. The evaluation and operation of the system was not without anomalies, and many were reproduced on the ground using identical hardware.

Some of the capabilities and engineering features of the MH-96 were later found to be superfluous in the X-15 application. In the initial design and flight qualification effort, a substantial focus was placed on hold modes, including and angle-of-attack hold mode, a heading hold mode, and a roll attitude hold mode. While these modes were designed to alleviate pilot workload and were evaluated in the qualification tests, they went unused by the operational pilots for virtually all subsequent flights. This most certainly is an artifact of evaluator pilots' experience with the hold modes in initial flights, where they tended to cause mode confusion and on multiple occasions resulted in pilots manually overpowering the trim actuators with the hold mode engaged. In fact, the somewhat famous incident of Neil Armstrong's Mach 3 Palmdale overflight was the result of an unintentional skip entry precipitated by a failure to recognize that the MH-96 hold mode was interfering with the entry angle-of-attack modulation [10].

Some unintentional behaviors were artifacts of limitations in the modeling of the aircraft during the MH-96 development, or practical limitations in its application. Most of these were known during development or discovered during the initial flight test campaign or in incidences in later flights.

1. Measured hysteresis effects in the X-15 control surface actuators were greater than those initially provided to the contractor, lowering the frequency and characteristics of the small amplitude servo limit cycle. Higher hysteresis levels also lowered the effective adaptation rate, implying that entries

**NASA Engineering and Safety Center
Technical Assessment Report**

Document #:
NESC-RP-14-00957

Version:
1.0

Title:
**A Comprehensive Analysis of the X-15
Flight 3-65 Accident**

Page #:
76 of 107

having high $d\bar{q}/dt$ would often operate for a brief period at supercritical gains. In most cases, this resulted in slightly higher amplitude limit cycles (3 degrees peak-to-peak), but the effects were otherwise benign [1].

2. RCS jet firings created a larger than expected transient gain reduction as an effect of servo response to the attitude rates induced by the RCS. The use of hysteretic engage/disengage logic was a result of this issue [7].

3. In quiescent operation (e.g. when powered up on the ground), system hysteresis could prevent the formation of the desired limit cycle and cause gains to ramp to maximum. This was alleviated in ground testing through preloading of the control surfaces, and, as predicted, did not occur in flight due to turbulence and aerodynamic loads.

4. Large pilot input commands were known to be sensed by the gain changer and cause transient reductions in gain. This is an artifact of this type of control architecture, given that a linear filter acting as a frequency-domain discrimination mechanism cannot distinguish between periodic signals with high power spectral density in the high-frequency range of interest and transient signals with rapid rise times. Limiter circuits were installed to mitigate this effect to some extent. In most flights, the transient gain reductions were small and went unnoticed by the pilot.

5. An unexplained servo transient anomaly persisted on the X-15-3 airframe that appeared unique to the MH-96 hardware implementation. The anomaly was manifested as a random servo "kick" resulting in a rapid but small amplitude motion of the servo. The direct control effects of the servo transients were negligible, but the unexpected transient was detected by the gain changer and caused temporary reductions in loop gain on the order of twenty seconds. Its exact cause was never found, but was probably a sensitivity to disturbances on the aircraft power bus [8].

6. Both types of failure monitoring circuits caused control system malfunctions due to false-positive sensing of failure conditions. The servo rate monitors frequently caused resets in a single channel, most likely due to the aforementioned servo transient anomalies. These were usually quickly noticed by the pilot and reset upon occurrence. In addition, a gyro rate monitor circuit was provided on each channel to detect full-scale gyro output failures by opening the failed channel in the event the gyro output exceeded 22.5 degrees per second. Under normal operational conditions, rates of this magnitude were not encountered. In the servo reset case, all gains associated with that channel were reduced to their minimum values so as to mitigate the risk of supercritical operation if a reset occurred at high dynamic pressure. However, if a reset occurred at low dynamic pressure, a several second time delay would elapse before the gains returned to sufficient values to enable the RCS.

7. Pilot display of MH-96 behavior was substantially absent from the initial design. It was improved to some extent as the result of initial flight tests, including relocation of the MH-96 status panel to be within the pilot's restrained field of view [10]. In addition to the lack of status information regarding the RCS system, the human interface with the AFCS remained markedly complex.

8. The mechanical interlink between the servoactuators and the control inceptor implied that adverse motion of the control surfaces was directly reflected through the mechanical linkages into both the center and side-stick controllers, sometimes with substantial forces. A severe "stick kick" phenomenon occurred when the servo overran the power actuator rate capability, which were much slower than the servos. This was resolved by the introduction of flow restrictors on the servos [9]. However, in all cases, servo motion commanded by the flight control system was reflected as stick motion. A secondary set of electric trim actuators (follow-up trim) was commanded to periodically recenter the stick [5]. The possibility of large amplitude and high force feedback motion to the stick remained, especially in the presence of large control surface motions involving the servos.

9. A divergent limit cycle existed in the MH-96 configuration pitch and roll axes as a result of a structural mode filter added just prior to MH-96 acceptance testing in 1961. This mode of failure was known to the program, definitely by 1965 (having occurred in another flight, although non-destructively), and possibly as early as 1962 (predicted by simulation). However, the exact reasons for this behavior may have been unknown until determined through the analysis associated with the present report.

A.2 MH-96 X-15 Model Development

An extensive effort was undertaken to construct an sufficiently detailed simulation of the X-15 flight control system so that both nominal and off-nominal behaviors that were believed to have contributed to the Flight 3-65 accident could be reproduced. As much of the X-15 design details are dispersed among multiple sources, constructing a model that is a reasonably accurate representation of X-15-3 at the time of the accident proved to be a substantial challenge. Some data was extracted from internal and publicly available research reports, but the vast majority of the configuration data associated with the flight control system was taken from the MH-96 contractor reports [7, 1, 11, 12, 10, 6, 5]. It is worth noting that these reports are not self-consistent and one must very cautiously interpret the data therein to ensure that the quoted information is representative of the final aircraft configuration after the "acceptance flight test" period in 1962.

The simulation was constructed in the MATLAB/Simulink environment so as to support both time-domain nonlinear simulation (for reproduction of limit cycle behavior) and frequency-domain describing function analysis (for prediction and forensic analysis of adverse nonlinear behaviors).

The objective of the X-15 simulation is to reproduce and analyze the behavior exhibited in the 3-65 accident. To that end, detailed environmental, navigation, and aircraft dynamics models are not required, since the dominant nonlinear effects appear in the servo, power actuator, and flight control elements. In the present simulation, the majority of the high-fidelity modeling is associated with the actuator and the MH-96 electronics.

A summary of the major simulation elements and their data sources appears in the following subsections.

A.2.1 Airframe Dynamics

For the purposes of the present control system analysis, a linear, time-invariant model of the short period pitch mode of the X-15 is sufficient to capture the rigid-body and aerodynamic effects on the control system. Since structural flexibility was not a key factor in the control system instability (having been sufficiently attenuated via filtering), structural modes were not included in the analysis. In addition, the normal acceleration (N_z) feedback channel of the MH-96 was not modeled as the expected characteristics appear using only the attitude dynamics.

Normalizing Eq. A.1 by dynamic pressure, the short-period airframe rate dynamics have the general form

$$G_p(s) = \frac{\bar{q}}{\bar{q}_0}\left(\frac{M_{\delta 0}\left(s + \frac{1}{\tau_a}\right)}{s^2 + 2\zeta_a\omega_a + \omega_a^2}\right) \tag{A.3}$$

where $M_{\delta 0}$, ω_a, and ζ_a are functions of Mach number and dynamic pressure and $\bar{q}_0$ is the reference dynamic pressure (taken as unity, $\bar{q}_0 = 1$). The simulated flight condition is that of the LCO onset at approximately 270 s MET, $\bar{q} = 390$ psf and Mach 4.7 with a moderate angle of attack of $\alpha \approx 5°$ (see Appendix B).

Flight data appearing in [13] was collected during the test program at various Mach numbers and angles of attack through free-decay fits. Data for the SAS-off (bare airframe) cases was used to estimate the natural frequency and damping ratio of the vehicle pitch mode as a function of Mach number in the

moderate angle-of-attack range. Based on interpolation to the aforementioned flight condition, it follows that $\omega_a = 2.56$ rad/sec (0.41 Hz) and $\zeta_a = 0.08$ at this flight condition. Natural short period damping of the X-15 pitch mode was quite low.
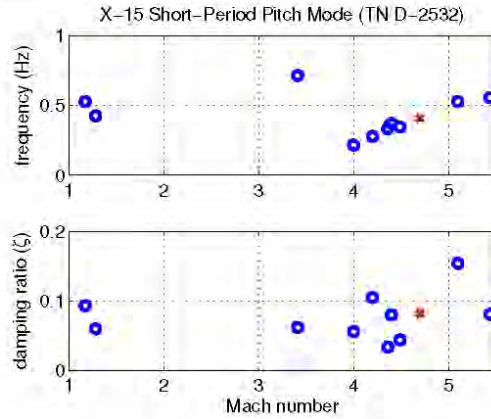

Figure A.3: X-15 short-period pitch data (bare airframe).

The control effectiveness parameter $M_{\delta 0}$ is determined from the power-off pitch moment data in [13] at the empty loading condition (Table 1).

Parameter	Description	Value
S	wing area	200.0 ft^2
$\bar{c}$	wing reference chord	10.27 ft
I_{yy}	pitch axis MOI, empty	8.7×10^4 slug $-$ ft^2
$C_{m\delta h}$	stabilator effectiveness	-0.7448 $\frac{1}{\text{rad}}$
$M_{\delta 0}$	control parameter ($\bar{c}SC_{m\delta h}/I_{yy}$)	-0.0176 $\frac{1}{\text{psf}-\text{sec}^2}$

Table 1: Power-off pitch moment data

The pitch zero is estimated from [12] at $\tau_a = 1.64$.

The short-period dynamics are mechanized in a state-space form and incorporated into a simple airframe model including the rate gyro dynamics (Figure A.4).

The rate gyro response is second order with parameters $\omega_n = 125$ rad/sec and $\zeta = 0.4$ [5]. A surface turbulence model is included with a break frequency of 1.0 rad/sec.

The dynamic pressure is variable and scheduled with respect to time. For simulation of the actual 3-65 entry, it is assumed that the Mach number and angle of attack (and thus the short-period mode parameters) are constant while the dynamic pressure is varied. The dynamic pressure profile for the entry is extracted from the as-flown flight data ranging from about 190 to 285 sec MET (referenced to ignition) (Figure A.5). For analysis of the limit cycle behavior, the dynamic pressure is fixed at the value where LCO began to appear in the flight data at approximately 270 sec MET, or $\bar{q} = 390$ psf.
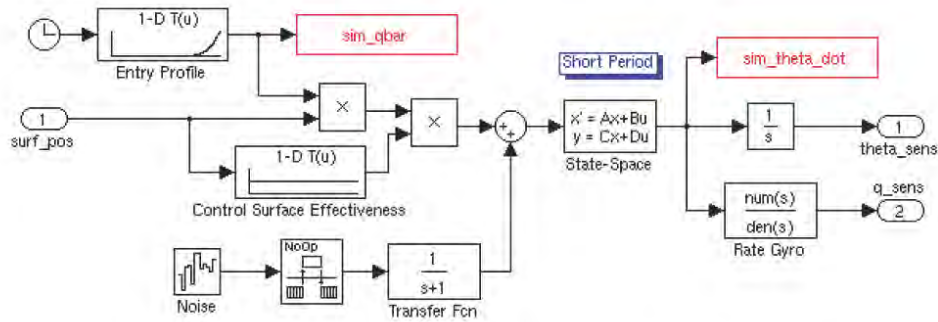
Figure A.4: X-15 short-period dynamics with sensor
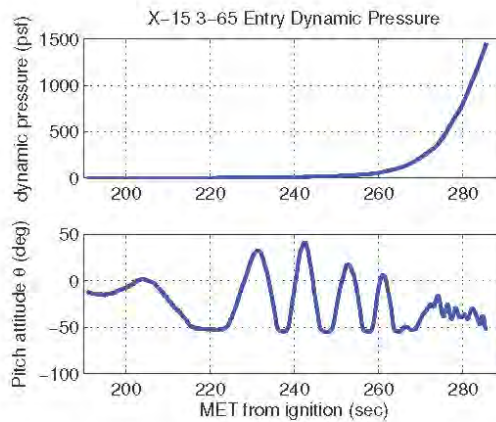
Figure A.5: X-15 3-65 entry dynamic pressure and MH-96 LCO

A.2.2 Servoactuator Model

The X-15 servoactuator is the dominant nonlinear element in the aircraft rate loop. The X-15 actuator was a two-stage power-assist design driven by a series hydraulic servo and hydraulic power actuator. The design of the servo for the MH-96 changed from a fully-integrating configuration to a semi-integrating configuration during the development of the MH-96 in order to improve low-frequency phase margin characteristics while still maintaining integrating trim capability [6]. In NASA FRC publications, the servo travel is given in units of inches (±1), corresponding to ±15 degrees of stabilator authority (out of 30 degrees total). The mechanical pilot interface to the power actuator provided another ±15 degrees of authority for the pilot [14]. The layout of the servoactuator system is shown in Figure A.6.

		Document #:	Version:
NASA Engineering and Safety Center **Technical Assessment Report**		**NESC-RP-14-00957**	**1.0**

Title:	Page #:
A Comprehensive Analysis of the X-15 Flight 3-65 Accident	80 of 107
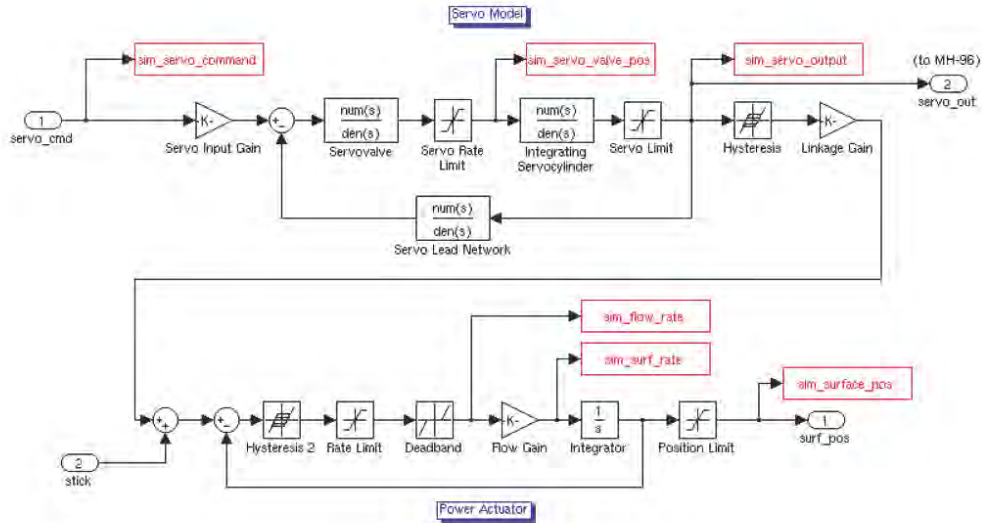
Figure A.6: X-15-3 servoactuator system

In the present simulation, a prescribed motion model the surface dynamics is used. Since the cantilever stabilator resonant mode was above 12 Hz [5], both the rigid-body and elastic motion of the stabilators is neglected. The servoactuator parameters are taken from Refs. [14, 7, 12, 5] and are shown in Table 2. Several critical servo loop gains are missing from the reports, especially [5], and were empirically adjusted to match other frequency response data (appearing as transfer functions or frequency response magnitude plots) or were calculated from equivalent circuit parameters (e.g. degree surface per unit μA).

Parameter	Value	Subsystem	Model
Servo input gain	1.0	Servovalve	$\frac{k\omega_n^2}{s^2+2\zeta\omega_n s+\omega_n^2}$, $\omega_n = 109$, $\zeta = 0.78$, $k = 6$
Servo rate limit	4.0 in/sec		
Servo travel limit	1.0 inch		
Servo/power actuator backlash	0.25 deg	Servocylinder	$\frac{1}{s(\tau s+1)}$, $\tau = 0.006$
Power actuator mechanical gain	15 deg/inch		
Power actuator/surface backlash	0.25 deg		
Surface flow gain	25.0 /sec	Servo lead network	$\frac{\tau_1 s+1}{\tau_2 s+1}$, $\tau_1 = 1.2$, $\tau_2 = 0.2$
Surface rate limit	25.0 deg/sec		
Surface position limit (absolute)	± 30 deg		

Table 2: X-15 servoactuator model parameters

The complexity of this full nonlinear model of the actuator can be compared with the commonly used approximation appearing in much of the X-15 literature;

$$H_A(s) = \frac{1}{0.15s + 1}. \tag{A.4}$$

A.2.3 MH-96 Model

The MH-96 autopilot model of the pitch axis is developed primarily using the information in Refs. [7, 1, 12, 15, 5] and is shown in Figure A.7.
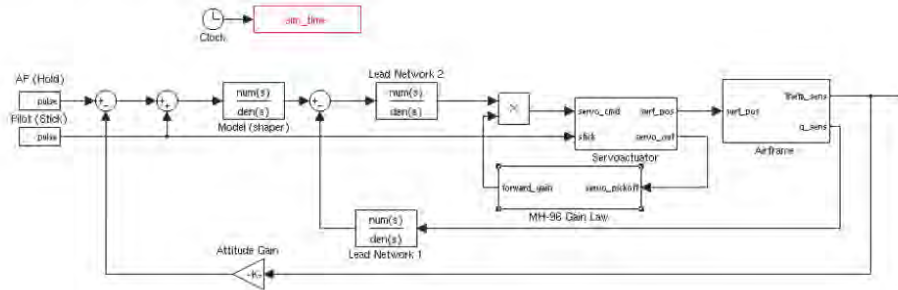
Figure A.7: MH-96 SAS loop model

The MH-96 consists of the SAS inner rate loop and the attitude hold loop. For the purposes of this study, the attitude hold loop is disabled as it was not activated on flight 3-65. The inner rate loop contains two filters; one is in the feedback (minor loop) configuration and the other is in the compensator (forward loop) configuration. In the present form, the MH-96 AFCS and X-15-{1,2} SAS are functionally identical if the MH-96 adaptation dynamics are disabled (fixed gain) and the "Lead Network 1" and "Lead Network 2" filters are modified accordingly.

In the MH-96 configuration, the pitch axis input filter (reference model) is given by a first-order lag of the form

$$H_M(s) = \frac{1}{0.5s + 1} \tag{A.5}$$

and the "Lead Network 1" filter is a lead-lag stage having the transfer function

$$H_{L1}(s) = \frac{1}{0.01s + 1}\left(\frac{0.1s + 1}{0.01s + 1}\right). \tag{A.6}$$

The "Lead Network 2" filter is a structural notch filter of order 9. The notch filter design appearing in the original design report [12] is compared with the magnitude and phase response of the reconstructed filter (Figures A.8 and A.9).
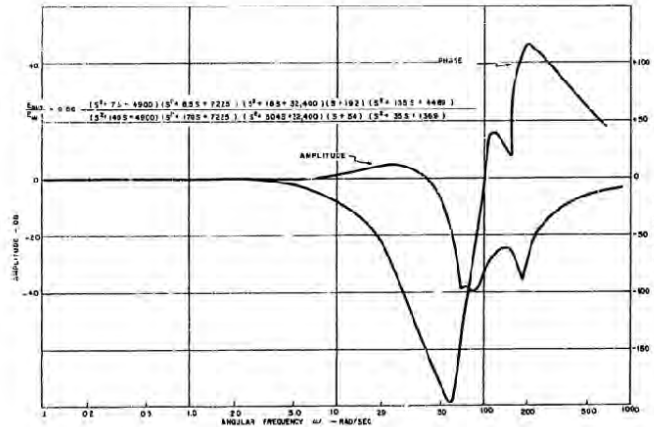
Figure A.8: Original notch filter
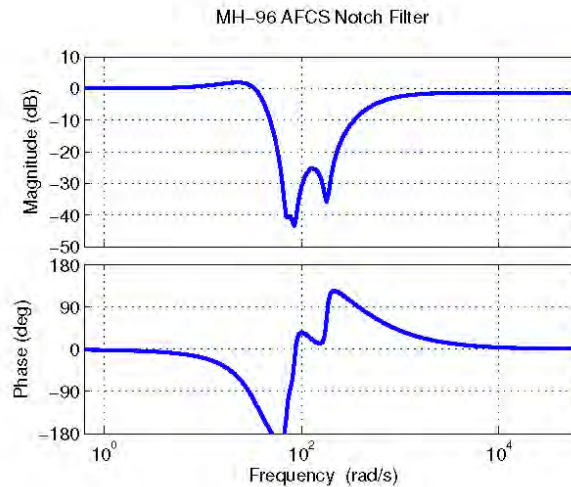
Figure A.9: Reconstructed notch filter

In the design configuration prior to the 1960-1961 modifications to attenuate the stabilator resonant modes, the form of the "Lead Network 1" and "Lead Network 2" filters differed and their original form can be found in [5]. They are given by

$$H_{L1}(s) = \frac{0.12s + 1}{0.02s + 1} \tag{A.7}$$

$$H_{L2}(s) = \frac{0.2s + 1}{0.02s + 1}. \tag{A.8}$$

It is important to note that while the fixed-gain and MH-96 inner loop designs are functionally nearly

identical, the aggressive notch filter is required in the MH-96 configuration to attenuate the high-frequency gain of the loop shaping filter (Equation (A.6)). The high gain characteristic of this lead network is necessary in the adaptive configuration to ensure that the desired limit cycle ("adaptive mode") appears at the specified frequency.

The MH-96 adaptation law (Figure A.10) consists of the servo LCO detector circuit, comprised of a high-pass filter, input limiter, and band-pass filter-rectifier. The rectified output is compared with a setpoint limit cycle amplitude (assumed to be on the order of the hysteresis magnitude, approximately 0.1 deg average power). The input limiter is set to a value of three times the hysteresis magnitude [5].
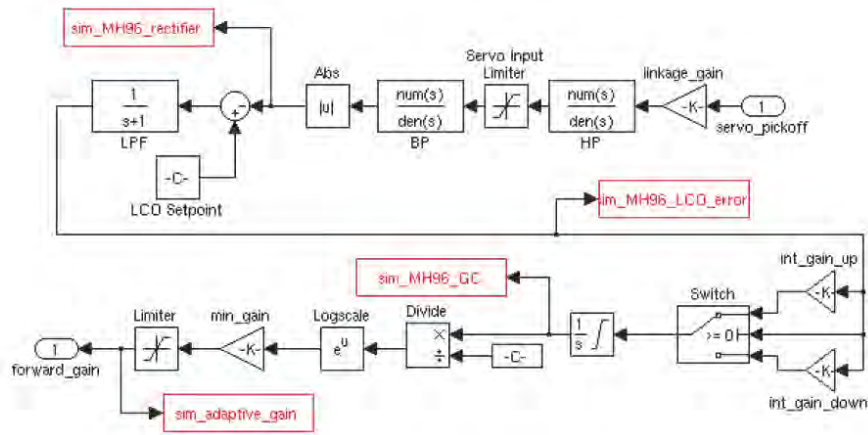
Figure A.10: MH-96 adaptation law

The adaptation gain scale of the MH-96 was nonlinear, having an exponential gain characteristic [1]. Furthermore, the down-gain is a factor two larger than the up-gain [16], which was set such that at the saturated input condition, the gain would reach full scale in approximately 20 seconds. Based upon the data in [5], the nonlinear gain function is approximated by

$$k_a(u) = k_0 e^{u/7.25} \tag{A.9}$$

where u is the gain changer integrator output and k_0 is the minimum gain. The minimum and maximum gains of the fixed-gain SAS and the MH-96 differed, and are given in Table 3.

	SAS [14]	MH-96 [5]
Minimum (deg/(deg/sec))	0.075	0.546
Maximum (deg/(deg/sec))	0.750	11.645

Table 3: SAS and MH-96 gain range

The band-pass and high-pass filters are described by the appropriate continuous-time transfer functions

given by

$$H_{BP}(s) \;=\; \frac{4.883s^2}{0.01405s^4 + 0.6725s^3 + 12.24s^2 + 132s + 877.9}, \qquad \text{(A.10)}$$

$$H_{HP}(s) \;=\; \frac{0.0521s}{0.0002558s^2 + 0.052s + 1}, \qquad \text{(A.11)}$$

respectively. In both cases the filter coefficients have been normalized to a maximum singular value of unity to avoid implementation of intermediate analog amplifier gains in the MH-96 model. The band pass filter is a mechanization of the original filter appearing in [5] with the center frequency adjusted to the expected post-flight-test servo limit cycle frequency of approximately 2.0-2.5 Hz.

A.3   Time-Domain Simulation

The MH-96/X-15 model was evaluated under nominal and off-nominal conditions to verify the implementation and characterize the sensitivity to inputs and flight condition. The individual simulation cases follow.

A.3.1   Nominal Adaptation Behavior

The nominal adaptation test case is designed to evaluate the gain changer behavior. The aircraft dynamics are held in a fixed-parameter configuration at a Mach number of 4.7 and a dynamic pressure of 400 psf. The gain cycling behavior consistent with the literature [17] is shown in Figure A.11. In this case the servo LCO frequency appears at the expected 3.5-4.0 Hz. The cycling behavior appears only in quiescent conditions and is substantially more pronounced with the original filter design. The modified (flight) design, consistent with the data found in [15], exhibits better steady-state convergence and lowers the servo LCO frequency to approximately 2 Hz (Figure A.12). In both cases, the resultant motion at the surface is on the order of 0.5 degree peak. As noted in the original design documentation, the attainable limit cycle frequency and amplitude depends strongly on the hysteresis and deadbanding in the actuator linkages.
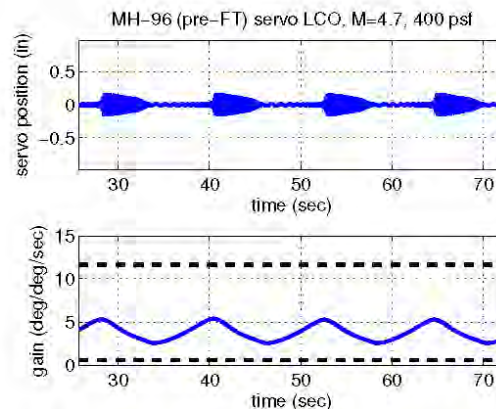
Figure A.11: Gain cycling (pre-flight-test configuration)
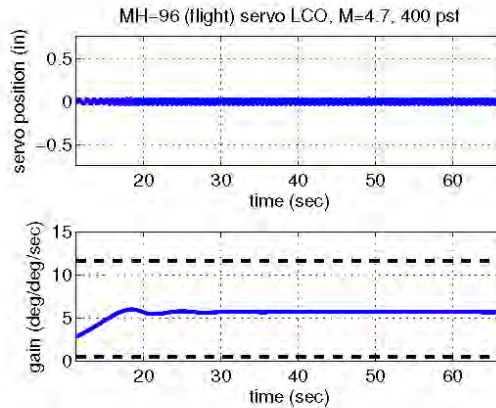
Figure A.12: Gain cycling (flight configuration)

The efficacy of the invariant-response design of the MH-96 can be illustrated using a transient response simulation of a pitch maneuver (Figure A.13). In this case, the attitude loop is closed ($k_P = 0.7$) and a 5 degree pitch attitude command is issued with a period of 10 seconds at a dynamic pressure of 400 psf and 800 psf. The MH-96 provides an aircraft transient response that is invariant with respect to the 2:1 variation in dynamic pressure, and tracks the reference model filter 1st order lag characteristic.
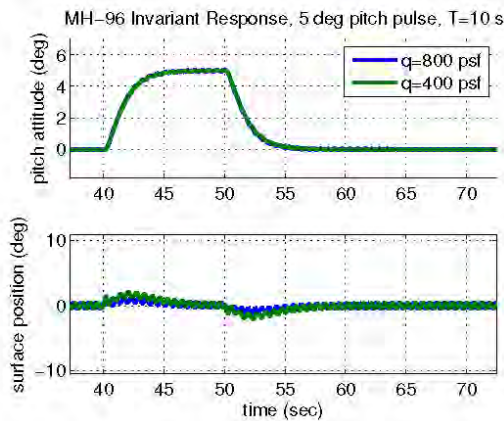
Figure A.13: MH-96 invariant model response

A.3.2 Entry Adaptation

The high dynamic pressure and dynamic pressure rate seen during the 3-65 anomalous reentry was within the design capability of the MH-96 adaptation gain dynamic range and adaptation rate so long as no exogenous disturbances caused saturation of the control surface actuators. This can be verified through simulation of the adaptation dynamics during the planned 3-65 entry (to approximately 800 psf) and the anomalous entry (exceeding 1500 psf). In both cases, since the system is operating in a ballistic mode prior to the entry, the adaptive gain is at maximum. Even when using the accident flight dynamic pressure

profile, the adaptive law is successful in establishing the desired servoactuator limit cycle and modulating the forward gain to the proper value (Figure A.14). This analysis result contradicts the author's early hypothesis that the adverse LCO was precipitated by a dynamic pressure rate-of-change exceeding the capability of the MH-96 gain changer.
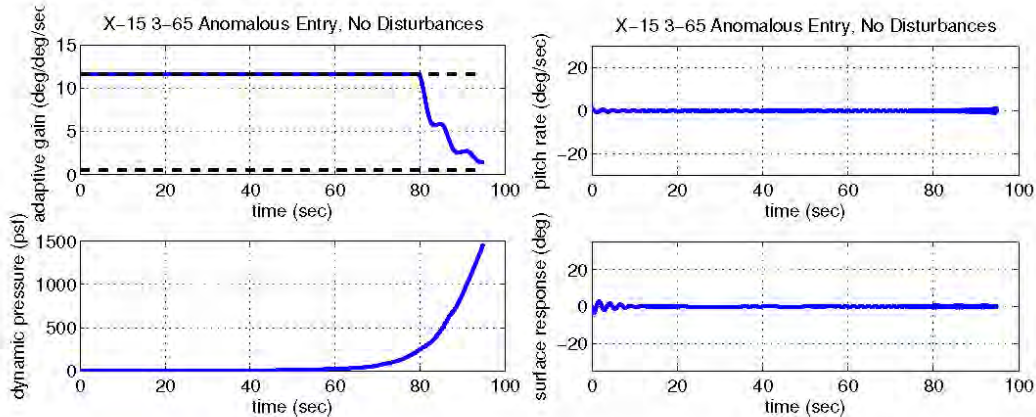
Figure A.14: MH-96 3-65 entry, no disturbances

A.3.3 Adverse LCO

The adverse LCO appears in the anomalous entry due to saturation of the control surface actuators such that the short-period pitch mode of the aircraft is simultaneously excited during the period when the gain adaptation would otherwise be rapidly reducing system gain to compensate for the rapid increase in dynamic pressure (Figure A.15).
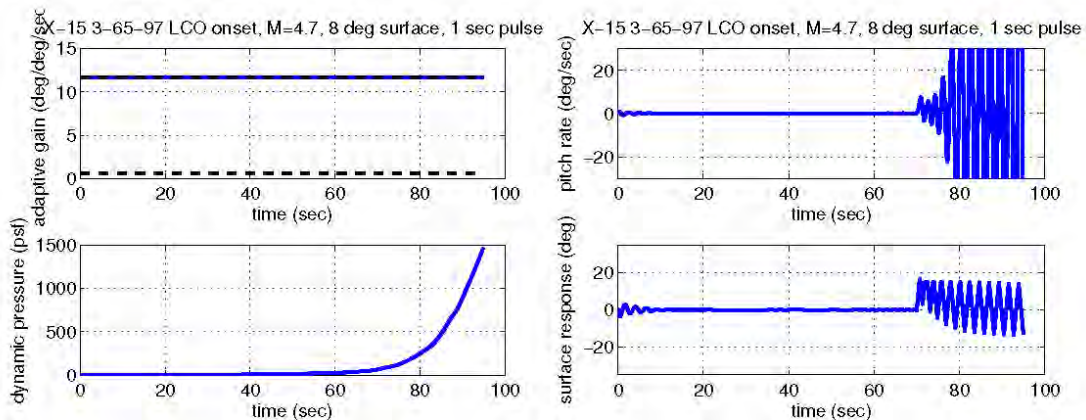
Figure A.15: MH-96 3-65 entry, pilot input

In this case, the actuator saturation is induced using a pilot stick pulse equivalent to 8 degrees of surface deflection with a 1 second period. The rapid pulse induces a combined response of the rigid-body short period dynamics that maintains actuator saturation. The MH-96 gain changer, no longer able to

identify and establish the desired small-amplitude LCO, maintains maximum gain [8]. In this high-gain condition, the short-period pitch mode is divergent.

The same divergent LCO can be induced in the system even in a fixed gain condition with fixed dynamic pressure, if the pilot input magnitude is large enough to induce rate limiting in the actuator (Figure A.16). This occurs with moderate gain levels exceeding those of the fixed-gain SAS but much below the MH-96 maximum gain. This implies that a more serious mechanism involving the fundamental stability of the SAS inner loop is responsible for the limit cycle behavior, since in the fixed-gain case the behavior persists.
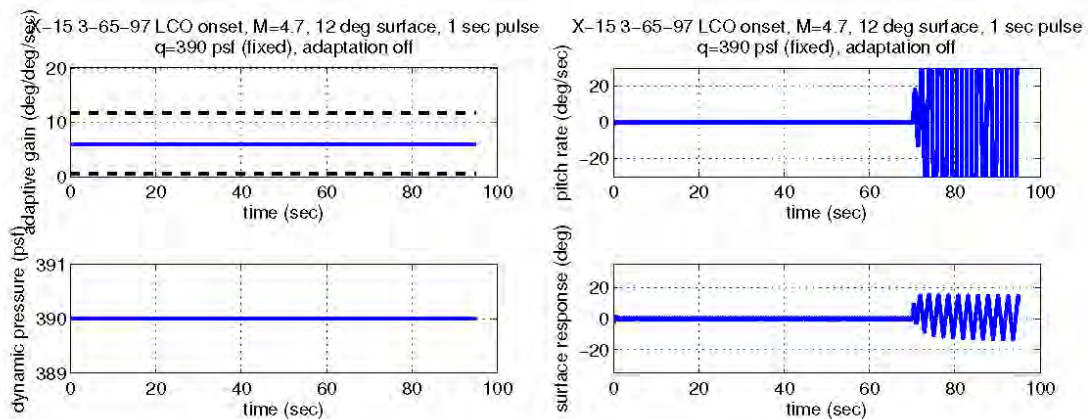
Figure A.16: Fixed dynamic pressure, large pilot input, fixed gain

It is illustrative to consider that the introduction of lag due to the implementation of the structural notch filter may be related to the apparent rate-limit divergent limit cycle oscillation. Under the time-varying 3-65 entry conditions, the system is simulated with an identical pilot input but with the original loop filter design (Eq. A.7). Although rate limiting is induced for a short time, the actuator does not couple with the short-period mode and thus no divergent oscillation is induced (Figure A.17).
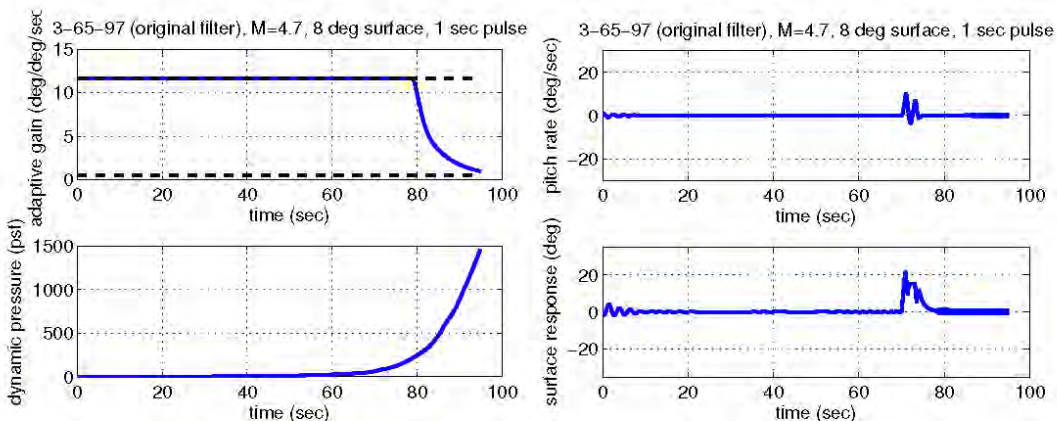
Figure A.17: 3-65 entry, large pilot input, original filter

From these results, it can be concluded that the structural notch filter introduced to mitigate the stabilator resonance destabilizes the inner loop independently of the adaptive gain mechanism, while the original design did not. An analytical investigation using numerical describing function analysis confirms this and appears in the following section.

A.4 Describing Function Analysis

Describing function (DF) analysis is a useful tool for predicting the existence of sustained periodic solutions of SISO nonlinear feedback dynamical systems [18]. The use of describing functions is based on several approximating assumptions, the most prevalent being that the response of a nonlinear dynamical system with output q and sinusoidal input $u = A \sin \omega t$ described by

$$\dot{z} = f(z, u) \tag{A.12}$$
$$q = h(z, u) \tag{A.13}$$

can be approximated by a complex-valued *describing function* $N(A, \omega)$ as a function of the input amplitude A and the input frequency ω. If the nonlinearity in Equations (A.12-A.13) is incorporated into the feedback path of an otherwise linear SISO plant, under certain conditions the describing function N can be used to approximate the nonlinear element for the purposes of analysis (Figure A.18).
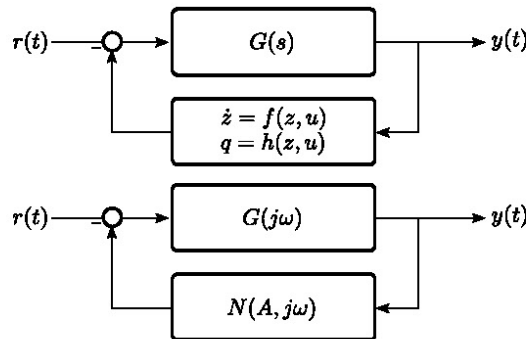
Figure A.18: Original and describing function approximation of feedback nonlinearity

In most introductory texts on describing function analysis, it is assumed that the nonlinearity is single-valued and static (memoryless), in which case $f = 0$ and $q = h(u)$; that is, the system has no dynamics. However, the theory does not preclude the use of a dynamic nonlinearity in the feedback path so long as the describing function is computable (e.g., the nonlinear system is locally stable with respect to bounded inputs), even if it cannot be determined analytically.

When the approximation N is incorporated into the loop, the linear Nyquist theorem predicts the existence of a sustained periodic oscillation (a limit cycle) at a particular frequency ω_k and amplitude A_j if the linearized system return difference function satisfies the equality

$$1 + G(j\omega)N(A, j\omega) = 0, \tag{A.14}$$

for some $\omega = \omega_k$ and $A = A_j$. This leads to the well-known sinusoidal inverse describing function relationship

$$G(j\omega) = -\frac{1}{N(A, j\omega)}. \tag{A.15}$$

The sinusoidal describing function N is computed from the truncation of a Fourier series expansion of the response of the nonlinearity to an input sinusoid. The complex number N has magnitude

$$|N| = \frac{\sqrt{a_1'^2 + b_1'^2}}{A} \qquad (A.16)$$

and angle

$$\angle N = \tan^{-1}\left(\frac{a_1'}{b_1'}\right) \qquad (A.17)$$

where a_1', b_1' are the real Fourier coefficients associated with the first harmonic, given by

$$a_1' = \frac{2}{T} \int_{-T/2}^{T/2} q(t)\cos(\omega t)\, dt \qquad (A.18)$$

$$b_1' = \frac{2}{T} \int_{-T/2}^{T/2} q(t)\sin(\omega t)\, dt. \qquad (A.19)$$

A.4.1 X-15 Analysis Overview

In the X-15 analysis, it is reasonably assumed that for the purposes of limit cycle prediction, the adaptive gain itself does not introduce dynamics (that is, the adaptation mode is separated in frequency from the limit cycle dynamics) and that the plant (airframe, filters, etc.) are linear.

The present form of DF analysis used herein for the prediction of the MH-96 limit cycle behavior is similar to the exact numerical describing function technique described by Klyde et al. [19] but is extended to facilitate direct analysis of the effect of the DF in-the-loop owing to the multivariable nature of the adaptive gain, DF frequency, and loop amplitude. Traditionally, inverse describing function analysis determines a frequency $\omega = \omega_k$ and amplitude $A = A_j$ at which Equation (A.15) is satisfied by determining, graphically, intersections of $G(j\omega)$ and $-N(A, j\omega')^{-1}$ in the complex plane for which $\omega = \omega'$, since each are an independent function of frequency. In the present analysis, the function $G(j\omega)N(A, j\omega)$ (Equation A.14) is computed over a set of discrete frequencies $\omega = \omega_k$, $k = 1, 2, \ldots, n$ and compared with the point $-1 + j0$ in the complex plane. This provides an equivalent criterion to Equation (A.15) but eliminates the additional frequency variable. At each unique amplitude A_j, the resultant curve can be interpreted similarly to a traditional Nichols or Nyquist plot, and provides a measure of equivalent (nonlinear) gain or phase margin with respect to the predicted LCO. This will be referred to as "DF-in-the-loop."

The nonlinear element under analysis is the servoactuator assembly, including the servovalve, servocylinder, and power actuator. At each discrete amplitude A_j, a frequency vector is constructed such that the describing function $N = N(A_j, j\omega_k)$ is computed over a discrete set of frequency points $k = 1, 2, \ldots n$ with $0.06 < \omega_k < 125$ rad/sec (approximately 0.01 - 25 Hz). For each j and k, the response of the servoactuator (degrees response with respect to degrees command) is computed numerically from a time-domain nonlinear simulation of the servoactuator element using Equations (A.16-A.19) above. In all cases, the time-domain simulation is allowed to reach steady state to avoid corruption of the Fourier coefficients by transient effects.

Finally, the numerical describing function $N(A_j, j\omega[k])$ is used directly to compute the forward transfer function $G(j\omega[k])N(A_j, j\omega[k])$ after conversion of the linear part to discrete time. A limit cycle *can* exist at some value of the forward loop gain if the curve $G(j\omega_k)N(A_j, j\omega_k)$ crosses the $-\pi$ phase line at any point and that point is within the gain authority of the adaptive law.

In this analysis, parametric uncertainty is not considered; these results assume a perfect implementation of the flight control electronics and X-15 parameters based upon a single test point. Limit cycle behavior, therefore, is more likely to occur in the actual system due to unmodeled dispersions.

A.4.2 Analysis of Small-Amplitude MH-96 LCO

The DF technique can be used to predict the small-amplitude servoactuator LCO at the converged value of the forward loop gain. From the flight configuration example shown above in Section A.3.1, the adaptive gain reaches a steady-state value of 5.7 deg/(deg/sec) at a dynamic pressure of 390 psf yielding a small-amplitude limit cycle of 2.58 degrees (taken at the servo input) and approximately 0.5 degrees at the surface with an LCO frequency of 1.6 Hz.

A DF approximation of the servoactuator with these parameters is computed and compared with the nominal linear model of the servoactuator. As can be seen in Figure A.19, the response of the actuator matches well at low frequencies but exhibits slightly more phase lag.
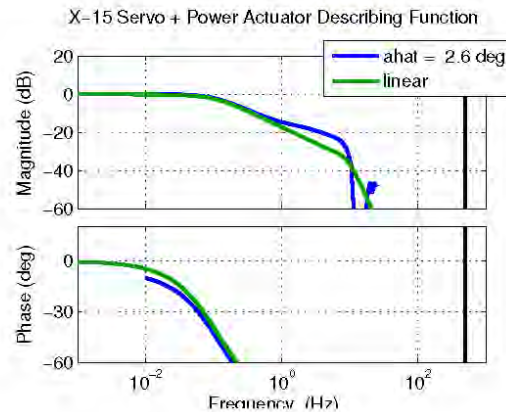
Figure A.19: X-15 servoactuator small-amplitude describing function

Note that in this analysis, the other actuator nonlinearities in addition to the basic rate limiting contribute to the divergent behavior. However, a describing function analysis of the power actuator alone confirms that the response matches well with the published results in the existing literature [20] (Figure A.20).
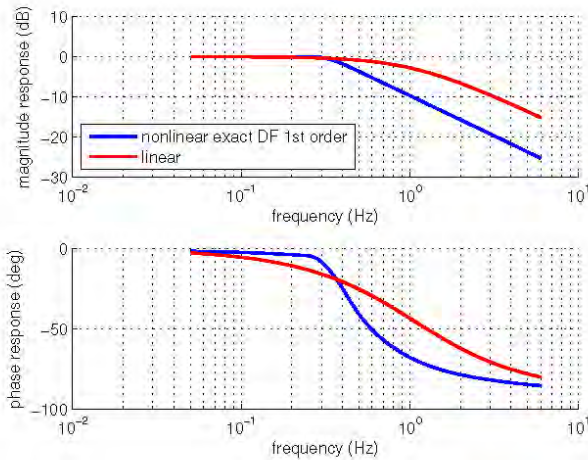
Figure A.20: Describing function analysis of X-15 power actuator only, 15 degree input amplitude

Using the servoactuator DF in-the-loop at the stated forward gain condition, the small-amplitude LCO is accurately predicted by the numerical analysis. Since the forward gain in the DF analysis matches the converged gain, the system intercepts the critical point. The $-\pi$ phase line is shown for comparison. It should be noted that the short period mode, appearing at approximately 0.4 Hz, has relatively little equivalent phase margin at this condition at stable values of the forward gain.
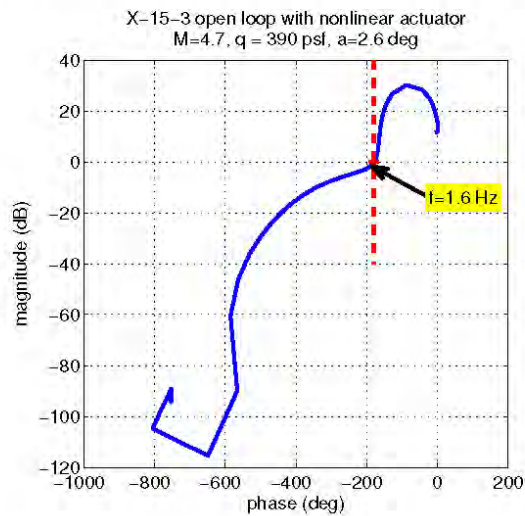
Figure A.21: X-15 servoactuator small-amplitude LCO prediction

A.4.3 Analysis of Large-Amplitude MH-96 LCO

Based upon the time-domain analysis, it was observed that the large-amplitude LCO tended to be precipitated by large inputs causing actuator rate saturation coupled with an excitation of the short-period pitch mode. In order to determine the possible transition amplitude for the adverse LCO, the amplitude-frequency parameter space was searched for a DF such that the short-period mode would approach critical stability when at the 3-65 entry conditions (maximum forward gain, 390 psf). The transition amplitude for this condition consists of a large servo command of approximately 80 degrees peak equivalent, or a command-to-authority factor of about 6:1. Large servo commands exceeding the servocylinder limit of 1 inch (15 degrees equivalent) will cause saturation in the servo, the power actuator, or both. The effects of saturation on the actuator frequency response are shown in Figure A.22. Near the short-period frequency, the effective phase lag is increased by approximately 25 degrees.
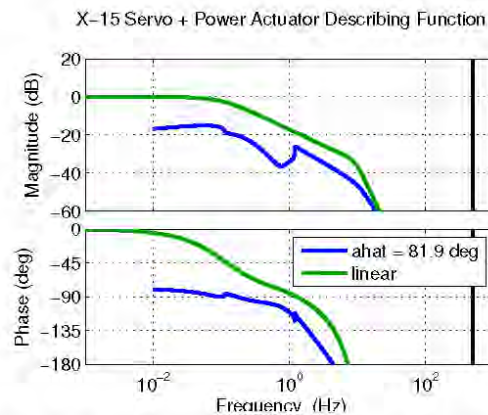
Figure A.22: X-15 servoactuator large-amplitude describing function

The coupled response with the servoactuator DF in-the-loop is shown in Figure . At a transition amplitude, the short-period mode phase margin approaches zero, predicting a periodic oscillation in the closed loop near a frequency of 0.55 Hz (simulation shows a frequency consistent with the short-period mode at 0.43 Hz). While not as accurate a predictor of the oscillation frequency as in the low-amplitude case, this is to be expected using the approximation technique since the dominant complex poles near this frequency are clearly associated with the short-period mode.

It was noted before in the analysis of the high-frequency desired LCO that the short-period mode had very little phase margin when operating at the critical gain (Figure A.21). In the design of the MH-96, an implicit assumption was that the system phase shaping (via filters in the rate feedback path) provided for a linear phase margin that was approximately invariant with respect to the forward gain. Based on a comparison of the original system response with the flight configuration using the structural notch filter, it appears that the introduction of the notch filter substantially degraded the phasing of the short period mode due to the introduction of additional low-frequency lag (Figure A.23). Even under these conditions, the original design maintains more than 30 degrees of phase margin for the short-period mode.
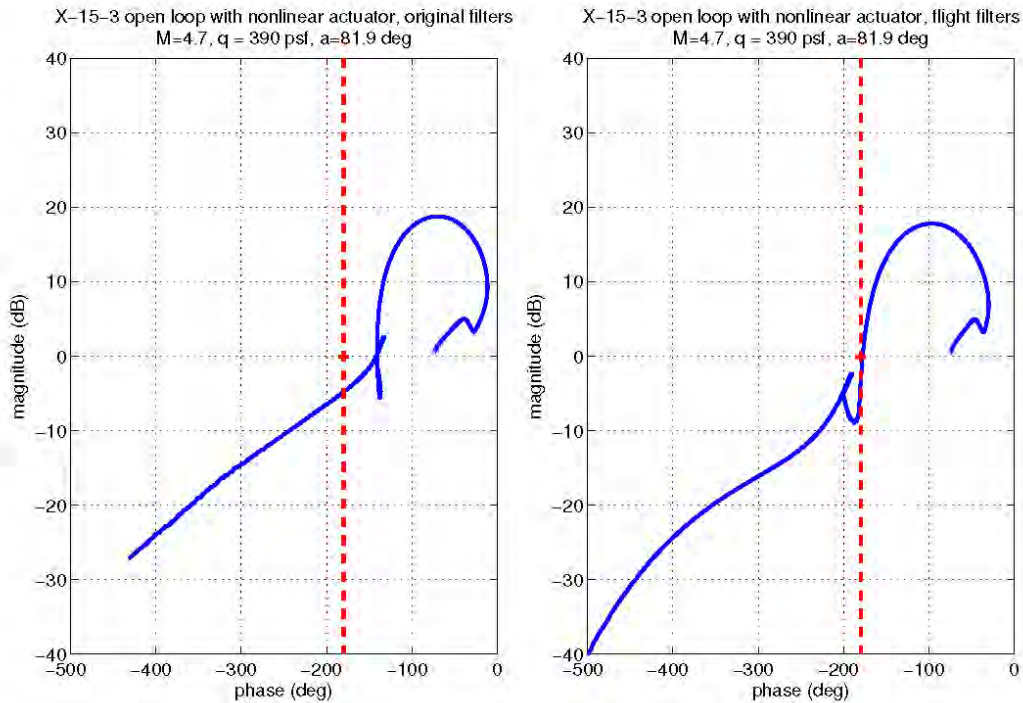
Figure A.23: X-15 servoactuator large-amplitude LCO prediction

Under the proper circumstances (including a flight condition where the bare airframe damping is small combined with a saturated servoactuator), the effective system lag was sufficient to destabilize the rigid body. This appears to have been a latent flaw in the design of the notch filter, whereas the original system design was not susceptible. However, the original filters did not provide sufficient attenuation for the problematic stabilator resonant modes, and lacking a detailed design study, it is unclear as to whether *any* design would have been feasible given the limitations in the analog filter implementation. Furthermore, while describing function techniques and the "equivalent lag" effects of saturated actuators were known at the time, it cannot be reasonably expected that the designers would have been able to analyze the robustness of the system in the level of detail presented herein due to limitations in computational resources.

A.5   Conclusions

The MH-96 adaptive flight control system was an exceptional example of practical and innovative flight control system engineering that substantially improved the capability of the X-15-3 airplane. Unfortunately, the realities of its implementation appear to have eventually so constrained the design that its robustness was substantially and unknowingly compromised, and a lack of attention to the human-machine interface substantially contributed to the loss of X-15 Flight 3-65.

References

[1] D. Mellen, G. Cole, and J. Lindahl, "Advanced Flight Vehicle Self-Adaptive Flight Control System, Part II: Design of MH-96 System," Tech. Rep. WADD-TR-60-651, Part II, Flight Control Laboratory, Wright Air Development Division, USAF Air Research and Development Command, February 1961.

[2] J. Blakelock, *Stability and Control of Aircraft and Missiles, 2nd Ed.* Wiley-Interscience, 1991.

[3] "Flight Control Design - Best Practices," Tech. Rep. RTO-TR-029, North Atlantic Treaty Organization Task Group SCI-026, December 2000.

[4] Royal Australian Air Force, "Determination of the Pitch and Roll Gain Limits for the F-111C Automatic Flight Control System," Tech. Rep. TN Aero 81, Aircraft Research and Development Unit, December 1987.

[5] J. Lindahl, W. McGuire, and M. Reed, "Advanced Flight Vehicle Self-Adaptive Flight Control System, Part VII: Final Report on Study, Development, and Test of the MH-96 System for the X-15," Tech. Rep. WADD-TR-60-651, Part VI, Air Force Flight Dynamics Laboratory, Research and Technology Division, USAF Systems Command, December 1963.

[6] J. Lindahl, W. McGuire, and M. Reed, "Advanced Flight Vehicle Self-Adaptive Flight Control System, Part VI: Final Flight Test Report," Tech. Rep. WADD-TR-60-651, Part VI, Air Force Flight Dynamics Laboratory, Research and Technology Division, USAF Systems Command, October 1963.

[7] B. Boskovich, G. Cole, and D. Mellen, "Advanced Flight Vehicle Self-Adaptive Flight Control System, Part I: Study," Tech. Rep. WADD-TR-60-651, Part 1, Flight Control Laboratory, Wright Air Development Division, Air Research and Development Command, USAF, September 1960.

[8] D. Bellman et al., *Investigation of the Crash of The X-15-3 Aircraft on November 15, 1967.* NASA Flight Research Center, January 1968.

[9] M. Thompson and J. Welsh, "Flight Test Experience With Adaptive Control Systems," tech. rep., NASA Flight Research Center, 1970.

[10] J. Lindahl, W. McGuire, and M. Reed, "Advanced Flight Vehicle Self-Adaptive Flight Control System, Part V: Acceptance Flight Tests," Tech. Rep. WADD-TR-60-651, Part V, Flight Control Laboratory, Aeronautical Systems Division, USAF Systems Command, May 1963.

[11] C. Exby, J. Gray, and J. Harrison, "Advanced Flight Vehicle Self-Adaptive Flight Control System, Part III: Support Equipment Study," Tech. Rep. WADD-TR-60-651, Part III, Flight Control Laboratory, Wright Air Development Division, USAF Air Research and Development Command, February 1961.

[12] M. Reed, J. Wolfe, and D. Mellen, "Advanced Flight Vehicle Self-Adaptive Flight Control System, Part IV: Notch Filter Development," Tech. Rep. WADD-TR-60-651, Part IV, Flight Control Laboratory, Aeronautical Systems Division, USAF Systems Command, June 1962.

[13] R. Yancey, "Flight Measurements of Stability and Control Derivatives of The X-15 Research Airplane to a Mach Number of 6.02 and an Angle of Attack of 25 Degrees," Tech. Rep. TN D-2532, NASA Flight Research Center, November 1964.

[14] R. Tremant, "Operational Experiences and Characteristics of the X-15 Flight Control System," Tech. Rep. TN D-1402, NASA, December 1962.

[15] D. Mellen, "The Development and Flight Test of An Adaptive Flight Control System for the X-15 Vehicle," tech. rep., Minneapolis-Honeywell, February 1963.

[16] B. Boskovich and R. Kaufmann, "Evolution of the Honeywell First-Generation Adaptive Autopilot and its Applications to F-94, F-101, X-15, and X-20 Vehicles," *J. Aircraft*, vol. 3, no. 4, pp. 296–304, 1966.

[17] Staff of the Flight Research Center, "Experience with the X-15 Adaptive Flight Control System," Tech. Rep. TN D-6208, NASA Flight Research Center, 1971.

[18] J. C. Hsu and A. U. Meyer, *Modern Control Principles and Applications*. McGraw-Hill, 1968.

[19] D. Klyde, J. McRuer, and T. Myers, "Pilot-Induced Oscillation Analysis and Prediction with Actuator Rate Limiting," *J. Guidance, Control, and Dynamics*, vol. 20, no. 1, pp. 81–89, 1997.

[20] D. Klyde and D. Mitchell, "Investigating the Role of Rate Limiting in Pilot-Induced Oscillations," *J. Guidance, Control, and Dynamics*, vol. 27, no. 5, pp. 804–813, 2004.

Appendix B. Reconstructed Flight Data

Flight data from X-15 Flight 3-65 appearing in this appendix were reconstructed from a photocopy of the original strip chart recordings (see Figure B-1) appearing in the 1968 AIB report [ref. 3]. As can be expected with data of poor quality, it is subject to some uncertainty and contains a number of filtering artifacts. It is, however, the best available representation of the aircraft states known to the authors.

Where data are lacking or incomplete in the original report, the data were reconstructed based on assumed atmospheric properties. Unfortunately, the trajectory parameters appearing in the report do not indicate which range reference atmosphere (RRA) was used for the reconstruction or the sources for the vehicle's Earth-relative velocity magnitude (composite range radar estimates are assumed). As a result, Mach number and dynamic pressure ($\bar{q}$) are estimated from other vehicle states assuming a quiescent 1976 Standard Atmosphere model.
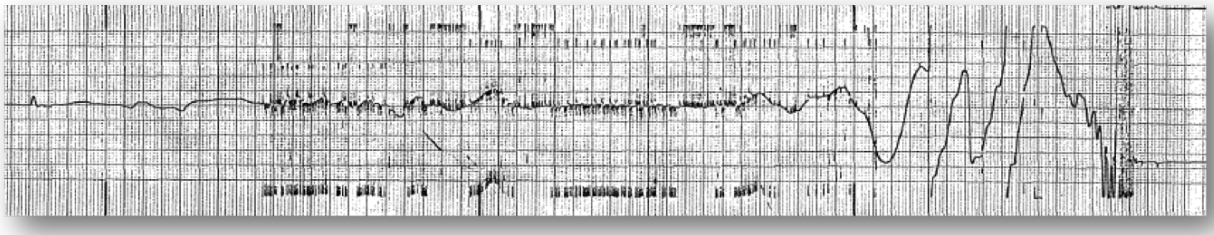
Figure B-1. Example of Original Strip Chart Recording

Data were time correlated by cross reference to key events appearing in Appendix K of reference 3 combined with a re-timing analysis of the digitized cockpit film. To generate plots (Figures B-2 through B-6), data were extracted from the original graphics via image processing, then interpolated and uniformly sampled at 10 Hz. The data were noise filtered with a zero-phase (forward-backward) second-order low pass filter (f_c = 1 Hz, ζ = 0.707). MET is referenced to ignition occurring at 10:30:08 PST on November 15, 1967.
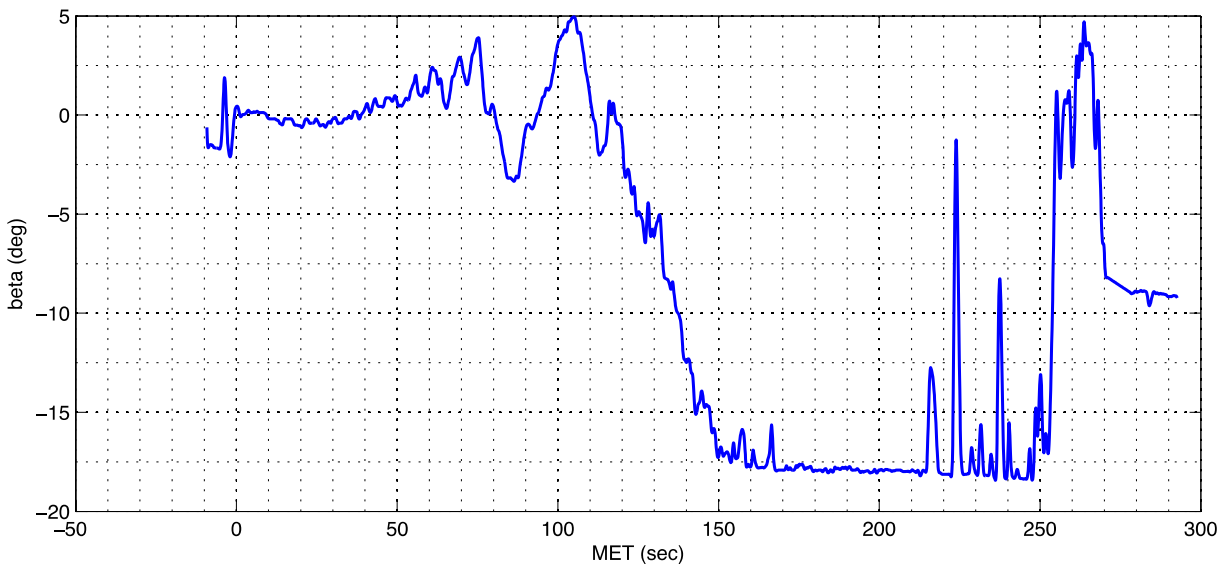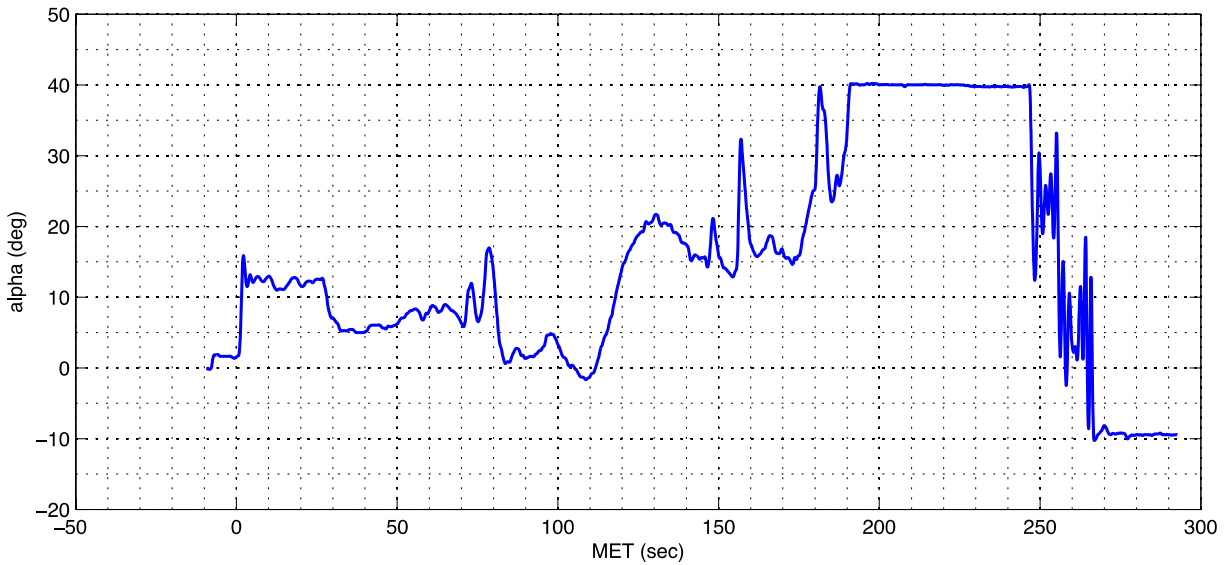
Figure B-2. Flight 3-65 Aerodynamic Angles
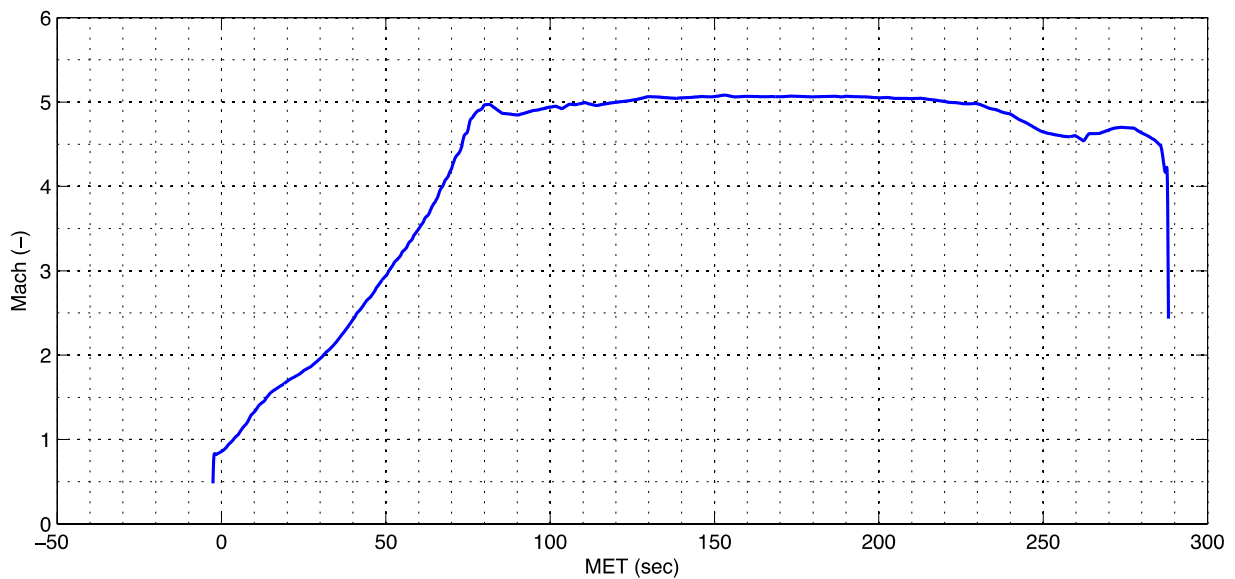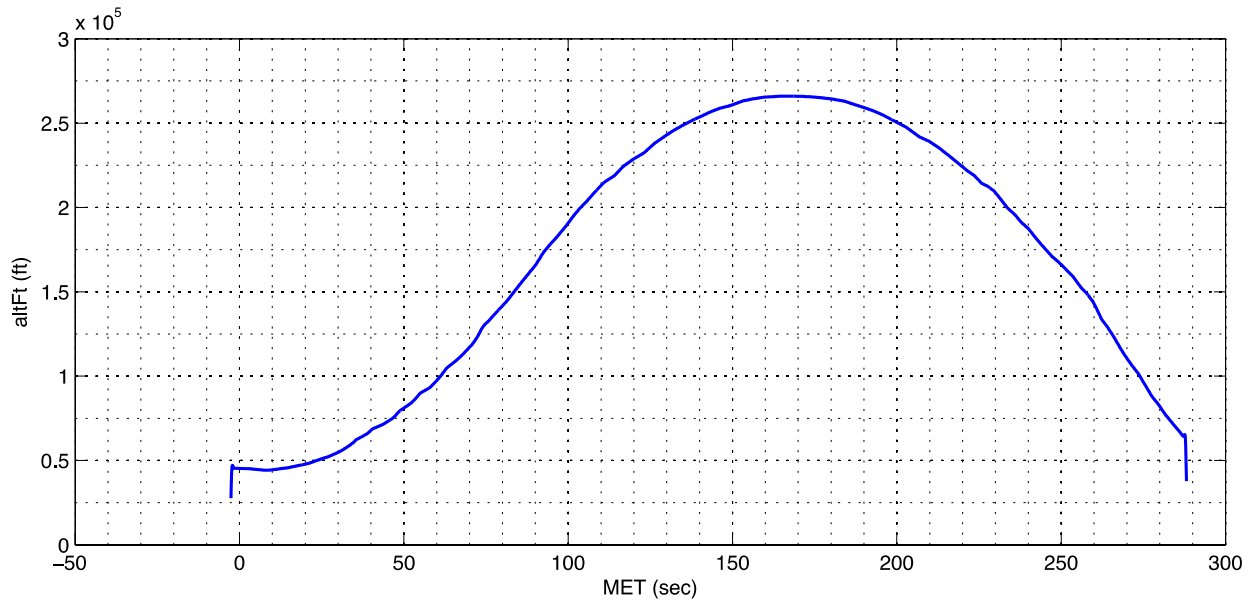
Figure B-3. Flight 3-65 Altitude and Mach Number
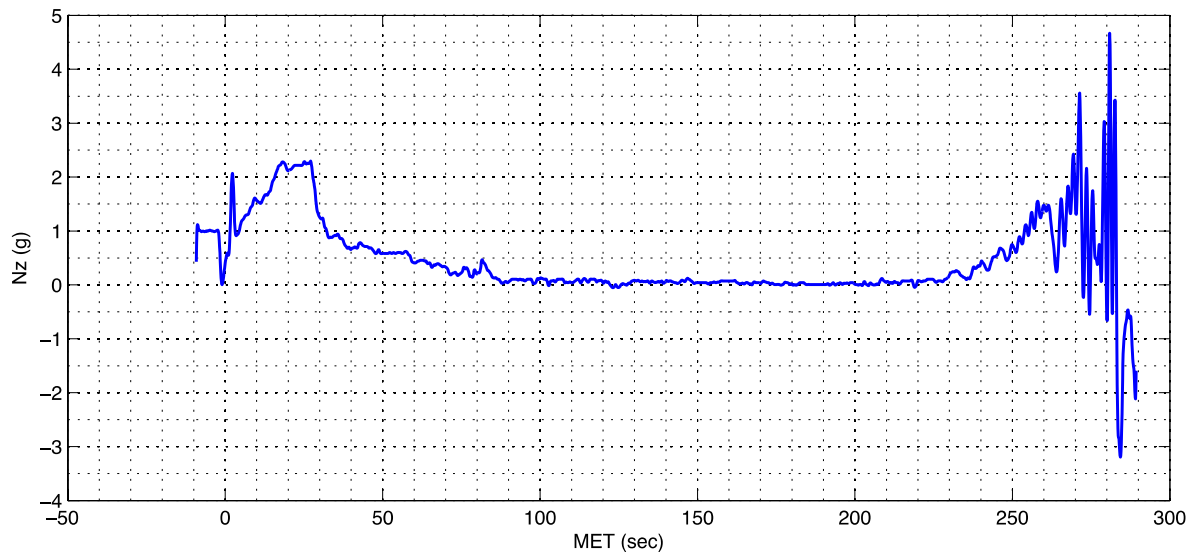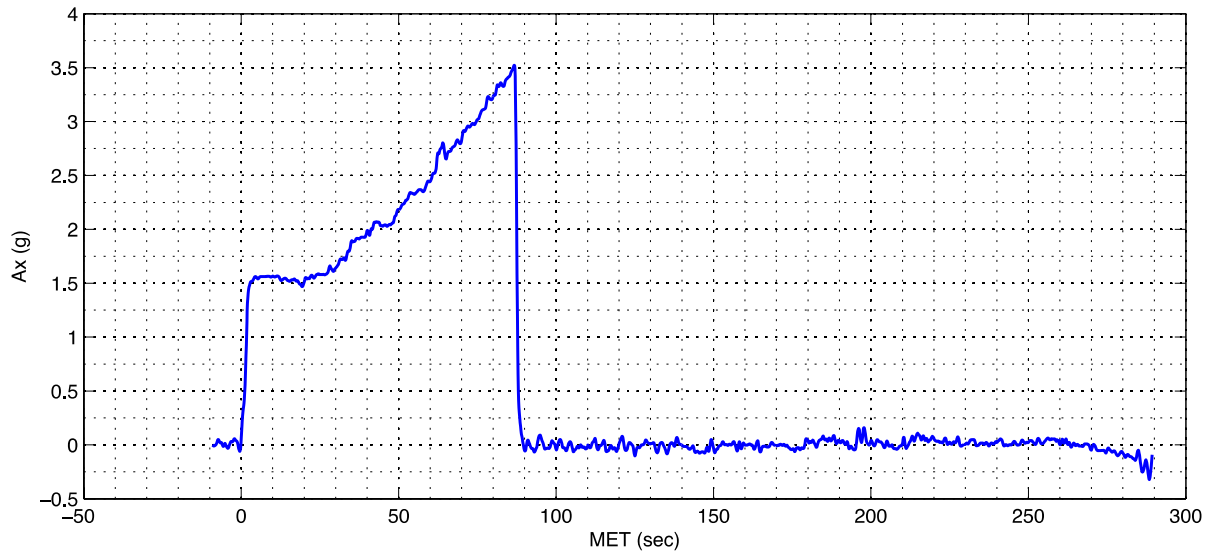
Figure B-4. Flight 3-65 Axial and Normal Acceleration
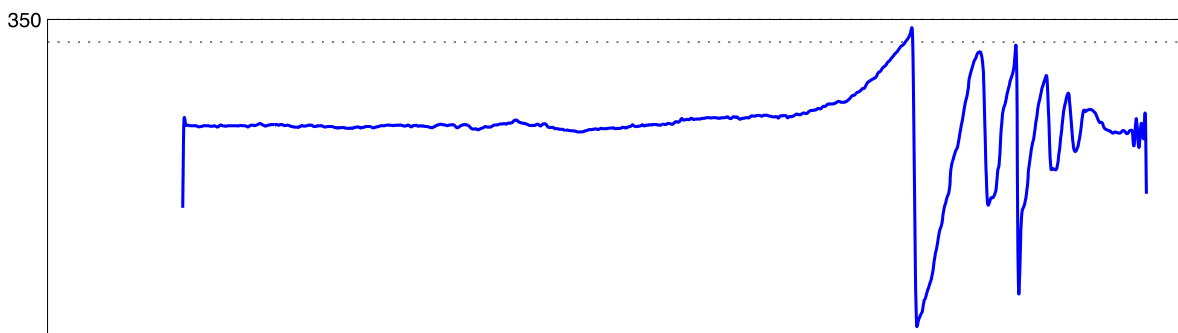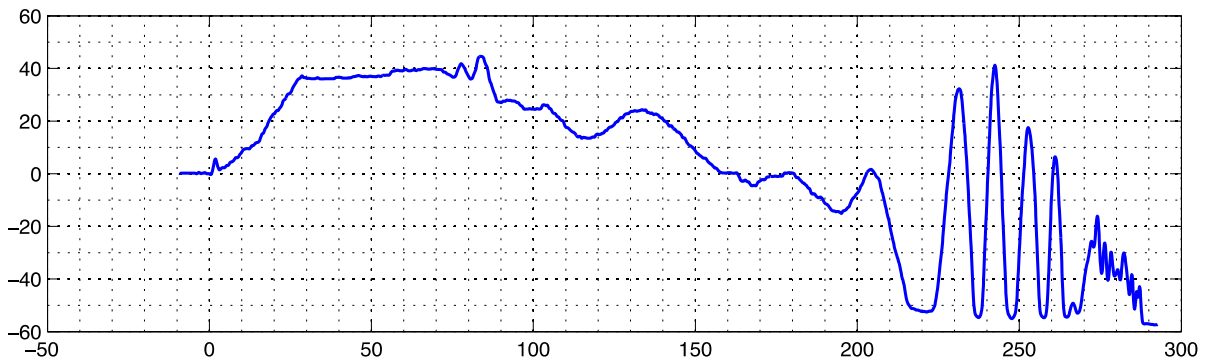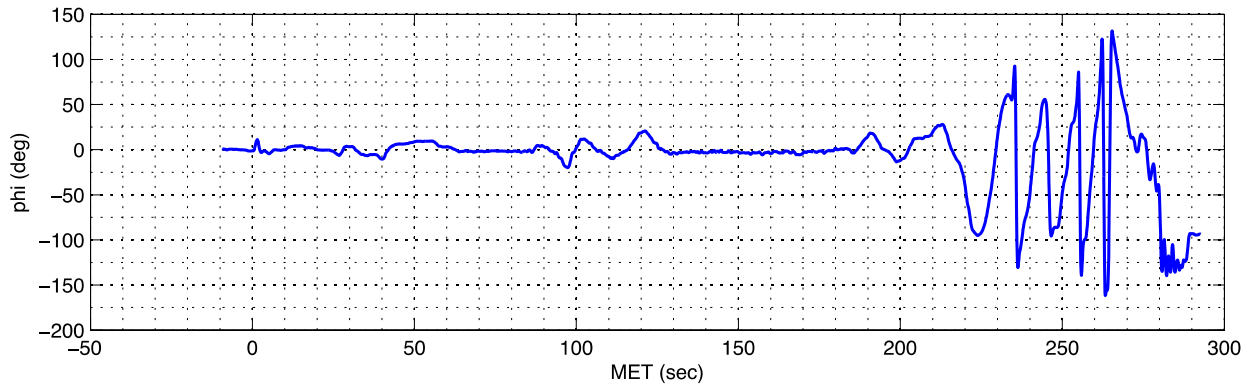
***Figure B-5. Flight 3-65 Attitude Angles (Earth relative, ψ = 0 true North;
magnetic variation 16° E)***
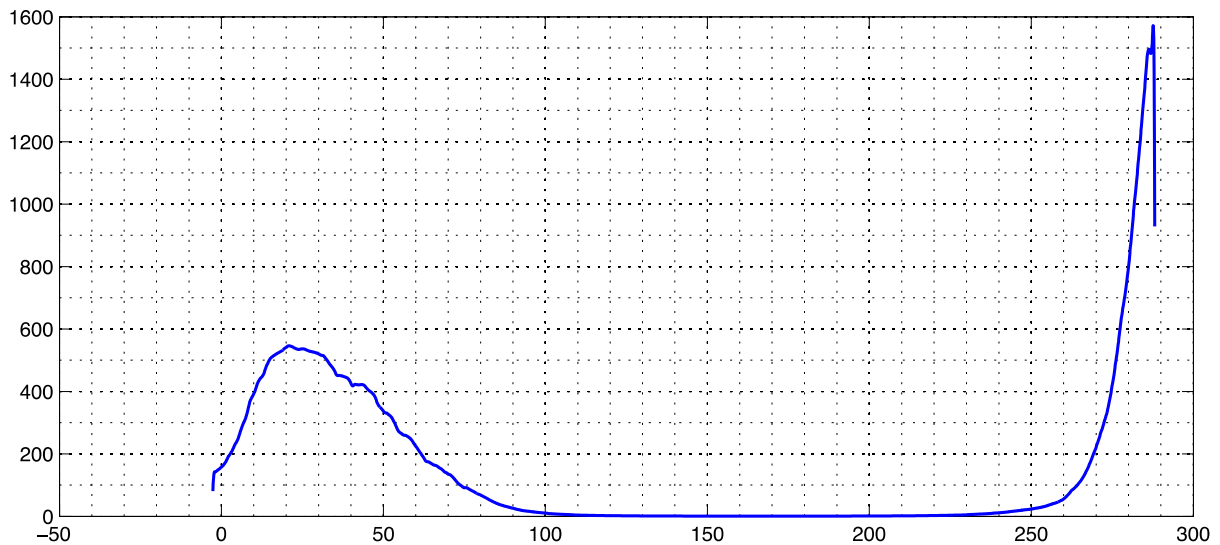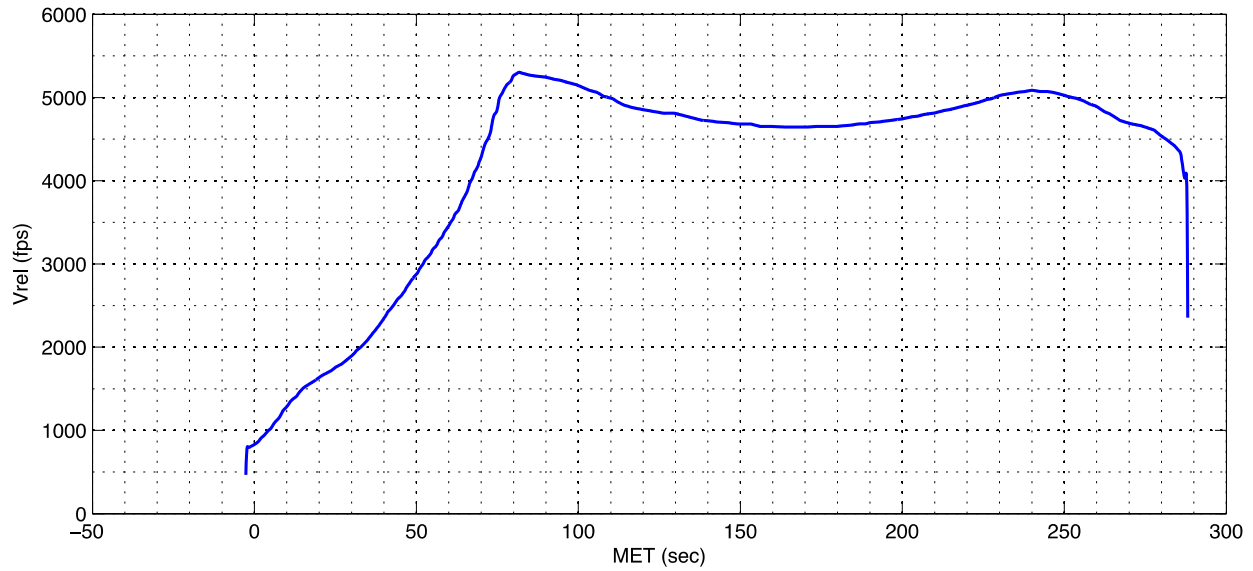
Figure B-6. Flight 3-65 Earth-relative Velocity Magnitude and Dynamic Pressure

The X-15-3 aircraft carried three 16-mm film cameras, one of which was attached to the inside of the pilot canopy (Figure B-7) and took photographs of the right side of the pilot panel at a rate of 2.5 frames per second [ref. 3].
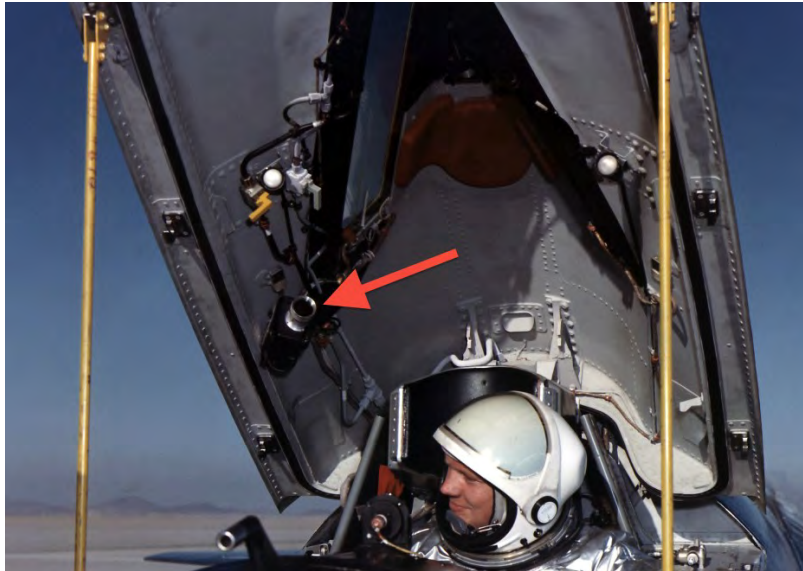
Figure B-7. Location of Film Camera on Canopy (DFRC)

Extracted frames from the cockpit film are shown in Figures B-8 through B-17. Critical events and pilot actions are identified in these events based on the re-timing analysis. A digitized version of the original film was found as a 29.97-fps digital video disc in the public domain. The frame timing from the 2.5-fps film to the 29.97-fps digital was not uniform, so the timing synchronization was based on observable events in the video assuming a uniform frame rate. This appears to yield a synchronization that is accurate to approximately +/–0.25 sec.

The first synchronization event is the rise in chamber pressure at engine ignition (approximately 1 second post release), which can be seen in the pilot's chamber pressure gauge at the top left of the engine instrumentation panel below the IFDS vertical tapes. According to the AIB report, this event occurs at 10:30:08.5 PST. The last event is the last film camera frame prior to sun exposure, which occurs at 10:34:54.4 PST. Based on this information, a total time span between these events of 4:45.9 is expected, and the frame timing was adjusted to achieve this.

Timecode information was added indicating the frame count (not correlated with the original film frame count, which is unknown), and the mission elapsed time referenced to ignition time. The recovered video starts about 12 seconds prior to ignition.

The synchronization is relatively accurate. The pilot can be seen to activate the PAI switch at MET + 84.7 seconds, corresponding to 10:31:33.2 PST. The AIB reports this event at 10:31:33.0.

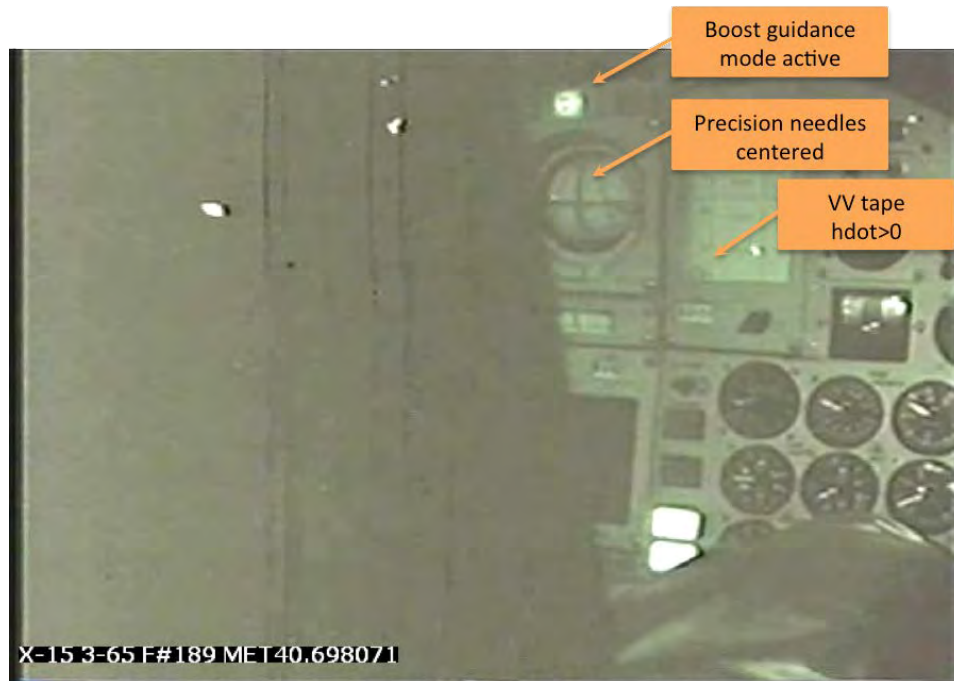*Figure B-8. Cockpit Film – Ignition Indicated by Increasing Chamber Pressure (MET = 0 seconds, 10:30:08 PST)*

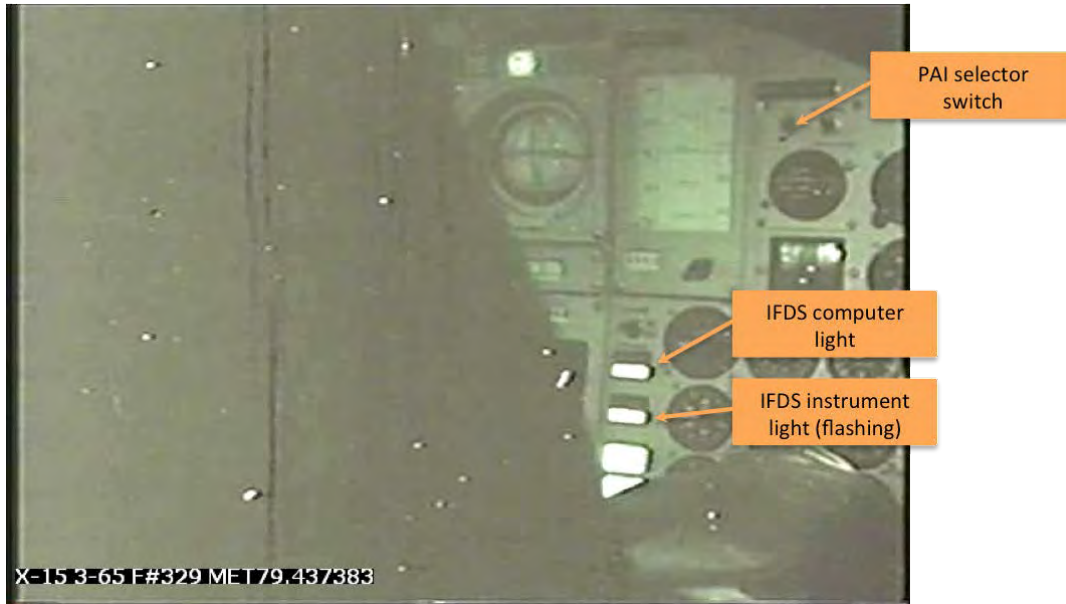*Figure B-9. Cockpit Film – Boost Phase (MET = 41 seconds, 10:30:49 PST)*

Figure B-10. Cockpit Film – Begin IFDS Malfunction (MET = 79 seconds, 10:31:27 PST)

Figure B-11. Cockpit Film – Pilot Engages PAI (MET = 84 seconds, 10:31:32 PST)

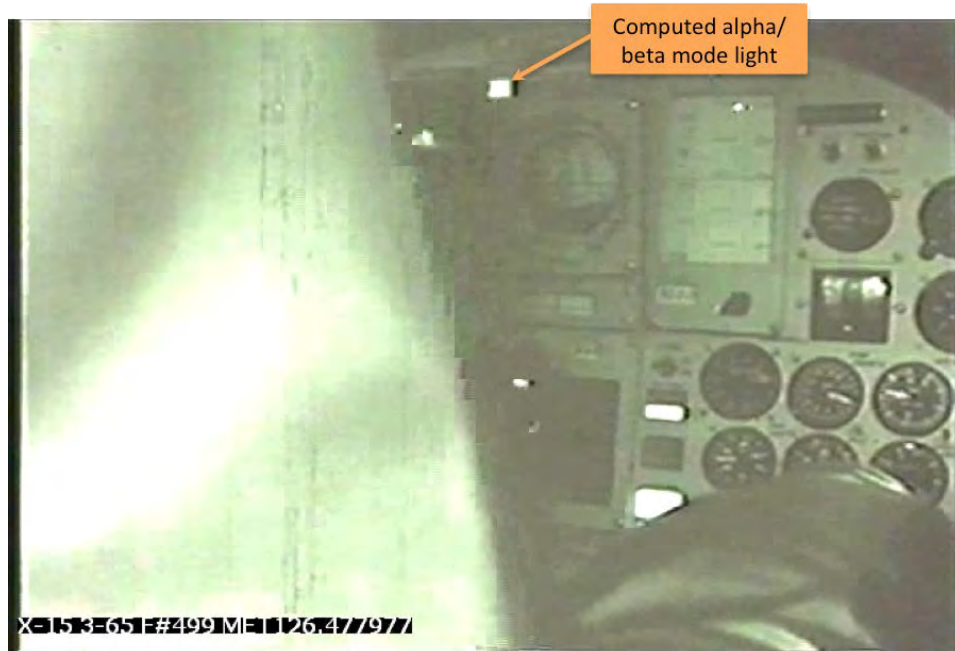*Figure B-12. Cockpit Film – Pilot Attempts IFDS Reset (MET = 87 seconds, 10:31:35 PST)*

Figure B-13. Cockpit Film – Pilot Selects Computed IFDS Aerodynamic Angles <50 psf
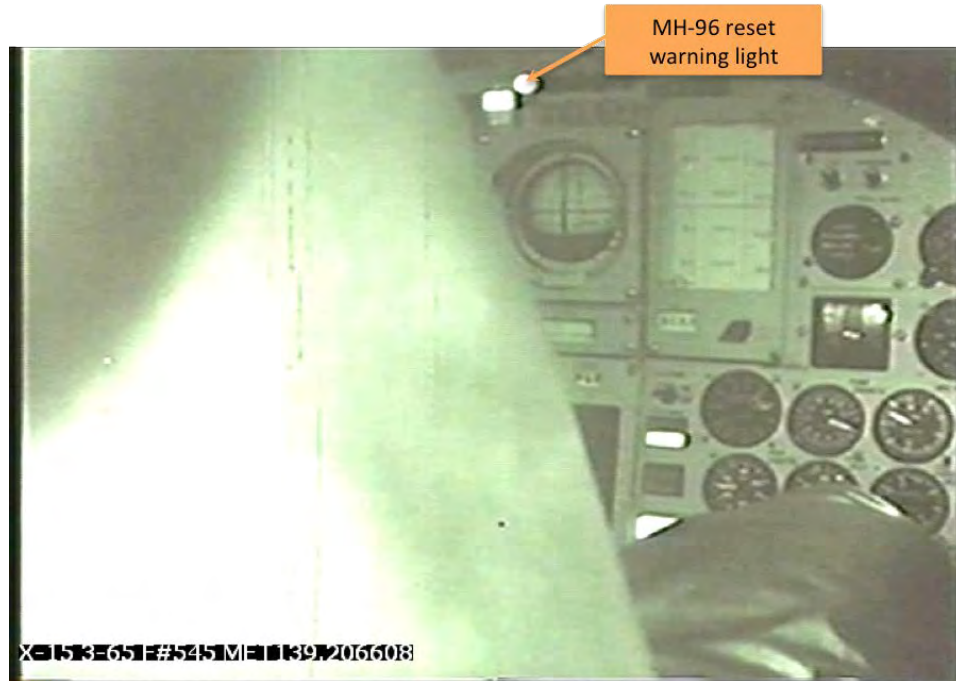*(MET = 126 seconds, 10:32:14 PST)*

Figure B-14. Cockpit Film – One of At Least Two MH-96 Disengages (MET = 139 seconds, 10:32:27 PST)
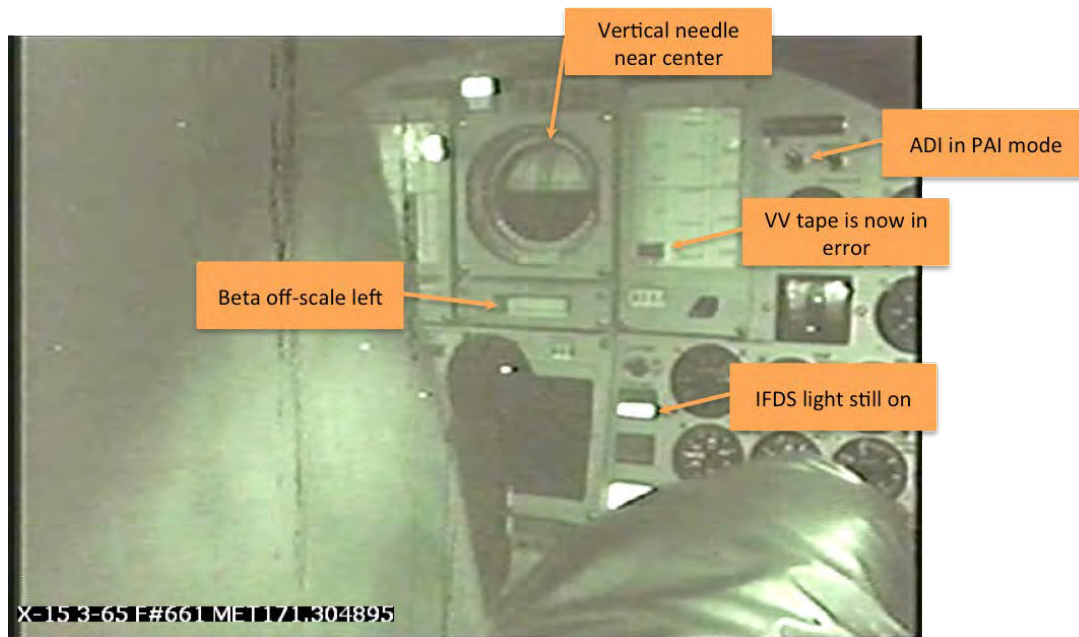
Figure B-15. Cockpit Film – Near Peak Altitude (MET = 171 seconds, 10:32:59 PST)
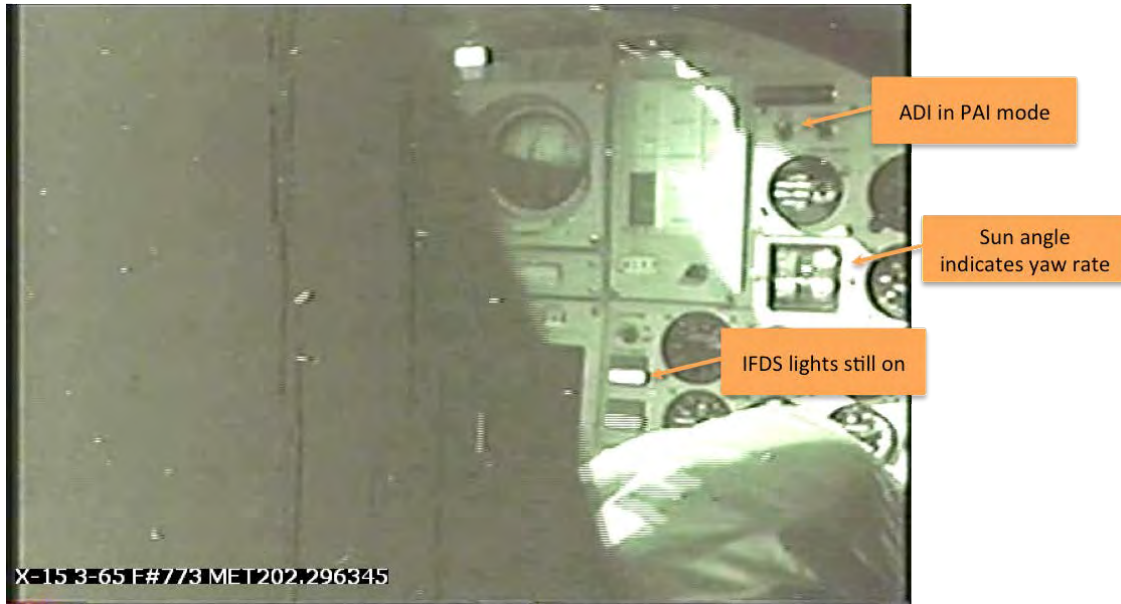
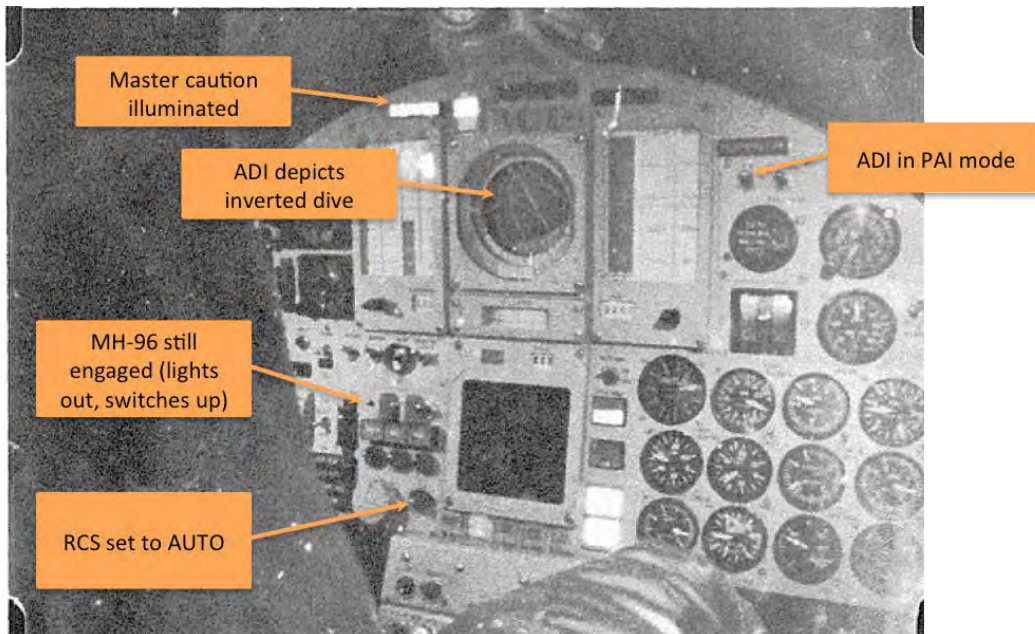*Figure B-16. Cockpit Film – Spin Entry (MET = 202 seconds, 10:33:30 PST)*

Figure B-17. Cockpit Film – Last Camera Frame (MET = 286 seconds, 10:34:54 PST)

REPORT DOCUMENTATION PAGE		*Form Approved* *OMB No. 0704-0188*

The public reporting burden for this collection of information is estimated to average 1 hour per response, including the time for reviewing instructions, searching existing data sources, gathering and maintaining the data needed, and completing and reviewing the collection of information. Send comments regarding this burden estimate or any other aspect of this collection of information, including suggestions for reducing this burden, to Department of Defense, Washington Headquarters Services, Directorate for Information Operations and Reports (0704-0188), 1215 Jefferson Davis Highway, Suite 1204, Arlington, VA 22202-4302. Respondents should be aware that notwithstanding any other provision of law, no person shall be subject to any penalty for failing to comply with a collection of information if it does not display a currently valid OMB control number.
PLEASE DO NOT RETURN YOUR FORM TO THE ABOVE ADDRESS.

1. REPORT DATE *(DD-MM-YYYY)* 01- 10 - 2014	2. REPORT TYPE Technical Memorandum	3. DATES COVERED *(From - To)* June 2014 - September 2014	
4. TITLE AND SUBTITLE A Comprehensive Analysis of the X-15 Flight 3-65 Accident		**5a. CONTRACT NUMBER**	
		5b. GRANT NUMBER	
		5c. PROGRAM ELEMENT NUMBER	
6. AUTHOR(S) Dennehy, Cornelius J.; Orr, Jeb S.; Barshi, Immanuel; Statler, Irving C.		**5d. PROJECT NUMBER**	
		5e. TASK NUMBER	
		5f. WORK UNIT NUMBER 869021.03.07.01.03	
7. PERFORMING ORGANIZATION NAME(S) AND ADDRESS(ES) NASA Langley Research Center Hampton, VA 23681-2199		**8. PERFORMING ORGANIZATION REPORT NUMBER** L-20481 NESC-RP-14-00957	
9. SPONSORING/MONITORING AGENCY NAME(S) AND ADDRESS(ES) National Aeronautics and Space Administration Washington, DC 20546-0001		**10. SPONSOR/MONITOR'S ACRONYM(S)** NASA	
		11. SPONSOR/MONITOR'S REPORT NUMBER(S) NASA/TM-2014-218538	

12. DISTRIBUTION/AVAILABILITY STATEMENT
Unclassified - Unlimited
Subject Category 16 Space Transportation and Safety
Availability: NASA CASI (443) 757-5802

13. SUPPLEMENTARY NOTES

14. ABSTRACT
The November 15, 1967, loss of X-15 Flight 3-65-97 (hereafter referred to as Flight 3-65) was a unique incident in that it was the first and only aerospace flight accident involving loss of crew on a vehicle with an adaptive flight control system (AFCS). In addition, Flight 3-65 remains the only incidence of a single-pilot departure from controlled flight of a manned entry vehicle in a hypersonic flight regime. To mitigate risk to emerging aerospace systems, the NASA Engineering and Safety Center (NESC) proposed a comprehensive review of this accident. The goal of the assessment was to resolve lingering questions regarding the failure modes of the aircraft systems (including the AFCS) and thoroughly analyze the interactions among the human agents and autonomous systems that contributed to the loss of the pilot and aircraft. This document contains the outcome of the accident review.

15. SUBJECT TERMS
Adaptive Flight Control System; NASA Engineering and Safety Center; X-15; Commercial off the Shelf; Attitude Director Indicator; Inertial Flight Data System

16. SECURITY CLASSIFICATION OF:			17. LIMITATION OF ABSTRACT	18. NUMBER OF PAGES	19a. NAME OF RESPONSIBLE PERSON STI Help Desk (email: help@sti.nasa.gov)
a. REPORT	b. ABSTRACT	c. THIS PAGE			
U	U	U	UU	112	19b. TELEPHONE NUMBER *(Include area code)* (443) 757-5802

Standard Form 298 (Rev. 8-98)
Prescribed by ANSI Std. Z39.18